Understanding the pathomechanisms leading to muscle alterations in Myotonic Dystrophy type 1: Consequences of CaMKII deregulation on the maintenance of neuromuscular junctions

Inauguraldissertation

zur

Erlangung der Würde eines Doktors der Philosophie

vorgelegt der

Philosophisch-Naturwissenschaftlichen Fakultät

der Universität Basel

von

Denis Falcetta

2020

Genehmigt von der Philosophisch-Naturwissenschaftlichen Fakultät
auf Antrag von

Prof. Dr. Markus A. Rüegg, Prof. Dr. Perrine Castets, Prof. Dr. Michael Sinnreich, Prof. Dr. Valérie Allamand

Basel, den 13.10.2020

Prof. Dr. Martin Spiess
Dekan

Acknowledgments

First and foremost, I would like to express my deep and sincere gratitude to my research supervisor Prof. Perrine Castets, for all the patience and energy she had to execute to guide me through the last past 4 years, especially in times where I lost confidence. It was a great privilege and honor to work and study under her guidance and I am extremely grateful for what she has offered me.

Special thanks go also to Prof. Markus A. Rüegg and Prof. Michael Sinnreich, who welcomed me in their research groups, allowed me to work on this exciting project, accepted to be part of my committee, and never failed to support me, whenever I was in need of their expertise and experience. Also I would like to express my gratitude to Prof. Valérie Allamand, who accepted to be part of my committee and for her helpful and critical advice during the committee meetings. Further, I want to give thanks to all the lab members from both laboratories for accepting me as an equal member of the group and for granting me their professional assistance at any time. All of you greatly contributed in making my work even more enjoyable. I would love to name you all, but I think reading this long list would exhaust everyone.

I am extending my heartfelt thanks to my girlfriend Rachel, who always stayed by my side, especially in rough times, in which she “had to” endure my emotional distresses and physical absences. You were my anchor and lifebuoy, and I could not have done this journey without you.

I am extremely grateful to my parents, siblings, and grandparents for their love, prayers, caring, sacrifices, and encouragement along the way.

I also want to thanks my best friends Carlos and Cristian for listening, caring, and alleviating my worries, when things were not going as planned.

Finally, my thanks go to all the facilities and people who have supported me to complete my research work directly or indirectly.

Abstract

Myotonic Dystrophy Type 1 (DM1) is a multisystemic autosomal dominant disorder and represents the most common form of muscular dystrophy in adults. DM1 is caused by a (CTG)n repeat expansion in the 3` UTR of the *DMPK* gene. Once transcribed, the aberrant (CUG)n transcripts form stable double-stranded structures, which sequester multiple RNA-binding proteins, resulting in the defective splicing of numerous genes. Since the discovery that RNA-gain-of-function constitutes a major pathological event in DM1, therapeutic strategies have mainly focused on targeting mis-splicing events to counteract the spliceopathy. Although refinement of experimental and therapeutic approaches have allowed a better understanding of DM1 pathophysiology, there is still no cure available. Over the last years, studies unveiled the contribution of different deregulated cellular processes to DM1 muscle pathology. In particular, previous results in the group showed that the key metabolic pathways AMPK and mTORC1 are perturbed in DM1 muscle. They further suggested a major deregulation of Ca^{2+}/calmodulin-dependent protein kinase (CaMK) proteins in DM1 muscle. To get further insights into the pathomechanisms underlying DM1, I investigated whether and how deregulation of CaMKIIs contribute to DM1 muscle affliction. CaMKIIs have been shown to be essential for muscle plasticity, including remodeling of muscle synapses. To this end, CaMKIIs regulate activation and translocation of key factors governing activity-dependent gene expression. In addition, CaMKIIs actively promote the recycling of AChRs to the surface of muscle membrane after their internalization, making them pivotal players in the maintenance of post-synaptic sites. Although studies have reported changes in pre- and post-synaptic compartments of neuromuscular junctions (NMJs) in muscle from DM1 patients and mouse models, a potential contribution of NMJ alterations to DM1 muscle pathogenesis remains under debate. Here I showed that the muscle-specific isoform of CaMKIIβ (CaMKIIβM) is lost in muscle of HSA^{LR} and $Mbnl1^{\Delta 3/\Delta 3}$ mice, two well-characterized DM1 mouse models. Fluorescent-based staining approaches of NMJs revealed that HSA^{LR} and $Mbnl1^{\Delta 3/\Delta 3}$ muscle exhibit an increased fragmentation of the motor endplates in both, basal conditions and when challenged with nerve injury. Analysis of activity-dependent pathways pointed to a deregulation of HDAC4 and synaptic gene expression, which may involve CaMKII deficiency in HSA^{LR} and $Mbnl1^{\Delta 3/\Delta 3}$ muscles. Moreover, I showed that AChR turnover is increased in muscles from HSA^{LR} and $Mbnl1^{\Delta 3/\Delta 3}$ mice under basal conditions. This was accompanied by a reduction in AChR recycling at post-synaptic sites of DM1 muscle, which may also arise from CaMKII deficiency. Lastly, $Mbnl1^{\Delta 3/\Delta 3}$ mice showed defective up-regulation of synaptic genes upon nerve injury, while AChR turnover was strongly increased. This abnormal response to denervation may involve yet unknown CaMKII-independent mechanisms. Overall, these findings suggest that defective maintenance of NMJs in DM1 muscle may involve CaMKII-dependent and -independent processes, and may be key events contributing to DM1 muscle pathophysiology.

Table of Contents

List of Abbreviations

ACh	Acetylcholine
AChE	Acetylcholinesterase
AChR	Acetylcholine Receptor
ADP	Adenosine diphosphate
ANXV	Annexin 5
AMPA	α-amino-3-hydroxy-5-methyl-4-isoxazolepropionic acid
AMPK	AMP-activated protein kinase
ASO	Antisense oligonucleotide
ATP	Adenosine triphosphate
ATP2A1	*ATPase sarcoplasmic/endoplasmic reticulum Ca^{2+} transporting 1*
BIN1	Bridging integrator 1
bHLH	Basic-helix-loop-helix
CACNA1C	Voltage-dependent P/Q-type calcium channel subunit alpha-1C
CaM	Calmodulin
CaMKII	Ca^{2+} /calmodulin-dependent protein kinase II
CaV1.1	Voltage-gated L-type calcium channel
CDK4	Cyclin-dependent kinase 4
CDK5	Cyclin-dependent kinase 5
Chrna1	*Cholinergic receptor nicotinic alpha 1 Subunit*
ClC-1	Chloride voltage-gated channel 1
CLCA	Chloride channel accessory
CLCN1	*Muscle specific chloride channel 1*
CNM	Centronuclear myopathy
CNS	Central nervous system
CtBP1	C-Terminal Binding Protein 1
CUGBP1	CUG binding protein 1
DACH2	Dachshund homolog 2
DGC	Dystrophin-glycoprotein complex
DHPR	Dihydropyridine receptor
DM	Dystrophia Myotonica/Myotonic Dystrophy
DMPK	Dystrophia Myotonica Protein Kinase
DM1	Myotonic Dystrophy type I/Steinert´s disease
DM2	Myotonic dystrophy type 2/proximal myotonic myopathy
DMD	*Duchenne muscular dystrophy*
DNA	Deoxyribonucleic acid
DOK-7	Downstream of tyrosine kinase-7
EAMG	Experimental autoimmune myasthenia gravis
ECC	Excitation-contraction coupling
EMG	Electromyogram
EPP	Endplate potential
ER	Endoplasmic reticulum
ERK	Extracellular signal regulated kinase
ERM	ETS translocation variant 5
F-actin	Filamentous actin
Fbox32	F-box only protein 32
FKBP1A	FKBP Prolyl Isomerase 1A
Fn14	Fibroblast growth factor-inducible 14

GABPα/β	GA Binding Protein Transcription Factor Subunit Alpha / Beta
G-actin	Globular actin monomers
GSK3β	Glycogen synthase kinase 3β
HDAC	Histone Deacetylase
Homer1	Homer Scaffold Protein 1
HSA	Human skeletal actin
HSA^{LR}	Human skeletal actin - long repeat
IR	Insulin receptor
hnRNPH	Heterogeneous nuclear ribonucleoprotein H
JNK	c-Jun N-terminal kinase
LC3	Microtubule-associated proteins 1A/1B light chain 3B
LRP-4	Low-density lipoprotein receptor-related protein 4
MBNL1	Muscleblind-like protein 1
MEF2	Myocyte-specific enhancer factor 2
mEPC	miniature endplate current
MG	Myasthenia gravis
MHC	Myosin heavy chain
miRNA	micro RNA
MLC	Myosin light chain
MN	Motor neuron
mRNA	Messenger RNA
MURF1	E3 ubiquitin-protein ligase TRIM63
MuSK	Muscle Associated Receptor Tyrosine Kinase
mTORC1	Mammalian target of rapamycin complex 1
MyoD	Myoblast determination protein 1
Myog	*Myogenin*
NaV1.4	Sodium channel protein skeletal muscle subunit alpha
NMD	Neuromuscular disorder
NMJ	Neuromuscular junction
PKA/B/C	Protein kinase A/B/C
RAB5	Ras associated protein RAB5A
RAN	Repeat-associated non-ATG translation
RAPSYN	43kDA receptor associated protein of the synapse
RBPs	RNA-binding proteins
RNA	Ribonucleic acid
RyR1	Ryanodine receptor 1
SCN4	Sodium Voltage-Gated Channel Alpha Subunit 4
SERCA1	Sarcoplasmic/endoplasmic reticulum Ca^{2+} ATPase 1
SIX5	Sine Oculis Homeobox Homolog 5
SH3GLB1	Src-Homology 3 Domain-containing GRB2-like protein B1
STAU1	Double-stranded RNA-binding protein Staufen homolog 1
SR	Sarcoplasmic reticulum
TnC/I/T	Troponin C / I / T
TSC	Tuberous sclerosis complex
TWEAK	Tumor necrosis factor-like weak inducer of apoptosis
UTR	Untranslated region
VGCC	Voltage-gated calcium channels
ZNF9	Zinc-finger protein 9

List of Schemes

List of Figures and Tables

PROJECT 1

PROJECT 2

Preface

Myotonic Dystrophy Type 1 (DM1) is a progressive disorder affecting multiple tissues and systems in patients. DM1 constitutes the most common form of muscular dystrophy in adults and follows an autosomal dominant mode of inheritance. Even though modern research and medicine has been refined over the years, current therapeutic approaches have only limited beneficial effects. Up to date, DM1 still ranks as a not curable disease and its pleiotropic nature makes disease-management of affected individuals challenging. The modest capability of modern drugs to treat DM1 is mainly due to our limited understanding of the overall underlying pathomechanisms.

My thesis aimed to get further insights into the complexity of the disease by investigating mechanisms that may contribute to DM1 muscle pathophysiology. To this end, this study addresses a long debated question on the role of NMJ perturbation to DM1-associated muscle affliction, and it delineates potential deregulation of mechanisms involved in NMJ maintenance and plasticity (Result - Project 1). In a side project, I also investigated whether proteins of the chloride channel accessory (CLCA) family may limit the consequences of the deficiency in ClC-1, a chloride channel affected in the disease, and thereby reduce myotonia in DM1 muscle (Result – Project 2).

This project was conducted in the groups of Prof. Michael Sinnreich (Department of Biomedicine, University of Basel) and of Prof. Markus A. Rüegg (Biozentrum, University of Basel) under the supervision of Prof. Perrine Castets (CMU, University of Geneva). Structurally, this thesis comprises an introduction of relevant topics addressed during my work, a result section including the Project 1 in the form of a paper manuscript followed by a description of the Project 2 in the form of a short report, and lastly a discussion on the work conducted and potential outlook.

1. Introduction

Skeletal muscle is one of the three muscle types found in the musculoskeletal system of vertebrates, along with cardiac muscle and smooth muscle. Like cardiac muscle, skeletal muscle is a type of striated muscle, which unlike the former, consists of muscle cells that are under voluntary control, exhibit fatigue, and have high-energy requirements. In humans, skeletal muscle accounts for ~40% of the total body mass and is regarded as the largest organ of the body [1]. Decades of research have remediated the functional spectrum of skeletal muscle, which has long been restrained to the pivotal conversion of chemical signals to mechanical energy, *e.g.* the generation of force for locomotion, heat generation, respiration and posture-maintenance. Skeletal muscle is a highly dynamic and plastic organ, whose proper function relies on precise- and well-orchestrated cellular processes [2]. Due to its intrinsic ability to sense and respond to changes in the metabolic-energetic environment, as well as to communicate with other organs through secreted molecules (myokines), skeletal muscle constitutes a pivotal organ for whole-body homeostasis [3]. Consequently, perturbations (*e.g.* genetic or environmental) of processes that affect the integrity and function of skeletal muscle and/or of the innervating motor neurons eventually lead to neuromuscular disorders (NMDs) [4]. NMDs encompass ~100 syndromes and are characterized by dysfunctions of the peripheral nerves (*e.g.* amyotrophic lateral sclerosis), Schwann cells (*e.g.* chronic inflammatory demyelinating polyradiculoneuropathy), the neuromuscular junctions (NMJ) (*e.g.* myasthenia gravis) or the muscle itself (*e.g.* muscular dystrophies) [5]. NMDs commonly present with a progressive and multisystemic pathophysiology and the severity of the clinical manifestations can range from non-life threatening muscle pain to lethal respiratory and cardiac abnormalities [6]. Although new therapeutic approaches, such as gene therapy, have paved the way for more elaborated and effective treatments, most NMDs are still not curable today [6].

In the following, an overview of skeletal muscle architecture and function together with NMJ organization and maintenance is given, followed by a detailed description of the specific muscular dystrophy Myotonic Dystrophy type I (DM1) and of DM1-associated pathomechanisms.

1.1 Skeletal Muscle: from architecture to function

1.1a Skeletal Muscle Architecture: a brief overview

Skeletal muscle is attached to bones through tendinous tissue [7]. Muscles are composed of discrete muscle fascicles, which are in turn constituted of numerous elongated, multinucleated muscle cells. The structural and functional subunits of skeletal muscle cells, also referred to as muscle fibers or myofibers, are the myofibrils. Myofibrils are composed of structural, regulatory and contractile proteins that run parallel to the longitudinal axis of the myofiber, forming partially overlapping units of two sets of alternating thin and thick myofilaments, known as sarcomeres. Sarcomeres are the basic contractile units responsible for force generation and their repeated occurrence throughout muscle fibers gives skeletal muscle its striated appearance. A sarcomere is defined as the confined region of a myofibril between

two cytoskeletal structures, known as Z-discs or Z-lines. The thin myofilaments are anchored to the Z-discs by α-actinin and extend like a lateral array towards the center of the sarcomere (M-line). The thick myofilaments attach to the M-line through myomesin and extend towards the Z-discs. The region, where the lateral arrays of both thin and thick myofilaments intercalate in an alternating manner relates to the visually distinctive darker A-band. Thin myofilaments are composed of two chains of filamentous actin (F-actin), which in turn consist of polymerized globular actin monomers (G-actin) carrying a myosin binding site. Along each side of the actin filaments run two continuous polymers of the regulatory protein tropomyosin, to which a heterotrimeric troponin complex is associated [8]. The troponin complex consists of troponin C (TnC), troponin I (TnI) and troponin T (TnT). Thick myofilaments are composed of myosin protein complexes, which consist of two myosin heavy chains (MHCs) and four myosin light chains (MLCs). The globular heads of the MHCs harbor the actin- and ATP binding sites needed for force generation [9, 10].

1.1b Membrane potential and Action potential

Like any excitable cell, the membrane potential of skeletal muscle fibers relies on the net electrochemical gradients of ions that are unevenly distributed between the extra- and intracellular compartments [11]. An action potential starts with the activation and opening of AChRs prompting the influx of Na^+ ions into the muscle fiber [12]. The net inward current generated is sufficiently positive to elevate the muscle membrane potential over the threshold required for the activation of the juxtaposed fast voltage-gated sodium channels (SCN4, Sodium Voltage-Gated Channel Alpha Subunit 4) [13, 14]. Once activated, sodium channels open and the membrane potential strikes up from its negative resting membrane potential of -70 to -90mV towards the Nernst equilibrium of sodium (+67mV) [15]. Contemporarily with the upstroke, mechanisms are set in motion that limit peak potential to +30mV. Firstly, as the sodium ions rush from the extracellular space inside the cytoplasm, the build-up of positive charge in the intracellular space initiates the inactivation of sodium channels. Secondly, the resulting intracellular positive charge activates rectifying potassium channels, which initiate the leakage of K^+ ions into the extracellular space thereby repolarizing the membrane. Once the membrane is repolarized to negative resting values, K^+ channels start to close and Na^+/K^+-ATPase pumps actively restore the original ion concentrations across the muscle membrane thereby undergoing a brief phase of hyperpolarization [16].

In skeletal muscle, nerve stimulation generally generates short trains of repetitive action potentials (tetanic stimulation) that propagate along the transverse tubular network (t-tubules) to the inside of the muscle [17]. Following repeated stimulation, K^+ accumulates in the extracellular space due to a shift in the equilibrium potential of K^+ (E_K) leading to depolarization of the t-tubular membrane [18]. The potential transmission of t-tubular depolarization to the surface membrane, *i.e.* the generation of new action potential in absence of stimulation, is averted through the high resting conductance of chloride ions (G_{Cl^-}). In normal skeletal muscle, G_{Cl^-} accounts for ~80% of the total resting membrane conductance

(G_M) and obtains its most significant contribution through the action of chloride channel 1 (ClC-1). Although its contribution to repolarization is rather small, ClC-1 provides the inhibitory chloride currents necessary for stabilization of G_{Cl^-} allowing the restauration of resting membrane potential after repetitive stimulation [19]. As the negative equilibrium potential of chloride (E_{Cl}) exceeds (E_K), this leads to the re-uptake of K^+ ions into the lumen of t-tubules thereby quenching extracellular K^+ accumulation [20, 21]. Consequently, resting membrane potential and sarcolemmal excitability are restored to basal levels, thereby impeding after-depolarization of the membrane and allowing muscle relaxation upon cessation of nerve stimulation.

1.1c The Excitation-Contraction Coupling process

Excitation-contraction coupling (ECC) links the depolarization of the muscle fiber membrane (sarcolemma) to muscle contraction. As mentioned beforehand, the evoked action potential propagates like a wave along the sarcolemma deep into the muscle fiber. It does so by spreading radially down a network of characteristic sarcolemmal invaginations, which run perpendicular to the surface, known as transverse tubules or t-tubular system [17, 22]. ECC occurs at specific junctional sites (triad junctions), where the t-tubular membranes closely associate with two terminal cisternae of the sarcoplasmic reticulum (SR) through the protein junctophilin 1 [23, 24]. Depolarization of the t-tubular membrane at the triadic region induces conformational change in the α_1-subunit of the voltage-sensing dihydropiridine receptor (L-type Ca^{2+} channel Cav1.1/DHPR). This in turn enables its allosteric interaction with the ryanodine receptors (RyRs) located at the terminal cisternae of the SR and the release of calcium from SR stores into the sarcoplasm [25, 26].

In skeletal muscle, calcium is stored and sequestered in close vicinity to the RYRs within the SR lumen by calsequestrin [27]. RyR-mediated Ca^{2+} release is modulated by structural and functional proteins regulating RyR integrity and activity, including triadin, junctin, S100A1 (S100 calcium-binding protein A1), FKBP1A (FKBP Prolyl Isomerase 1A), Homer1 (Homer Scaffold Protein 1), calsequestrin and CaM (calmodulin) [28]. Once released, Ca^{2+} binds to TnC located on the actin myofilaments of the sarcomeres. This results in the structural displacement of tropomyosin and TnI, allowing exposure of their myosin binding sites. At this stage, the myosin heads of the myofilaments are energized by binding to ADP+Pi molecules. Upon release of the phosphates, the myofilaments bind to the unblocked myosin binding sites on the actin myofilaments forming a cross-bridge. Powered by the chemical energy stored in the myosin heads, the two myofilaments slide past each other, thereby releasing the bound ADP, a process referred to as sliding filament theory. Binding and hydrolysis of a new ATP molecule dissociates the myofilaments from each other resuming the initial rigor state ready for the next cycle [29, 30]. Muscle contraction terminates with the removal of Ca^{2+} from the cytosol back to the SR lumen through the action of SERCA (sarco/endoplasmic reticulum Ca^{2+}-ATPase) pumps [31]. Ca^{2+} removal is further supported by its uptake into mitochondria, as well as through the action of Na^+/Ca^{2+} exchanger pumps located at the sarcolemma [32]. With the decrease in cytoplasmic Ca^{2+} concentration, Ca^{2+} dissociates

from TnC leading to the reset of sarcomere length, which in turns restores the blockage of the myosin binding sites on the actin filaments through tropomyosin and TnI [32-34].

1.2 The Neuromuscular Junction: organization and maintenance

Moving voluntarily in a given environment is an ability essential to animals, including humans. Converting intent into action requires tightly regulated communication between the central nervous system (CNS) and skeletal muscle fibers. Neuromuscular junctions (NMJs) are specialized chemical synapses ensuring the transmission of the neural activity to skeletal muscle. The availability of new genetic techniques and suitable animal models have greatly contributed to the identification of NMJ components and mechanisms important for NMJ development and maintenance. Defects in the pre- and/or post-synaptic compartments of the NMJ affect the contractile properties of the muscle. A defective muscle response to neural input may have detrimental effects on fundamental functions within skeletal muscle tissue and result in muscle weakness, fatigue or even paralysis [6]. Albeit impairments of the neuromuscular transmission is a phenomenon identified in numerous pathological conditions, current therapeutic approaches are still in its infancy.

1.2a NMJ morphology and signal transduction

Like other chemical synapses, the NMJ comprises pre- and post-synaptic moieties separated by a synaptic space [35]. The pre-synaptic site corresponds to the axonal nerve terminal of a branched lower motor neuron (MN) that arises from cell bodies located in the ventral horn of the spinal cord [36]. Nerve terminals are the site of containment, storage, release and re-uptake of synaptic vesicles that carry the neurotransmitter acetylcholine (ACh) [37]. They are enveloped by non-myelinating, peri-synaptic glia cells (Schwann cells), which in turn are capped by fibroblast-like cells, referred to as kranocytes [37-39]. Once the incoming neuronal signal reaches the nerve terminal, voltage-gated calcium channels (P/Q Ca^{2+}-channels or VGCCs) trigger the influx of Ca^{2+} into the nerve terminal evoking the fusion of synaptic vesicles with the terminal membrane at the active zones. This results in the release of quantal packages (6000-10000 molecules) of ACh into the synaptic cleft [40].

Skeletal muscle fibers are coated along their axis by a sheath of extracellular material that passes the synaptic cleft and extends into the junctional folds of the postsynaptic muscle membrane, referred to as basement membrane or basal lamina [41]. Basal lamina consists predominantly of structural glycoproteins, such as collagen IV, laminins and nidogen-2, thereby forming a scaffold-like structure [41, 42]. Besides its mechanical role, it actively contributes to regenerative and developmental processes of the NMJ. Moreover, the basal lamina maintains the enzyme acetylcholinesterase (AChE) to the synaptic site [41, 42] through its binding to the two anchoring proteins collagen Q and perlecan, as well as to the post-synaptic protein MuSK (Muscle Associated Receptor Tyrosine Kinase) [43, 44]. As soon as ACh molecules start to diffuse towards the post-synaptic skeletal muscle fiber membrane, a portion of the molecules is hydrolyzed by AChE thereby invoking cessation of the neurotransmission [42].

The post-synaptic side of the NMJ organizes in junctional folds of membrane, which harbor the components involved in the propagation of the action potential. The folds increase the volume of the synaptic space thereby serving as an amplification system of neuromuscular transmission [45]. Once the ACh molecules reach the post-synaptic region, they bind and activate nicotinic acetylcholine receptors (AChRs) in a 2:1 ratio. The ionotropic AChRs are members of the Cys-loop receptor family, which in turn belongs to the superfamily of ligand-gated ion channels [46, 47]. They reside densely packed at the crest of the post-synaptic junctional folds [48]. Release of one ACh-containing vesicle (one quanta) results in a net inward current of 3-4 nA into the muscle fiber, referred to as quantal current or miniature endplate current (mEPC) [49]. As an action potential in the nerve terminal leads to the fusion of numerous synaptic vesicles and therefore to the release of several ACh quanta, the summed opening of thousands of AChRs results in the depolarization of the sarcolemma by around 30-40mV, known as endplate potential (EPP). The evoked EPP is higher than the needed threshold to elicit an action potential at the fiber membrane, a mechanism referred to as the safety factor of neuromuscular transmission [50]. ACh action terminates by the unbinding of the molecules from their receptors and their subsequent hydrolysis by AChE into choline and acetate. The cycle completes with the re-uptake of choline into the nerve terminal, where it can be re-used as a substrate for the synthesis of new ACh molecules and re-packed into synaptic vesicles [51].

1.2b AChR properties and maintenance

The efficiency of neuromuscular transmission depends on various structural and physiological features of the NMJ. These include pre-synaptic characteristics, such as nerve terminal size, quantal release and ACh concentration, as well as post-synaptic attributes like Na^+-channel and AChR localization, number and composition [49]. In adult muscle, AChRs reside densely clustered (10,000-20,000 molecules/μm^2) at the crest of the post-synaptic junctional folds, where they form characteristic continuous plaque- or pretzel-like shaped structures [52, 53]. AChRs are transmembrane pentameric glycoproteins composed of α, β, ε, and δ subunits in a 2:1:1 stoichiometry (α2βεδ). During transition from pre-natal to post-natal development, the composition of AChRs switches from α2βγδ to α2βεδ, thereby changing inherent electrophysiological properties of the receptors, such as mean channel duration of opening upon activation and ion conductance [54]. Upon nerve injury, the inverse switch from the adult isoform ε to the embryonic form γ occurs, which reverses (γ to ε) during re-innervation [55-57]. Alongside with the switch of AChR subunits, development and de/re-innervation cycles are accompanied by changes in the metabolic stability and lifetime of AChRs. At functional adult NMJs, AChRs have a half-life time of ~10-14 days, which dramatically decreases to 1-2 days upon denervation [58-60]. Of note, similar short half-life is observed for extra-synaptic AChRs during early post-natal development [61, 62]. Although it was first hypothesized that AChR stability is predominantly determined by AChR subunit composition, studies have demonstrated that their metabolic stability rather relies on the insertion of new receptors into the membrane surface [62]. Indeed, turnover of AChRs is regulated by well-

orchestrated processes, including their biosynthesis, exocytic delivery to the postsynaptic membrane, endocytic removal, activity-dependent recycling, and degradation [63]. Therefore, perturbations of any of these processes is likely to alter the metabolic stability and availability of AChRs at the membrane surface, potentially compromising neuromuscular transmission.

1.2c Signaling involved in the regulation of AChR turnover

Over the past decades, researchers have delineated some of the molecular mechanisms governing AChR turnover in skeletal muscle. Studies conducted in murine models, such as experimental autoimmune myasthenia gravis (EAMG) mice have greatly contributed to elucidate processes involved in AChR turnover. Myasthenia gravis (MG) is predominantly associated with a defective autoimmune response against AChRs leading to a decrease in AChR number and density at post-synaptic sites. As a consequence of NMJ deterioration, neuromuscular transmission is impaired resulting in severe muscle weakness [64]. Interestingly, muscle of EAMG rats presents with an increased rate of AChR internalization and degradation suggesting that changes in AChR turnover are likely to contribute to NMJ deterioration observed in affected individuals [65, 66].

- *Mechanisms regulating the dynamics of AChRs at the sarcolemma*

Biosynthesis and assembly of AChR subunits occur within the endoplasmic reticulum (ER). Following glycosylation in the Golgi apparatus, AChRs are escorted via exocytic vesicles to the cell surface by the 43kDa receptor associated protein of the synapse (rapsyn) [67, 68]. Once inserted in the membrane, AChRs are tethered to clusters via rapsyn and linked to the underlying actin cytoskeleton via β-dystroglycan [68]. In the presence of neural activity, establishment of the AChRs-rapsyn network is thought to be predominantly regulated trough activation of the agrin/MuSK/Lrp4/Dok-7 signaling pathway [37, 49]. Indeed, studies in murine models and cultured myotubes have shown that deficiency of any of these components attenuates AChR clustering and NMJ formation [49].

Previous reports have shown that AChR internalization occurs via endocytic pathways [66, 69, 70]. Whereas studies conducted in EAMG mice and C2C12 cells have suggested a lipid-raft-mediated internalization of AChRs, cross-linking studies in cultured frog muscle cells rather pointed to the involvement of a clathrin/caveolin-dependent mechanism [71, 72]. A more recent study has implicated the GTPase RAB5, as well as the proteins CDK5 and SH3GLB1 in the regulation of AChR endocytosis at early stages [63, 73].

Once internalized, AChRs are either recycled back to the post-synaptic membrane, where they intermingle with pre-existing receptors, or targeted for autophagosomal degradation. Using pulse/chase fluorescence-based assays, Bruneau et al. have demonstrated the existence of different AChR pools (*i.e.* pre-existing, recycled, newly synthesized) within a synapse in living mice [74]. Upon denervation, AChR recycling decreases and a great proportion of the internalized receptors are directed for degradation. The process is reversed by muscle stimulation, suggesting that motor innervation is crucial

for AChR stabilization [75]. Studies using time-lapse imaging techniques in innervated and denervated adult mouse muscles have demonstrated the antagonistic roles of protein kinase C (PKC) on one hand, and PKA and CAMKII on the other hand, in regulating AChR recycling [62, 76, 77]. While PKA prevents the removal of pre-existing AChRs and promotes receptor recycling back to the membrane, PKC rather restricts their recycling, hence promoting their degradation [76]. Consistently, PKC inhibition and PKA activation were sufficient to restore AChR recycling at denervated NMJs [76]. Up to date, it remains unclear, if PKA/PKC/CaMKII-dependent regulation of AChR recycling occurs through direct phosphorylation of AChR or if other target molecules are involved. The role of CaMKII in AChR regulation will be discussed in the next section (1.2d).

As mentioned before, AChR half-life decreases during catabolic conditions, including starvation, functional denervation, and pathological disorders. Studies insinuate that, while AChR recycling is suppressed, their removal and degradation rate increase at NMJs of denervated muscle [75, 78]. A body of evidence suggests that clearance of AChRs occurs predominantly through the process of selective autophagy. Genetic ablation of the autophagic marker Atg7 (*Atg7*$^{-/-}$ mice) led to an increase in AChR turnover, which was accompanied by higher number of AChR-containing vesicles and altered NMJ morphology [79]. In mice with fasting-induced atrophy, endocytosed AChRs co-localized with multiple autophagosomal components, including LC3 and p62/SQSTM1 [73]. In this context, studies have reported that NMJ remodeling under atrophic conditions, *i.e*. the increase in AChR turnover, is partially dependent on the E3 ubiquitin-ligase Murf1/Trim63. Indeed, investigations showed that Murf1 is enriched at NMJs and interacts with AChR-containing carriers through the endocytosis- and autophagy-regulating factor SH3GLB1 (Bif-1). Moreover, attenuation of Murf1 (*Murf1*$^{-/-}$ mice) increased AChR stability at the membrane surface and reduced muscle atrophy in the context of denervation [80]. Overall, these findings suggest that autophagy-related perturbations are likely to alter NMJ remodeling by affecting AChR degradation, and thereby AChR turnover. Autophagy perturbation may in particular play a role in NMJ deterioration upon aging, and may thereby contribute to sarcopenia (*i.e.* age-associated muscle affliction).

- <u>*Mechanisms regulating synaptic gene expression*</u>

Following muscle innervation, expression of synaptic genes, such as *Chrn* and *Musk* is maintained in sub-synaptic myonuclei (*i.e.* fundamental nuclei), while it is repressed in extra-synaptic myonuclei. This regionalization involves, on one hand, permissive mechanisms at the NMJ, with the release of pre-synaptic factors, including agrin and neuregulin. Among these, activation of agrin/Lrp4/MuSK signaling pathway plays a central role. Targeted expression of synaptic genes in fundamental myonuclei is conferred by a shared DNA regulatory sequence (N-box). N-box-dependent gene expression is thought to be mediated by transcription factors of the Ets family (GABPα/GABPβ dimers and Erm), as well as via activation of the ERK and JNK signaling pathways [81, 82].

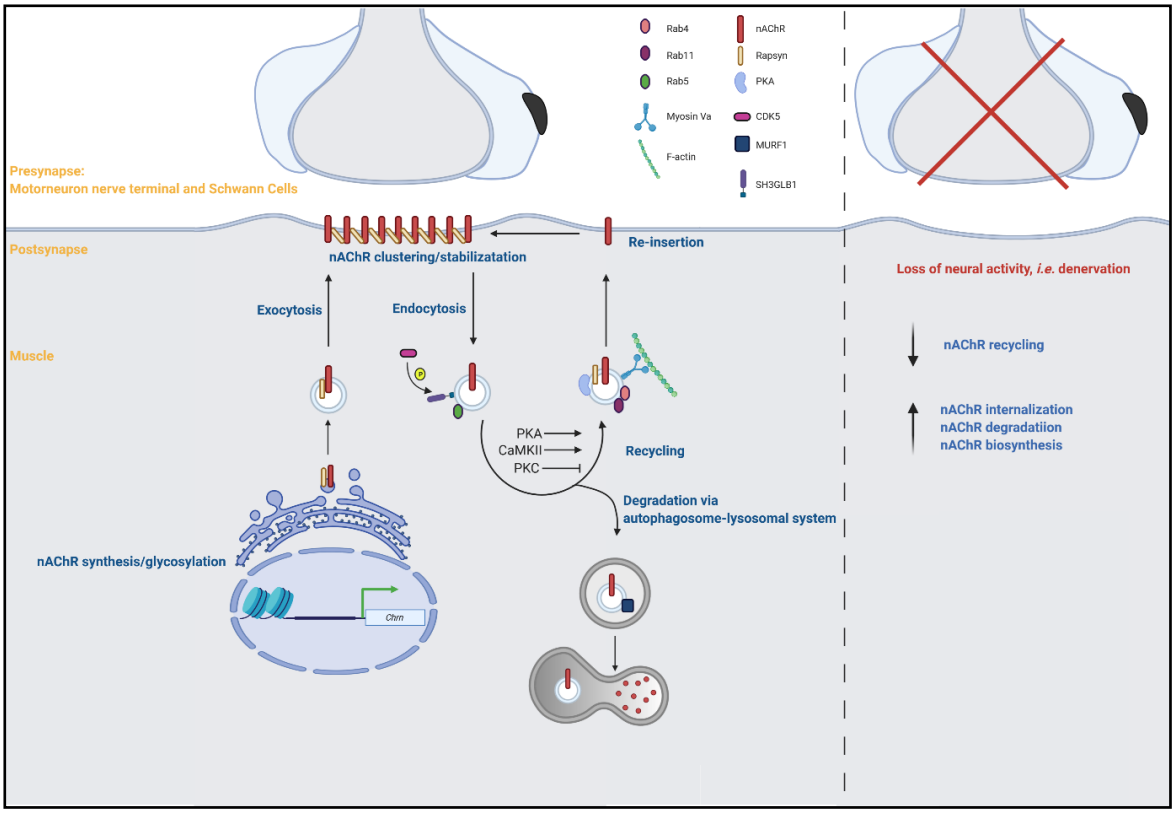

Scheme 1: AChR life cycle.

Adapted from Rudolf et al. [63]. Following their biosynthesis and glycosylation in the ER and Golgi, AChRs are delivered to the membrane surface accompanied by rapsyn. Here, they are clustered juxtaposed the nerve terminal. Upon endocytic internalization, AChRs are either recycled back and re-inserted into the membrane surface, or degraded via selective autophagy. Decision of their fate is regulated by the action of CaMKII, PKA and PKC. Recycling of AChR-containing vesicles involves myosin Va, PKA type 1, and rapsyn, while their degradation occurs in a MuRF1-dependent manner. Trafficking of the AChR-containing vesicles involves the proteins SH3GLB1 and Rab5/4/11. Loss of neural activity promotes AChR biosynthesis, internalization and degradation, whereas it suppresses AChR recycling.

Other transcription factors that regulate the expression of genes important for NMJ formation in developing and adult muscle are members of the basic-helix-loop-helix (bHLH) proteins, including MyoD and myogenin [83]. This is mediated by their binding to a shared sequence (E-box) in the promoter region of their target genes. Over the last decades, myogenin has emerged as the favorite candidate in the regulation of activity-dependent *Chrn* expression. In innervated muscle, transcriptional activity of myogenin is inhibited through Ca^{2+}-dependent activation of its upstream kinases PKC [84] and CaMKII [85, 86]. In the presence of electrical activity, the transcriptional expression of *Myog* (encoding myogenin) is also repressed by different effectors. This includes HDAC9 splice variant, MITR, which inhibits *Myog* expression *via* recruitment of HDAC1 and HDAC3 and binding to MEF2 [87]. Repression of *Myog* would also involve DACH2, MSY3 and CtBP1 [88, 89]. On the other hand, myogenin expression during development and upon denervation leads to the up-regulation of *Chrn* expression [90-93]. Recent reports have shown that myogenin expression upon denervation depends on the up-regulation and nuclear re-localization of active HDAC4 from synaptic sites. Once in myonuclei,

HDAC4 would relieve *Myog* repression at least by suppressing the expression of the transcriptional co-repressors DACH2 and MITR, thereby allowing the expression of synaptic genes [87, 94]. Further investigations are needed to identify the other mechanisms and regulatory effectors, which contribute to this finely-tuned re-induction of the developmental program allowing synaptic gene expression throughout the fiber upon denervation.

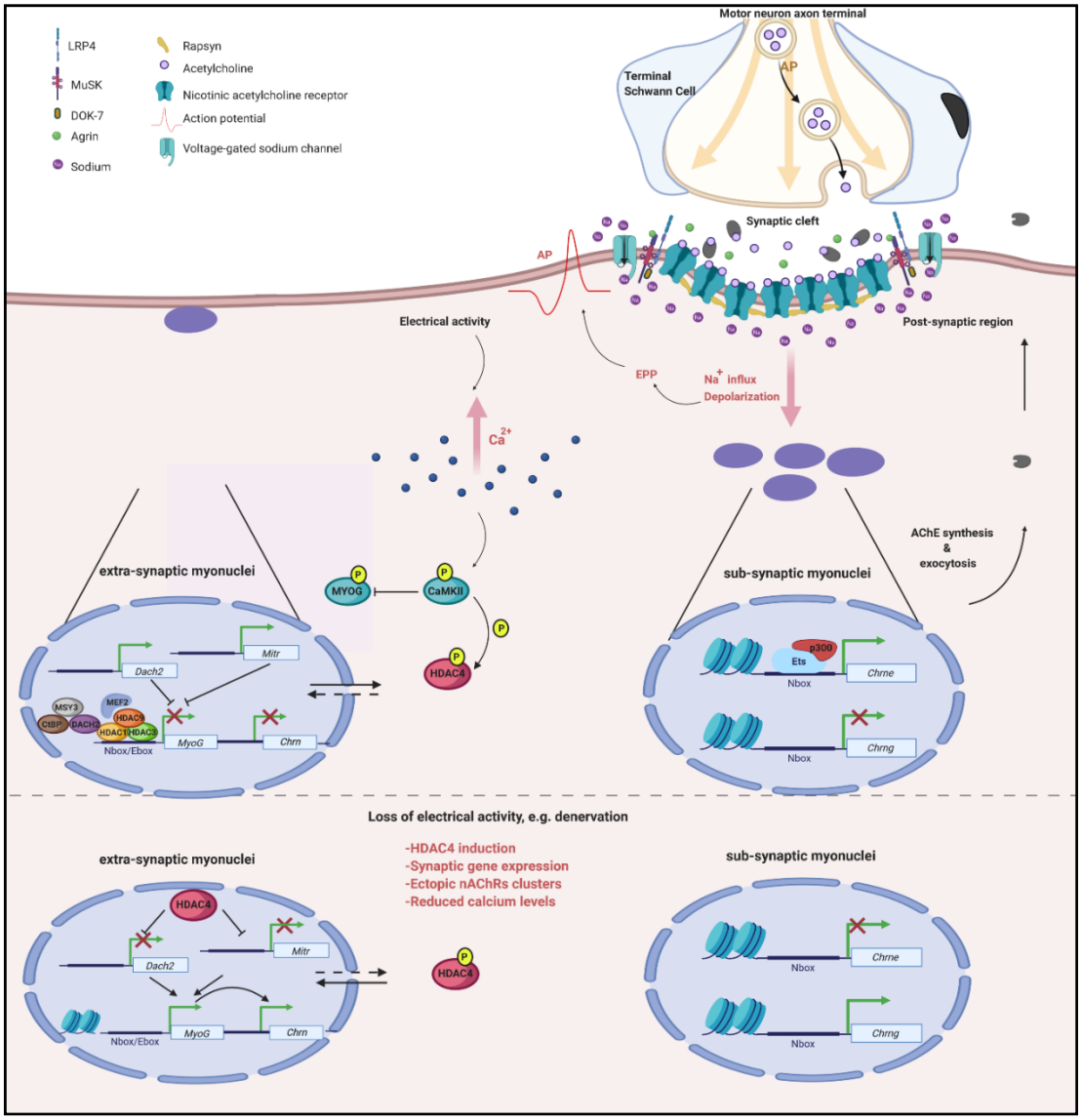

Scheme 2: Synaptic gene expression in skeletal muscle.
In the presence of neural activity, expression of synaptic genes is maintained in sub-synaptic myonuclei and suppressed at extra-synaptic sites. Targeted synaptic gene expression at synaptic sites is mediated through agrin/LRP4/MuSk signaling pathways. Nbox-dependent transcription of synaptic genes involves at least the recruitment of Ets transcription factors to the Nbox promoter region of specific targets. In extra-synaptic myonuclei, expression of synaptic genes is suppressed by MITR, DACH2, MSY3, and CTBP. This involves direct repression of *MyoG* expression through binding of co-repressors to the Ebox promoter region. In addition, transcriptional activity of myogenin is also inhibited through direct phosphorylation by CaMKIIs. Upon loss of neural activity, *i.e.* denervation, expression of synaptic genes at extra-synaptic sites is enabled through alleviation of the repressive mechanisms on myogenin expression, leading to the formation of ectopic AChRs clusters. This is mediated by the upregulation and nuclear import of HDAC4, which then represses the transcriptional co-repressors MITR and DACH2. At synaptic sites, absence of electrical activity leads to switch in the expression pattern of synaptic genes, such as the re-expression of AChR γ-subunits and repression of AChE synthesis.

1.2d Role of CaMKII in skeletal muscle and at the NMJ

Ca^{2+}-dependent expression of target genes is essential for skeletal muscle function and adaptation. Members of the Ca^{2+} / calmodulin-dependent kinase II (CaMKII) family play an essential role in decoding changes in amplitude, duration and frequency of Ca^{2+} transients, and translating them to specific transcriptional programs [95]. CaMKIIs are serine/threonine kinases and their capacity to transduce oscillating Ca^{2+} signals is determined by their structure, localization and isoform. Molecularly, CaMKIIs form homo- and hetero-multimeric holoenzymes composed of 12 identical subunits, which arrange in two sets of 6 subunits and assemble in a poke and wheel pattern. Each subunit constitutes a C-terminal association domain followed by regulatory domain and a N-terminal catalytic/kinase domain. Separate binding of Ca^{2+}/CaM to the regulatory domain of a subunit activates the kinase domain, thereby relieving auto-inhibition and enabling inter-subunit auto-phosphorylation [96]. CaMKII auto-phosphorylation leads to autonomous Ca^{2+}-independent kinase activity upon cessation of the activating signal, *i.e.* when Ca^{2+} concentration decreases to basal levels. This property is considered as a major frequency-decoding mechanism, especially after repeated muscle contraction [97, 98].

- *Role of the CaMKII family in muscle physiology*

Mammalian skeletal muscle expresses multiple isoforms of CaMKII (CaMKII-α, -β, -γ and -δ), each encoded by a different gene, with numerous splice variants being expressed [99]. Investigations on the role of CaMKIIs in skeletal muscle have primarily focused on elucidating their ability to link different patterns of muscle excitation to regulation of Ca^{2+}-dependent gene transcription. CaMKIIs have been shown to regulate Ca^{2+}-dependent transcription of contractile, metabolic, and synaptic genes, including *Chrn*, *Slc2a4*, *Atp2a2*, *Actn1, Atf1* and *Myh* genes encoding MHC isoforms [95]. Evidence suggests that part of CaMKII-dependent regulation of gene transcription is mediated via their ability to modulate subcellular localization of class II HDACs, and therefore histone acetylation [100]. In this context, studies conducted in cardiomyocytes have demonstrated that CaMKIIs promote nuclear export and block nuclear import of HDAC4 through direct phosphorylation, leading to a predominant cytosolic localization and derepression of target genes, such as MEF2 [101]. Moreover, the same group showed that HDAC5 acquires responsiveness to CaMKII signaling via oligomerization with HDAC4 leading to the co-export into the cytosol [102]. Of note, *in vitro* studies suggest that CaMKII-dependent decoding of distinct frequencies of Ca^{2+} oscillations may be regulated in an isoform-specific manner [103]. Indeed, studies conducted in murine muscle suggest that different durations of muscle activity lead to auto-phosphorylation of distinct CaMKII isoforms [99]. However, investigation elucidating specific functions of distinct CaMKII isoforms in muscle tissue are scarce. Overexpression of CaMKIIα/β in regenerating murine muscles has been shown to promote expression of SERCA2, ANXV and fast myosin type IIA/X, and to accelerate ECC and relaxation [99]. Studies conducted in aged and denervated muscles have implicated CaMKIIγ up-regulation in the adaptional response to muscle wasting [95]. Investigations in regenerating muscles form *mdx* suggested a potential contribution of increased

CaMKIIδ levels in metabolic remodeling [104]. In heart, nuclear splice variants of CaMKII α- and δ isoforms (α_B and δ_B) have been reported to regulate gene expression in ventricular myocytes, while upregulation of CaMKIIδ_A is associated with pathological cardiac hypertrophy [105, 106]. Alternative splicing of CaMKIIβ results in the muscle-specific CaMKIIβM isoform, which localizes at the membrane of SR by help of a non-kinase variant of CaMKIIα (α-kap). Here, CaMKIIβM has been shown to modulate activity-induced Ca^{2+} release and uptake through phosphorylation of RyR1, phospholamban and SERCA [107-111]. Of note, CaMKIIβ and CaMKIIβM exhibit differential Ca^{2+} sensitivity due to discrepancies in their CaM activation constant and auto-phosphorylation kinetics [112-114]. Hence, it is conceivable that discrete changes in intracellular Ca^{2+} concentrations from distinct subcellular pools may lead to the activation of specific CaMKII isoforms with individual decoding properties resulting in a differential regulation of downstream targets.

- *Role of CaMKII in synaptic gene regulation*

As mentioned before, nerve-evoked muscle activity leads to increased intracellular Ca^{2+} concentrations and suppresses AChR expression by inhibiting the transcriptional activity of myogenin. Early studies in chick muscle have suggested that myogenin inactivation is mediated through phosphorylation by Ca^{2+}-activated PKC [84]. However, recent investigations have revealed that activity-induced suppression of *Chrn* expression in mammalian muscle depends primarily on CaMKII activity. Studies conducted in primary rat muscle cells have demonstrated that CaMKII inhibits binding of myogenin to AChR promoter through direct phosphorylation [85, 86, 90]. Of note, depletion and pharmacologic inhibition of PKC did not block activity-dependent AChR suppression in Ca^{2+}- and electrically-stimulated muscle cells [86]. In addition, CaMKIIs have been shown to directly regulate HDAC4 activity and its cytosolic-nuclear translocation, which indirectly regulates the expression of activity-dependent genes through de-repression of MITR and Dach2 *(see section 1.2c)*. Taken together, these findings suggest that CaMKIIs are key effectors in the regulation of myogenin and AChR expression under different physiological conditions.

- *Role of CaMKII in AChR dynamics*

In a recent study, Martinez-Pena y Valenzuela et al. showed that direct muscle stimulation or pharmacological elevation of intracellular Ca^{2+} levels enhance AChR recycling at innervated and denervated NMJs. Conversely chelation of intracellular Ca^{2+} or pharmacological inhibition of CAMKII activity decreased recycling of AChRs and resulted in their intracellular accumulation after internalization. *In vivo* overexpression of different CaMKII isoforms (β, δ, γ) revealed the solely co-localization of muscle-specific CaMKIIβM isoform with AChRs at synaptic sites. As mentioned before, denervation prevents AChR recycling, while promoting receptor degradation. In this context, electrical stimulation of denervated muscle prevented AChRs degradation after receptor internalization and promoted their delivery back to the surface membrane. Interestingly, inhibition of CaMKII activity

negated this effect [77]. Of note, studies have reported that myosin Va is essential for the recruitment of AChR-containing vesicles upon recycling to post-synaptic sites [62, 115]. Interestingly, studies conducted in rat brain have demonstrated that activity- and $Ca2^{+}$-dependent recycling of AMPA receptors is mediated through myosin V motor proteins, which in turn are regulated by CaMKIIs [116]. Therefore, similar mechanisms may apply in the microdomain underlying NMJs. Taken together, these findings suggest that 1) translocation of internalized AChRs back to the membrane surface depends on muscle activity and 2) that CaMKIIβM plays a major role in re-routing AChRs from the degradative to the recycling pathway. Hence, it is likely that deregulation of CaMKIIs will perturb NMJ maintenance and that it may contribute to muscle weakness and atrophy in specific pathological conditions.

1.3 Myotonic Dystrophy Type I: from genetic to muscle dysfunction

1.3a Genetic cause of Myotonic Dystrophies

Myotonic Dystrophies (*Dystrophia Myotonica*, DM) are monogenic autosomal dominant neuromuscular disorder and the most common form of muscular dystrophy in adults with a global prevalence of 1:20000 [117]. DM are progressive and multisystemic diseases that affect various tissues, such as skeletal muscle, brain, heart, lungs, eyes, the gastrointestinal and endocrine systems. Up to date, two variant forms of DM have been defined, DM1 (Steinert`s Disease, OMIM #160900) and DM2 (proximal myotonic myopathy, OMIM #602668). DM1 and DM2 share several phenotypic features along with common aspects of the underlying molecular pathomechanisms. DM1 and DM2 both arise from a microsatellite repeat expansion in non-coding regions of a specific gene and are associated to clinical features characteristic to each individual form.

DM1 is more prevalent, commonly more severe, and caused by heterozygous expansion of (CTG)n trinucleotide repeats in the 3` untranslated region (UTR) of the *DMPK* (*dystrophia myotonica protein kinase*) gene located on chromosome 19q13.3. On the other hand, DM2 derives from a pathogenic expansion of (CCTG)n tetranucleotides in the intronic region of the *ZNF9* (Zinc-finger protein 9) gene situated on chromosome 3q21 [118]. Noteworthy, DM1 shows a genotype-phenotype correlation that is not observed in DM2, in which the trinucleotide expansion length relates to the age of onset and the severity of the disease. Generally, longer CTG repeats decrease the age of onset and aggravate disease manifestation. Typically, alleles that exceed 37 CTG repeats are considered as anomalous, between 38 and 49 repeats as asymptomatic and greater than 50 repeats as pathological. Due to their instable nature, trinucleotide repeats are prone to expand or contract during the processes of mitosis and meiosis [119].

Today, clinical diagnosis of DM1 occurs through non-genetic and genetic testing. Concurrently to the examination of suggestive clinical features and family history, molecular genetic testing has become the gold standard method for diagnostics. To this end, DNA testing for the causative CTG expansion in the *DMPK* locus by PCR or southern blot are used to confirm the diagnosis and circumvent the need for additional distressing tests [120-122]. Modern diagnostic has allowed to surrogate former invasive

methods like biopsy punches by less invasive and favorable approaches. Aforetime, muscle biopsies have been used by pathologist to identify alterations indicative of DM.

1.3b Clinical manifestations in DM1

Individuals affected by DM1 show a high heterogeneity in the manifestation and course of the disease. To provide an utilitarian conceptual framework, DM1 has been categorized in four main classes: congenital, childhood-onset, adult onset and late onset/asymptomatic [121]. Each class may manifest typical clinical features ranging from mild to severe that influence the quality of life of the patient to different degrees. Despite its pleiotropic nature, DM1 primarily compromises skeletal muscle, with symptoms encompassing a delayed muscle relaxation (*e.g.* myotonia), muscle pain, progressive muscle weakness and wasting.

- *Myotonia origin and evaluation*

Myotonia defines as the delayed relaxation of skeletal muscle after initial contraction. Clinical myotonia manifests as muscle stiffness that patients experience as the inability to relax their hand after a grip or the impaired capacity to chew, swallow and talk. The repeated contraction of an affected muscle leads to an amelioration of the myotonia, known as the "warm-up" phenomenon. Inversely, cold and stress typically provoke myotonia. Myotonia is caused by an overt excitability of the plasma membrane of skeletal muscle fibers. Consequently, voluntary contraction or electrical stimulation provokes repetitive muscle fiber action potentials, also referred to as myotonic runs or myotonic discharges. In DM1, as in most myotonic disorders, the increase in sarcolemmal excitability has been attributed to a decrease in the resting chloride conductance (G_{Cl}) due to a deficiency in the chloride channel protein 1 (ClC-1) [123]. Myotonia is evidenced by direct percussion of the thenar eminence and finger extensor muscles. Electrical myotonia is evaluated with a needle electromyography (EMG), which records the repetitive muscle fiber potential discharges and displays them on an electromyogram. Generally, myotonic discharges appear as fibrillation potentials with amplitudes ranging from 1µV to 1mV and firing rates between 20 to 80Hz. Compared to healthy individuals, who display an evoked discharge for only few milliseconds, affected individuals exhibit myotonic runs from tens of seconds to minutes [124, 125]. Noteworthy, modern evaluation of myotonia via EMG in patients has permitted to assess and distinguish profiles of perturbed ion-channels indicative of myotonic disorders. Although the electrophysiological pattern of DM1 patients largely coincides with profiles reminiscent of chloride channel malfunction, recent findings suggest a more intricate situation. Notably, Acket et al. have observed an atypical profile in 40% of the examined patients that cannot be fully explained by chloride channel disturbances alone [126, 127]. Congruently, several studies have related the perturbed electrical and contractile properties in DM1 to a dysfunction of voltage-gated sodium channels, as well as small-conductance calcium-activated potassium channels [128-131]. Hence, these findings suggest that DM1-associated myotonia may result from the dysfunction of more than one specific ion channel.

- *Muscle wasting and weakness*

Other cardinal features besides myotonia that relate to skeletal muscle alterations in DM1 are progressive muscle wasting and weakness. DM1 patients exhibit a characteristic distribution of affected muscles, which typically include the cranial, trunk and distal limb muscles with a preferential affliction of the neck flexors, finger flexors/extensors and foot dorsiflexors. Generally, wasting and weakness of cranial muscle reveal as temporal and masseter atrophy, ptosis and facial weakness [132, 133]. Consequently, loss in muscle strength may present with difficulties in lifting their head, balance and walking [133, 134]. A 5-year prospective study with DM1 patients reports changes in isometric leg muscle force of -6 to -18% , as well as deteriorations in different parameters of balance and gait [135]. Some DM1 patients gradually display a proximal limb muscle affliction as the disease progresses. Weakness of the oropharyngeal and diaphragmatic musculature may also compromise respiratory capacity and lead to clinical manifestations that range from nocturnal hypoventilation to respiratory failure.

Histologically, DM1 muscle displays fiber size variations from small angulated to hypertrophic fibers together with an overall increment in the proportion of type 1 fibers and a selective type 1 fiber atrophy [136]. Common features in DM1 muscle include an increase in endomysial connective tissue, as well as centrally located nuclei, pyknotic nuclear clumps, ring fibers, and sarcoplasmic masses within the muscle fibers [137]. Concomitant with voluntary muscle affliction, affliction of involuntary muscles like the gastrointestinal tract and the accessory digestive organs can manifest in constipation, cholelithiasis and swallowing difficulties. Moreover, DM1 commonly presents with progressive cardiac conduction abnormalities that may lead to a severe tachyarrhythmia and eventually atrioventricular block, thereby significantly contributing to the morbidity and mortality of affected individuals [138].

- *Non-muscle clinical manifestations*

Another system affected in DM1 is the central nervous system (CNS). Although CNS clinical features are variable, cognitive and behavioral impairments frequently occur. In DM1 patients, changes include daytime hyper-somnolence, fatigue, apathy, memory impairment and executive dysfunction. Other systemic features comprise metabolic, endocrine and ocular perturbations like insulin resistance, increased cholesterol levels, hypertriglyceridemia, a reduced fertility, balding and posterior iridescent cataracts [121, 139].

1.3c Pathogenic mechanisms associated with DM1

Historically, Hans Gustav Wilhelm Steinert and colleagues first described the classical clinical manifestations of DM1 in 1909 [140]. The identification of the causative mutation was not uncovered before the coming of 1992, when researchers revealed the presence of CTG repeat expansion in the 3` UTR of the *DMPK* gene [141-143]. Since then, several pathomechanisms involved in DM1 pathophysiology have been suggested.

- *Deficiency for DMPK and adjacent genes*

The inactivation of genes around the DM1 locus has been early suggested to contribute to DM1. In this scenario, the CTG repeats lead to the incorrect transcription of the mutated *DMPK* locus and consequently to a loss of the DMPK protein. Although initial studies using *DMPK* heterozygous and homozygous knockout mouse models have reported DM1-associated alterations, such as cardiac conduction alterations and features of a progressive myopathy [144, 145], recent studies failed to recapitulate these observations [146]. CTG repeat expansions may also alter locally the chromatin structure and its methylation status and thereby affect the expression of *DMPK*-adjacent genes. In this regard, studies conducted in DM1 cells have reported CTG expansion-mediated downregulation of the expression of the gene *SIX5* (*sine oculis homeobox homolog 5)* [147, 148]. Of note, heterozygous *Six5* knockout mice display cataracts, reduced male fertility and cardiac abnormalities, but do not reiterate skeletal muscle alterations associated with DM1 [149-152]. Although DMPK and SIX5 haplo-insufficiency does not recapitulate the full-range of DM1 pathology, the findings suggest that it contributes to certain aspects of the disease.

- *The hypothesis of RNA toxicity: what we learnt from DM1 animal models*

Following investigations using HSA^{LR} mice demonstrated the major role of (CUG)n-induced RNA-toxicity in DM1 muscle pathology. HSA^{LR} mice express an expanded and untranslated CTG repeat tract (~250 CTG) in the last exon of an inserted fragment of the human skeletal actin (*HSA, Acta1*) gene and reiterate multiple histopathological and functional alterations found in DM1 muscle. More specifically, HSA^{LR} muscle presents with ribonuclear foci, fiber size variation, ring fibers, features reminiscent of a progressive myopathy and myotonia. Moreover, HSA^{LR} muscle reproduces characteristic DM1-associated molecular characteristics, including the sequestration of specific splicing factors (*e.g.* MBNL1) by (CUG)n transcript repeats into ribonuclear foci [153, 154]. The significant contribution of reduced cytoplasmic MBNL1 availability and activity to DM1 spliceopathy will be discussed below.

Later on, mice ubiquitously expressing *DMPK* transcripts carrying the toxic CTG expansion have further help to understand the multisystemic presentation of DM1. DM300 mice display several DM1-associated molecular and functional abnormalities, including growth retardation, ribonuclear inclusions in different tissues (skeletal muscle, heart, CNS), histological alterations, myotonia, progressive muscle weakness and age-dependent alterations in glucose metabolism [155-157]. Interestingly, DM300 was the first mouse line that reproduced the expansion-biased intergenerational instability observed in DM1, which resulted in the generation of homozygous DMSXL mice carrying >1000 CTG repeats [158-160]. DMSXL mice express sense and antisense mutant *Dmpk* transcripts that accumulate into distinct nuclear foci in multiple tissues [160]. Phenotypically, DMSXL mice show cardiac and respiratory alterations, reduced muscle strength, lower motor performance, cognitive and behavioral deficits, but fail to reiterate the full-range of DM1-associated skeletal muscle alterations [160-163]. Nevertheless, these mouse models provided proof for the inherent toxic effect of pathological expanded (CUG)n transcripts. Of

note, overexpression of only 5(CTG) repeats in mice (DM5) was sufficient to reduce lifespan and cause cardiac conduction abnormalities and myotonia, suggesting that high expression of non-pathological repeats can be also pathogenic [164].

- *DM1: a spliceopathy involving several splicing factors*

Toxic RNA gain-of-function has emerged as the predominant causative event in the pathophysiology of DM1. In this scenario, transcription of the mutated *DMPK* allele generates anomalous (CUG)n-bearing transcripts that aggregate and form ribonuclear inclusions, also known as ribonuclear RNA foci. The aberrant transcripts *trans*-interfere with RNA-binding proteins (RBPs), which are important for correct alternative splicing and mRNA processing. Consequently, the deregulated activity of RBPs leads to the defective splicing of numerous pre-mRNAs [165]. RBPs that are deregulated in DM1 include members of the muscle blind-like proteins (MBNL), CUG-binding protein eva-like family member 1 (CUGBP1, also known as CELF1), hnRNP H (heterogeneous nuclear ribonucleoprotein H) and STAU1 proteins [166-169]. Among them, the antagonistic splicing factors MBNL1 and CUGBP1 have evolved as pivotal contributors to RNA-mediated pathogenesis in DM1.

a) MBNL1 as a central factor involved in DM1 pathogenesis:

Studies conducted in transgenic HSA^{LR} and *Mbnl1* knockout mice have provided significant support for the contribution of a MBNL1-dependent mis-splicing to DM1 pathology. Cytosolic MBNL1 is depleted in muscle fibers from DM1 patients and from HSA^{LR} muscle due to its sequestration by the pathologically expanded (CUG)n mRNA into nuclear foci [170, 171]. This has been related to the high affinity of exon 3-bearing MBNL1 isoforms for the expanded (CUG)n mRNA, which is allegedly stabilized in a double-stranded hairpin conformation [167, 172]. Consistently, $Mbnl1^{\Delta 3/\Delta 3}$ mice display clinical manifestations characteristic of DM1, including cognitive impairments, cataracts, myotonia and histological muscle alterations reminiscent of a progressive myopathy [173, 174]. Importantly, MBNL1 re-locates from the nucleoplasm to the cytosol upon post-natal skeletal muscle development and thereby participates in the transition of embryonic-to-adult splicing pattern of numerous pre-mRNAs [170]. Pre-mRNAs abnormally processed in DM1 and important for skeletal muscle physiology include *Clcn1* (encoding ClC-1), *Atp2a1* (encoding SERCA) and *Ryr1* (encoding RYR1) [175, 176]. Strikingly, comparative analysis between HSA^{LR} and $Mbnl1^{\Delta 3/\Delta 3}$ mice has revealed that depletion of MBNL1 contributes to more than 80% of the (CUG)n-mediated mis-splicing events in HSA^{LR} mice [177].

b) Contribution of CUG-BP1 in DM1 pathogenesis:

CUG-binding protein 1 (CUGBP1) regulates alternative mRNA splicing and translation. While CUGBP1 levels decrease in tissues of heathy individuals during development, DM1 heart and skeletal muscle show increased CUGBP1 steady state levels and activity [178-180]. CUGBP1 gain-of-function arises from a (CUG)n-mediated increase in PKC activity, which results in CUGBP1 hyper-

phosphorylation and RNA-protein complex stabilization [181]. Studies conducted in mice with tissue-specific CUGBP1 overexpression support the contribution of CUGBP1 deregulation in DM1 muscle pathology. Transgenic overexpression of CUGBP1 in muscle leads to growth retardation, histopathological features, and changes in the expression and translational activity of proteins important for myogenesis [182]. Moreover, overexpression in heart and skeletal muscle reproduces common DM1-associated pathological characteristics, including myopathy and defective splicing of cardiac troponin T (c*Tnnt2*), myotubularin-related 1 gene (*Mtmr1*), and *Clcn1 [183]*. Consistently, conditional overexpression in murine skeletal muscle reiterates histological and molecular alterations found in DM1 muscle, including centrally nucleated and atrophic muscle fibers, endomysial tissue infiltration and common mis-splicing events [184].

Overall, these studies have provided strong support for a major contribution of MBNL1- and CUGBP1-mediated toxic RNA-gain-of-function to DM1 pathogenesis, especially by favoring an adult-to-fetal shift in the expression pattern of numerous genes.

- *Potential RNA-independent mechanisms*

The occurrence of repeat-associated non-ATG translation (RAN) in microsatellite repeat expansion disorders has introduced a new level of complexity [185]. RAN translation enables the generation of mutant proteins from multiple reading frames of coding and non-coding repeat expansions without canonical AUG initiation codon usage [186]. This has even more far-reaching implications in disorders, where the repeat expansion mutations are bidirectionally transcribed [187]. RAN translation could hence bring about the generation of mutant proteins through all three reading frames from each single (CUG)n●(CAG)n-bearing transcript, giving rise to homopolymeric peptides (*i.e.* poly(Gln), poly(Ser), and poly(Ala)) [188]. Interestingly, a study in human DM1 tissues and DMSXL mice revealed the presence of poly(Gln) aggregates in myoblasts, skeletal muscle, heart and blood [187]. Moreover, the aggregates appeared to colocalize with caspase-8, which plays a pivotal role in the extrinsic apoptotic signaling pathway [187, 189]. In contrast to the known effects of the RNA-mediated toxicity, the contribution of such potential protein toxicity to DM1 pathogenesis is still elusive.

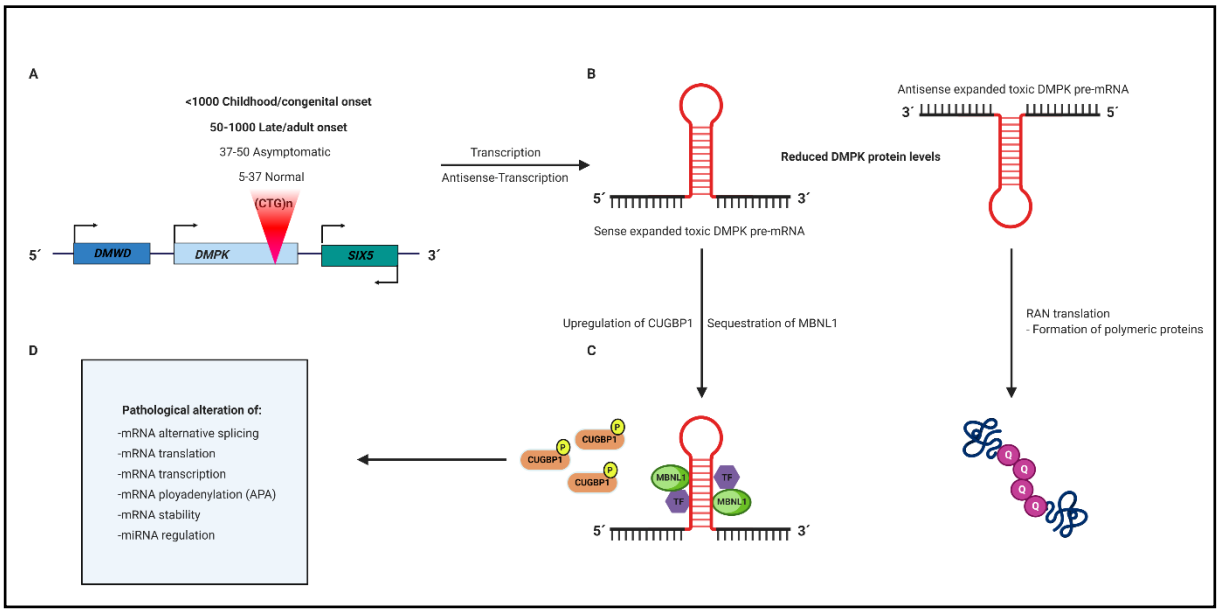

Scheme 3: Molecular pathomechanisms of DM1.

Adapted from André et al. [190]. A) Schematic representation of expanded (CTG)n repeats in the 3` UTR of the *DMPK* gene. In DM1 patients, the (CTG)n repeat fragment surpasses the 5-37 triplet repeats present in healthy individuals. The size of the repeat expansion positively correlates with the severity of the disease. B) Sense and antisense transcription of the mutated *DMPK* gene generates (CUG)n-containing mRNAs that form double-stranded hairpin structures, leading to reduced DMPK protein levels. C) Expression of (CUG)n-bearing mRNAs results in leaching different transcription factors (TF) and deregulation of the localization and function of RNA-binding proteins (RBPs) involved in pre-mRNA alternative splicing, mRNA translation and stability. In particular, sequestration of the splicing factor MBNL1, as well as stabilization and hyper-phosphorylation of CUGBP1 constitute major events in DM1-associated RNA-gain-of function. In addition, formation of polymeric proteins through repeat-associated non ATG translation (RAN) of antisense (CUG)n mRNAs has been proposed. D) These processes lead to pathological alterations of mRNA alternative splicing, transcription, translation, stability, polyadenylation (APA), and to dysregulation of miRNAs.

1.3d Pathomechanisms leading to muscle dysfunction in DM1

- *Molecular mechanisms leading to myotonia*

In muscle from DM1 patients and DM1 mouse models, myotonia is predominantly caused by reduced chloride membrane conduction due to the loss-of-function of ClC-1 [154, 173, 176]. ClC-1 loss-of-function derives from the aberrant splicing of *Clcn1* pre-mRNA by retention of exon 2 and inclusion of exon 6b and/or 7a. These changes introduce a premature termination codon that ultimately leads to nonsense-mediated decay of the truncated mRNA [191]. Noteworthy, *in vivo* overexpression of MBNL1 in HSA^{LR} muscle restores normal splicing of *Clcn1* and reverses myotonia [192]. Moreover, antisense oligonucleotide-induced exon skipping in HSA^{LR} and $Mbnl1^{\Delta 3/\Delta 3}$ mice corrects for *Clcn1* mis-splicing and reduces myotonia.

- *Deregulation of Ca^{2+}-associated signaling*

As for myotonia, DM1-associated muscle wasting is attributed to splicing defects of pre-mRNAs that are under the control of MBNL1 and CUGBP1. Mis-splicing events affect proteins that govern Ca^{2+}

homeostasis and are therefore crucial for ECC in muscle fibers. Early studies conducted in DM1 muscle cells have reported elevated intracellular Ca^{2+} concentrations [193]. In this context, muscle from patients and HSA^{LR} muscle exhibit an increased expression of the embryonic isoforms of RyR1, SERCA1 and CaV1.1 [175, 194, 195]. The aberrant alternative splicing of the corresponding genes arise from the exclusion of exon 70, exon 22 and exon 29, respectively. *In-vitro* studies conducted in myotubes have shown that the expression of the juvenile RyR1 isoform results in decreased channel activity concomitant with an enhanced depolarization-dependent Ca^{2+} release [196]. Furthermore, mis-splicing of *CACNA1C* has been shown to alter CaV1.1 activity and that the degree of mis-splicing correlates with the severity of muscle weakness in DM1 muscle [194]. Moreover, forced splice-shifting of *CACNA1C* by antisense oligonucleotides (ASO) in HSA^{LR} mice increases CaV1.1 channel gating leading to an increase in Ca^{2+} current and Ca^{2+} transient peaks [194]. In addition, *in vitro* studies have demonstrated a 50% reduction in microsomal Ca^{2+} re-uptake activity of the mis-spliced variant SERCA1b when compared to the adult isoform SERCA1a [197]. As mentioned before, CaMKII are other key Ca^{2+}-associated molecules indispensable for muscle plasticity. Studies have reported DM1-associated mis-splicing of CaMKII isoforms in several tissues. Indeed, muscle from DM1 patient and HSA^{LR} mice shows defective splicing of *Camk2b*, with an exclusion of exon13 [177, 198]. Moreover, mis-splicing of *Camk2d* pre-mRNA in brain from $Mbnl1^{\Delta 3/\Delta 3}$ mice and patients leads to an increased expression of the fetal isoform containing exons 14–16 (exon 14–15 in human) [177, 199]. Hence, the defective expression of Ca^{2+}-handling proteins is likely to contribute to DM1 muscle pathology.

- <u>*Mis-splicing of cytoskeletal proteins*</u>

Expression of cytoskeletal proteins, such as components of the dystrophin-glycoprotein complex (DGC), is affected in different hereditary muscular diseases, including Duchenne and Becker muscular dystrophy [200]. In DM1 muscle, the *DMD* gene, encoding dystrophin, is mis-spliced by exclusion of exon 78 leading to an up-regulated expression of the embryonic isoform, without affecting total protein amount and distribution [201]. Of note, studies have reported that forced *DMD* exon 78 skipping in wild-type mice leads to skeletal muscle alterations reminiscent of DM1, including ring fibers, sarcoplasmic masses, and Z-band disorganization [202]. Moreover, mis-splicing of the pre-mRNA encoding α-dystrobrevin by inclusion of exon 11A and exon 12 may alter the binding to α-syntrophin and perturb signal transduction in DM1 muscle [203]. Changes in the splicing pattern of the gene encoding BIN1 (bridging integrator 1, also known as amphyphysin2) is another event occurring in DM1 muscle [204]. Noteworthy, genetic mutations in the *BIN1* gene are responsible for the autosomal form of centronuclear myopathy (CNM) [205]. Centronuclear myopathies are characterized by prominent muscle weakness and atrophy and exhibit histopathological features found in DM1, such as ultrastructural changes of the t-tubular system [205, 206]. In CNM, alternative splicing of *BIN1* by inclusion of exon 11 generates a muscle-specific isoform that harbors a phosphoinositide-binding domain important for t-tubule biogenesis and invagination [207, 208]. In DM1 muscle, exclusion of

exon 11 results in the expression of an inactive form of BIN1 [204]. Interestingly, AAV-mediated overexpression of active BIN1 (+exon11) in DM1 cells leads to the restauration of the altered t-tubular membrane structures [204]. Moreover, forced BIN1 exon 11 skipping in mice promotes t-tubule alterations and muscle weakness [204]. Overall, these studies suggest that the defective expression of proteins important for skeletal muscle integrity and function may also contribute to DM1-associated muscle weakness and atrophy.

- *Deregulation of metabolic pathways*

DM1 patients commonly present with insulin resistance [121]. Studies conducted in DM1 myoblasts and muscles from DM300 mice have reported defects in insulin-stimulated glucose metabolism [156, 209]. Later investigations revealed that pre-mRNA encoding insulin receptor (IR) is mis-spliced in muscle from DM1 patients and mouse models leading to the increased expression of a non-muscle variant with lower signaling properties (IR-A) [180, 210]. Therefore, deregulations in signaling cascades downstream of IR activation have been suggested. In this context, muscle from DMPK-deficient mice presented with metabolic abnormalities that were associated with reduced phosphorylation of Akt (Ser473) and GSK3-β (Ser9) after insulin treatment [211]. Recent studies revealed that activity and stability of GSK3β are increased in DM1 muscle, leading to a reduction in D3/CDK4-dependent phosphorylation of CUGBP1 thereby altering its translational activity [212]. Accordingly, inhibition of GSK3β in DM1 cell culture and HSA^{LR} mice restored cyclin D3 levels and ameliorated muscle weakness and myotonia. Deregulation of the PKB/Akt-mTOR signaling pathway may also contribute to DM1-associated muscle wasting and weakness [213]. Indeed, several studies have demonstrated that key metabolic processes governed by the PKB/Akt-mTOR, such as autophagy, are altered in DM1. In atrophic DM1 flies, overexpression of mTOR restored muscle mass and reduced autophagy and apoptosis, two processes that have been found to be increased in DM1 cells [214]. Consistently, mice with an inducible expression of 960 CTG repeats showed severe muscle loss, associated with increased levels of activated AMPKα and higher expression of autophagy markers, such as Atg7 and Beclin-1 [215]. In contrast, investigations in our lab showed that AMPK signaling is impaired in HSA^{LR} muscle under starved conditions, while mTOR signaling remains active [216]. Changes in the Tweak-Fn14 signaling may also contribute to muscle wasting in DM1. Tweak-Fn14 has been shown to activate multiple processes, including autophagy [217] While being expressed in moderate amounts in healthy muscle, expression of Tweak and Fn14 is up-regulated under catabolic conditions, such as denervation and starvation which contributes to muscle atrophy [217]. Basal Fn14 levels are increased in muscle tissue from DM1 patients and DM5 mice. Interestingly, blockage of Tweak-Fn14 signaling with anti-Tweak antibodies improved muscle histology and function in mutant mice, hence suggesting that the pathway contributes to DM1-associated muscle wasting [218]. In parallel, studies have reported that the ubiquitin-proteasome system is deregulated in DM1 muscle. This involves an increase in trypsin-like proteasome activity, as well as upregulation in Fbxo32 (Atrogin-1) and Murf1 expression [157]. In this

context, studies have demonstrated that the expression of the microRNAs mir-7 and mir29b/c, which inhibit Murf1 expression, is downregulated in DM1 muscle [219, 220]. Overall, these studies suggest that perturbations in key metabolic pathways, such as autophagy, are likely to contribute to DM1 muscle pathology.

2. Problematic and Aims of the study

Over the last years, investigations in the DM1 field have delineated several pathological consequences arising from the toxic RNA-gain-of-function. Recently, deregulations in key cellular processes and signaling pathway have been shown to contribute to the pleiotropic nature of the disease. As DM1 affects primarily the neuromuscular system, investigations of the pathomechanisms contributing to muscle affliction are of major importance. In this study, I focused on evaluating potential alterations of muscle synapses, *i.e*. the neuromuscular junctions (NMJs), in DM1 muscle, and investigated whether changes in processes involved in their maintenance are affected. Although NMJ alterations have been observed before in DM1 muscle and mouse models, the causative mechanisms and signaling pathways remain unknown.

Here, I focused on the potential contribution of the deregulation of CaMKIIs in NMJ deterioration. Previous studies have suggested 1) that CaMKIIs isoforms are mis-spliced in DM1 muscle, and 2) that they play an essential role in the maintenance of NMJs by indirectly regulating synaptic gene expression and promoting AChR recycling. CaMKIIs regulate synaptic gene expression by inhibiting myogenin activity and HDAC4 nuclear import. The group recently reported that mTORC1-mediated inhibition of PKB/Akt alters denervation-induced AChR turnover in an HDAC4-dependent manner. In parallel, another study in the group has demonstrated that the AMPK and mTORC1 signaling pathways are perturbed in DM1 muscle, which was accompanied by perturbations in autophagy. Interestingly, several reports have established that autophagy modulates NMJ remodeling by regulating AChR degradation and turnover. Based on these observations, we hypothesized that deregulation of AMPK and mTORC1, of the autophagy flux, and of CaMKII isoforms may alter AChR dynamics and thereby NMJ maintenance in DM1 muscle.

The overall goal of my PhD is hence to analyze the contribution of NMJ perturbation to DM1 pathogenesis and to identify mechanisms leading to these changes. Using and comparing two well-known mouse models for DM1, I hence aimed specifically 1) to delineate the extent of NMJ deterioration in DM1, and whether it arises from muscle perturbation; 2) to assess the response of DM1 muscle to nerve injury and remodeling at the NMJ; 3) to characterize the deregulation of CaMKIIs and evaluate its contribution to NMJ defects and muscle affliction.

3. Results

3.1 Project 1

3.1.1 Manuscript

The following version of the manuscript will be soon submitted.

CaMKII deregulation and changes in neuromuscular junctions in Type I Myotonic Dystrophy

Denis Falcetta[1,2], Marine Théodore[1], Shuo Lin[2], Lionel Tintignac[1], Jochen Kinter[1], Markus A. Rüegg[2], Michael Sinnreich[1], Perrine Castets[3]

1. Neuromuscular centre, Department of Biomedicine, University Hospital Basel, Klingelbergstrasse 50/70, CH-4056 Basel, Switzerland
2. Biozentrum, University of Basel, Klingelbergstrasse 50/70, CH-4056 Basel, Switzerland
3. Department of Cell Physiology and Metabolism, Faculty of Medicine, University of Geneva, 1 rue Michel Servet, CH-1211 Geneva, Switzerland

* Corresponding author: Perrine Castets, perrine.castets@unige.ch, +41 22 379 52 35

Abstract

Myotonic Dystrophy type I (DM1) is a multisystemic neuromuscular disorder, which constitutes the most common form of muscular dystrophy in adults. Previous reports have suggested that neuromuscular junctions (NMJ) deteriorates in skeletal muscle in DM1. However, the underlying pathomechanisms and its contribution to muscle affliction remain unknown. Here, we compare changes in NMJ and activity-dependent signalling in HSA^{LR} and $Mbnl1^{\Delta 3/\Delta 3}$ knockout mice, two well-known mouse models for DM1. Both models display increased fragmentation of motor endplate, associated with high turnover of acetylcholine receptors (AChR) and increased expression of synaptic genes. These changes correlate with the loss of the muscle-specific isoform of Ca^{2+}/calmoduline-dependent kinase protein II (CaMKII) in DM1 muscle. Upon nerve injury, AChR turnover further increases in DM1 muscle, despite defective synaptic gene up-regulation. Our study points to CaMKII-dependent and -independent mechanisms, which compromise NMJ maintenance and thereby muscle function in DM1.

Introduction

Myotonic Dystrophy type I (DM1) is caused by a (CTG)n repeat expansion located in the 3'UTR of the *DMPK* (*Dystrophia Myotonica Protein Kinase*) gene, leading beyond other symptoms, to muscle wasting, weakness and inability to relax (*myotonia*) [141, 143]. RNA-hairpins formed by the abnormal transcribed (CUG)n repeats lead to the sequestration of splicing factors. The consecutive mis-splicing of specific genes, like the *CLCN1* gene encoding the chloride channel ClC-1, is determinant in the pathogenesis of DM1-associated muscle alterations [167, 170]. Similarly, mis-splicing of several genes encoding proteins of Ca^{2+}-associated signalling pathways have been identified and shown to contribute to muscle affliction. Especially, we and others previously suggested that mis-splicing of *CAMK2* genes, encoding Ca2+/calmodulin-dependent kinase II (CaMKII) proteins, is a hallmark of DM1 [199, 216, 221]. However, the functional consequences of CAMKII deregulation in skeletal muscle and its contribution to DM1 pathogenesis remain largely unknown.

CaMKIIs are determinant for the maintenance of the neuromuscular junctions (NMJ), the chemical synapses connecting motor neurons to muscle fibres. Previous reports showed that CaMKIIs promote the recycling of the acetylcholine receptors (AChR) upon their internalization in the sub-synaptic regions of the muscle fibres (*i.e.* the motor endplate) [77]. Moreover, CaMKIIs contribute to the repression of synaptic genes in non-synaptic regions of innervated muscle, by inhibiting the myogenic factor myogenin and the histone deacetylase (HDAC) 4 [86, 222, 223]. Hence, functional deficiency in specific CaMKII isoforms may affect NMJ maintenance, by altering the expression pattern and the dynamics of synaptic proteins.

Early studies pointed to NMJ-associated abnormalities, such as multiple, enlarged endplates or angular muscle fibres in DM1 muscle biopsies [224-227]. The lack of denervation markers, such as non-junctional AChR clusters, rejected the idea of important denervation process as part of DM1 pathomechanisms [228]. Interestingly, NMJ alterations have been reported in DMSXL mice and *Mbnl1; Mbnl2* compounds knockout mice, two mouse models for DM1, as well as in C. *elegans* DM1 mutant [161, 229]. Moreover, nuclear foci, characteristic of DM1-associated accumulation of toxic RNA, were detected in sub-synaptic nuclei, which may locally alter the expression of synaptic genes [230]. Hence, whether and how NMJ deteriorate in DM1 muscle, and its contribution to muscle pathology, remain ill-known.

Here, we analysed and compared changes in NMJ and activity-dependent signalling in HSA^{LR} and $Mbnl1^{\Delta 3/\Delta 3}$ mice, two DM1 mouse models. Results obtained in these models provide insights on DM1-associated muscle perturbations affecting NMJ maintenance. Both mouse models show endplate fragmentation, associated with slight increase in AChR turnover and synaptic gene expression. Extensive characterization of CaMKIIs reveals a predominant loss of the muscle-specific isoform of CaMKIIβ (CaMKIIβM), which may affect activity-dependent pathways, such as HDAC4, as well as AChR recycling. Interestingly, DM1 muscle also responds abnormally to nerve injury, with a defective

up-regulation of synaptic genes. Hence, DM1 triggers NMJ deterioration, which may involve CaMKII deregulation and contribute to muscle affliction in patients.

Results

Mbnl1$^{\Delta 3/\Delta 3}$ and *HSA*^{LR} mice show similar DM1 muscle phenotype

To evaluate NMJ changes in DM1, we selected the *Mbnl1*$^{\Delta 3/\Delta 3}$ and *HSA*^{LR} mouse lines, two mildly affected DM1 models, in order to limit the effect of muscle alterations on NMJs and to delineate the contribution of post-synaptic signalling perturbation (*i.e.* in the muscle) to the defects. *Mbnl1*$^{\Delta 3/\Delta 3}$ are depleted for *Mbnl1* exon 3, leading to ubiquitous depletion of the splicing factor MBNL1 (*i.e.* including muscle and motor neurons; MBNL1, *Muscleblind-like protein 1*) [173]. In contrast, *HSA*^{LR} mice express an *HSA* transcript with long (CTG)n repeats only in skeletal muscle [153]. To assess the potential impact of muscle affliction on NMJ changes, we first compared muscle phenotype in both models. There was no dystrophic sign in muscle from 3-months-old mutant mice (Figure 1A, B), as previously reported [153, 173]. Dystrophic signs remain mild in 9- and 12-months-old *Mbnl1*$^{\Delta 3/\Delta 3}$ and *HSA*^{LR} mice, respectively (Figure 1A, B). Alterations, such as internalized nuclei, vacuoles and degenerated fibres, were present in *Mbnl1*$^{\Delta 3/\Delta 3}$ muscle and in the *gastrocnemius* muscle from *HSA*^{LR} mice. In contrast, alterations were sparse in *tibialis anterior* (TA) and *extensor digitorum longus* (EDL) muscles from *HSA*^{LR} mice (Figure 1A, B). Both *Mbnl1*$^{\Delta 3/\Delta 3}$ and *HSA*^{LR} muscles display myotonic phenotype, as shown by the increased late relaxation time of EDL muscle after *ex vivo* tetanic stimulation (Figure 1C-E). In contrast, specific muscle force (sP0) was not affected in 3-month-old mutant mice (Figure F, G), consistent with previous reports showing late onset of muscle weakness in these models [153, 173]. To evaluate DM1-associated mis-splicing, we then quantified the inclusion of exons 7a and 22 of the *Clcn1* and *Atp2a2* genes, encoding ClC-1 channel and SERCA (*Sarco/Endoplasmic Reticulum* Ca^{2+}*-ATPase*) pump, respectively. Inclusion of *Clcn1* exon 7a was strongly increased in *Mbnl1*$^{\Delta E3/\Delta E3}$ muscle, and accompanied by major reduction in total transcript levels of *Clcn1* (Figure 1H, I). *Clcn1* mis-splicing and down-regulation were comparable in *gastrocnemius* muscle from *HSA*^{LR} mice (Figure 1J, K). In contrast, as for muscle phenotype, TA muscle from *HSA*^{LR} mice showed milder changes in *Clcn1* splicing and no reduction in the overall expression of *Clcn1* transcripts (Figure 1J, K). Similarly, abnormal exclusion of *Atp2a1* exon 22 was more pronounced in *gastrocnemius* muscle, than in TA muscle, in *HSA*^{LR} mice (Figure 1L), with no changes in total *Atp2a1* expression (Figure 1M). These results confirm that both mouse models display mild muscle alterations, with close DM1-associated phenotype in *Mbnl1*$^{\Delta 3/\Delta 3}$ muscle and *HSA*^{LR} *gastrocnemius* muscles, and milder changes in TA/EDL muscles from *HSA*^{LR} mice.

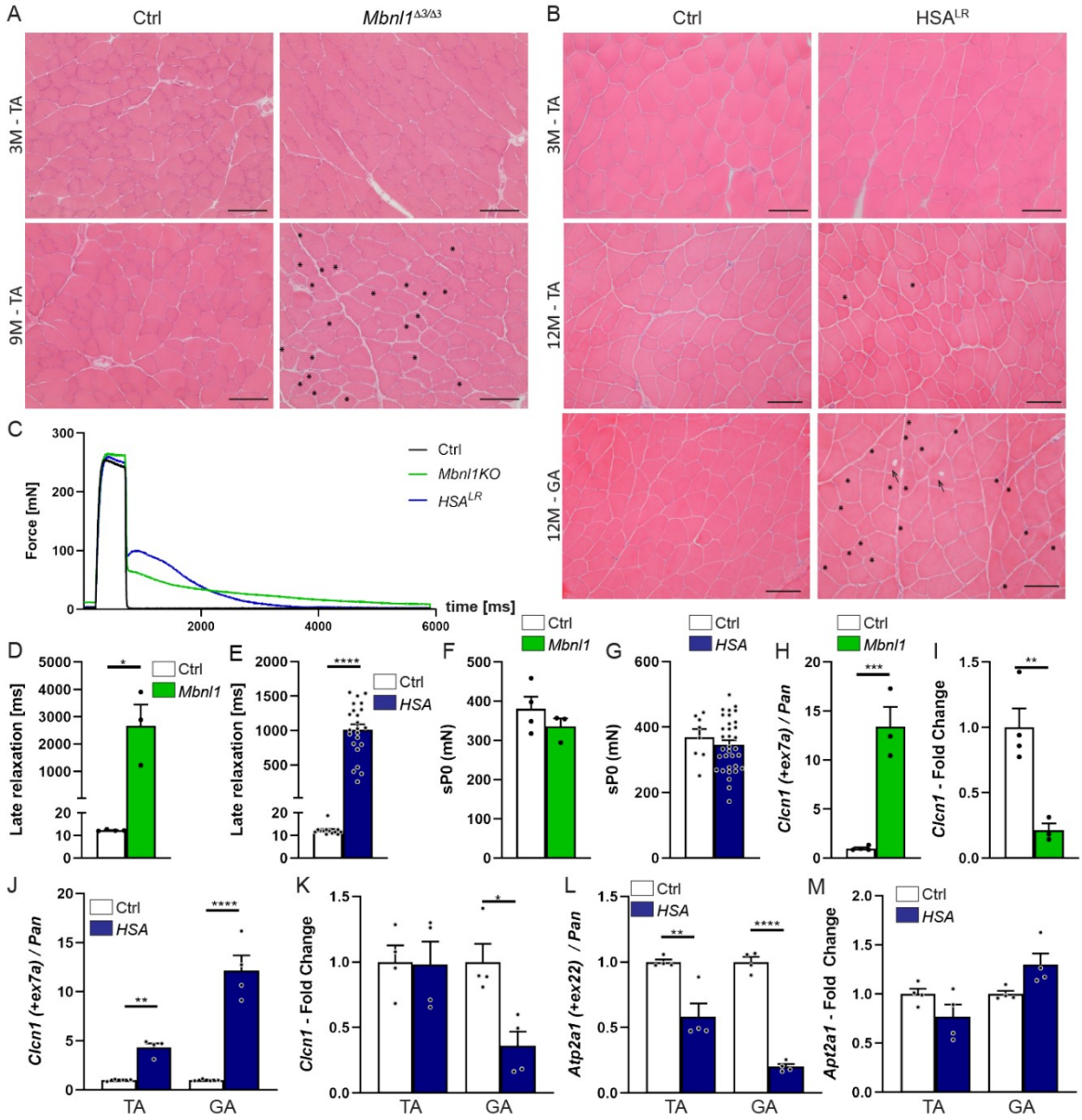

Figure 1: Muscle affliction in *Mbnl1*$^{\Delta 3/\Delta 3}$ and *HSA*^{LR} mice.

A,B) H&E coloration reveals limited histopathologic alterations in muscles from 3- and 9-month-old *Mbnl1*$^{\Delta 3/\Delta 3}$ and *HSA*^{LR} mice. Asterisks and arrows point to internalized nuclei and vacuoles, respectively. Scale bar, 100 µm. C-E) Late relaxation time upon stimulation is increased in EDL muscle from 3-month-old *Mbnl1*$^{\Delta 3/\Delta 3}$ (C,D) and *HSA*^{LR} (C,E), as compared to control mice. n = 4 Ctrl / 3 KO (D); 13 Ctrl / 23 HSA (E). F, G) Specific tetanic force (sP0) of EDL muscle is unchanged in 3-month-old *Mbnl1*$^{\Delta 3/\Delta 3}$ (F, n = 4 Ctrl / 3 KO) and *HSA*^{LR} (G, n= 8 Ctrl / 33 HSA). H-K) Quantitative PCR reveals reduction in exon 7a inclusion of the *Clcn1* gene (H, J) and in its total expression (I, K) in TA muscle from *Mbnl1*$^{\Delta 3/\Delta 3}$ mice (H, I) and gastrocnemius muscle from *HSA*^{LR} mice (J, K). Milder changes are observed in TA from *HSA*^{LR} mice (J, K). n = 4 Ctrl / 3 KO (H, I); 4 Ctrl / 4 HSA (J,K). L, M) Quantitative PCR analysis of the splicing (inclusion of exon 22; L) and of the total expression (M) of the *Atp2a1* gene in TA and *gastrocnemius* muscles from *HSA*^{LR} mice (n=4 Ctrl / 4HSA). Expression of spliced variants is normalised on total expression. Total expression is normalized on *Tbp* expression. In all panels, data represent mean ± SEM. *p<0.05, **p<0.01, ***p<0.001, ****p<0.0001, unpaired 2-tailed Student's t test.

NMJs deteriorate in *Mbnl1*$^{\Delta 3/\Delta 3}$ and *HSA*^{LR} mice

We next analysed NMJ structures in EDL, TA and *gastrocnemius* muscles from 3-month-old and 9- or 12-month-old *Mbnl1*$^{\Delta 3/\Delta 3}$ and *HSA*^{LR} mice. Pre- and post-synaptic compartments were stained with antibodies against neurofilament/synaptophysin and with α-bungarotoxin (Btx), which binds specifically to AChRs, respectively. The overall organization of the NMJs was preserved in mutant mice (Figure 2A, B). In particular, denervated motor endplate, abnormal axonal termination and extra-synaptic clusters of AChRs were rarely observed in mutant muscle, as in control muscle (*data not shown*). There was also no major defect in the distribution of sub-synaptic nuclei (Figure 2A, B). However, the number of fragments forming the motor endplate was increased in muscle from both 3- and 9-month-old *Mbnl1*$^{\Delta 3/\Delta 3}$ mice, compared to age-matched controls (Figure 2C). Interestingly, a similar increase in endplate fragmentation was observed in *HSA*^{LR} mice, including both the affected *gastrocnemius* and spared TA/EDL muscles (Figure 2D). As the *HSA*^{LR} transgene is not expressed in nerve in *HSA*^{LR} mice, the results suggest that post-synaptic (*i.e.* muscle) perturbations contribute to NMJ deterioration. Moreover, it is unlikely that the increased endplate fragmentation was caused by the limited degeneration/regeneration ongoing in mutant muscle, especially at 3 months of age.

DM1 muscle shows major deficiency for CaMKIIβM

As CaMKIIs have been shown to contribute to the regulation of the expression and the recycling of AChRs [77], we hypothesized that NMJ deterioration in DM1 muscle may arise from CaMKII deficiency. Indeed, we recently reported that the expression pattern of CaMKIIβ and γ/δ proteins is altered in *HSA*^{LR} muscle [216]. We confirmed by Western Blot that the expression of the muscle-specific isoform of CaMKIIβ (*i.e.* CaMKIIβM), is drastically reduced in *HSA*^{LR} *gastrocnemius* muscle (Figure 3A, B). Moreover, abnormal pattern around the size of CaMKIIγ/δ suggested the expression of alternative CaMKII isoforms in mutant muscle (Figure 3A). Levels of phospho-CaMKIIβM (Ser286), as compared to total CaMKIIβM, were reduced, suggesting that auto-phosphorylation, and therefore activity, of CaMKIIβM is reduced in *HSA*^{LR} muscle (Figure 3C). Interestingly, CaMKIIs showed very similar expression pattern in *Mbnl1*$^{\Delta 3/\Delta 3}$ muscle (Figure 3D), with drastic reduction in CaMKIIβM levels (Figure 3E) and decrease in its auto-phosphorylation (Figure 3F). To identify the different isoforms expressed in DM1 muscle and the predominant regions of mis-splicing in the genes *Camk2b, 2g* and *2d*, we took advantage of RNA-seq results obtained in *HSA*^{LR} *gastrocnemius* muscle. Based on the reads, we compared splicing events occurring in *Camk2* genes in *HSA*^{LR} and control muscles. In *Camk2b*, exclusion of the exon 13 and of the exons 18 to 20 was strongly increased in *HSA*^{LR} muscle, compared to control (Supplementary Figure 1A, B). We confirmed the exclusion of *Camk2b* exon 13 in *HSA*^{LR} muscle with PCR and sequencing of the amplicons (Supplementary Figure 1C, D). Moreover, the product including exons 18 to 20, encoding the variable inserts A, B and C of CaMKIIβM, was not detected in *HSA*^{LR} muscle (Supplementary Figure 1D).

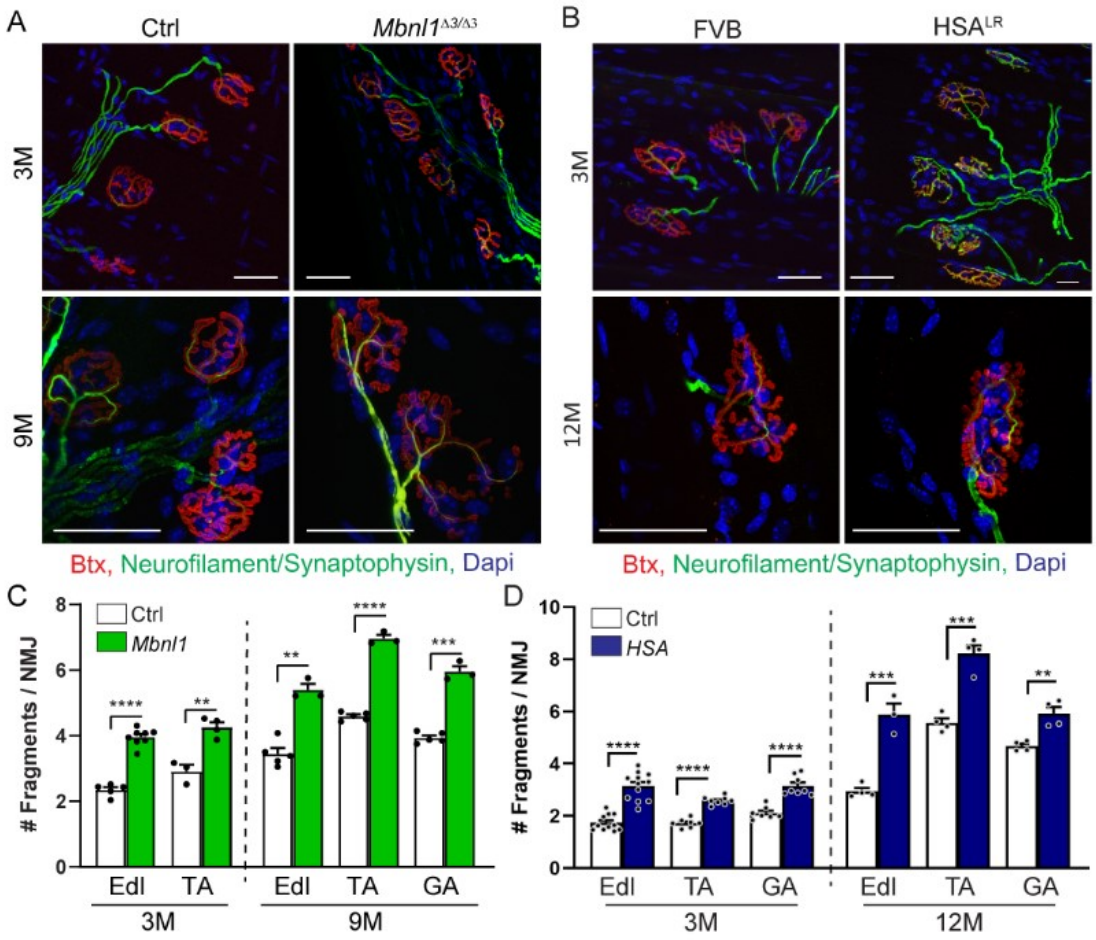

Figure 2: Altered NMJ maintenance in *Mbnl1*$^{\Delta E3/\Delta E3}$ and *HSA*^{LR} mice.

A,B) Fluorescent images of innervated muscle from 3- and 9-month-old *Mbnl1*$^{\Delta 3/\Delta 3}$ mice (A) and 3-and 12-month-old *HSA*^{LR} mice (B), showing NMJ regions stained with Dapi (blue), α-bungarotoxin (red) and antibodies against Neurofilament/Synaptophysin (green). Scale bar, 50 µm. C, D) Quantification of the number of fragments per NMJ in EDL, TA and *gastrocnemius* muscles from 3- and 9/12-month-old *Mbnl1*$^{\Delta 3/\Delta 3}$ (C) and *HSA*^{LR} (D) mice. n=5/8 (EDL 3M), 3/4 (TA 3M), 5/3 (all muscles 9M) Ctrl/KO (C); 11/12 (EDL 3M), 7/8 (TA 3M), 7/8 (GA 3M), 4/3 (EDL 12M), 4/4 (TA and GA 12M) Ctrl/HSA (D). Data represent mean ± SEM. **p<0.01, ***p<0.001, ****p<0.0001, unpaired 2-tailed Student's t test.

For *Camk2g*, the main changes detected with RNA-seq results corresponded to the increased inclusion of the exons 13, 15 and 19 in HSA^{LR} muscle (Supplementary Figure 1E, F). Of note, exons 15/19 are usually referred to as exons 14/18 because of the very low inclusion of exon 13. Sequencing of the products obtained by amplifying the region from exons 14 to 21, confirmed the increased inclusion of exons 15 and 19 in HSA^{LR} muscle (Supplementary Figure 1G). In contrast, RNA-seq and sequencing of amplicons failed to identify major splicing changes in *Camk2d* between HSA^{LR} and control muscles (*data not shown*).

As CaMKIIβM was predominantly perturbed in HSA^{LR} muscle, we further quantified splicing changes affecting the expression of *Camk2b* by qPCR. Exclusion of exon 13 was 4 times increased (Figure 3G) and inclusion of exons 18 to 20 was reduced by half (Figure 1H) in *gastrocnemius* muscle from HSA^{LR} mice, compared to controls. Similar extent of mis-splicing was found in the less affected TA and EDL muscles (Figure 3G, H). Moreover, there was a significant increase in total *Camk2b* expression in all three muscles from HSA^{LR} mice, compared to controls (Figure 3I). Interestingly, inclusion of exons 13 and 18-20 was strongly reduced in $Mbnl1^{\Delta 3/\Delta 3}$ muscle (Figure 3J, K). This was also accompanied by increased levels of total *Camk2b* transcripts in mutant muscle (Figure 3L). Together, these results indicate that changes in MBNL1-dependent splicing of *Camk2b* strongly alter the expression of CaMKIIβ isoforms, leading to the loss of the muscle-specific variant in DM1 muscle.

Expression and dynamics of AChRs are perturbed in DM1 mice

CaMKIIs contributes to NMJ maintenance, by regulating AChR dynamics at the motor endplate [77]. To get further insights on the mechanisms underlying NMJ deterioration in DM1 muscle, we measured the turnover of AChRs, by double labelling "old" stable and newly formed receptors with two sequentially injected fluorescent Btx [231, 232]. The assay could be applied to TA and EDL muscles, only. Interestingly, AChR turnover was higher in both EDL and TA muscles from 3-month-old $Mbnl1^{\Delta 3/\Delta 3}$ mice, as compared to controls (Figure 4A, B). Turnover tended to increase in HSA^{LR} muscle, as well, even though higher variability and milder changes were observed as compared to $Mbnl1^{\Delta 3/\Delta 3}$ mice (Figure 4C, D). As CaMKIIs promote AChR recycling at the endplate [77], we further evaluated AChR recycling at the sarcolemma of DM1 muscle. To this end, we labelled AChRs present at the sarcolemma at t0 with Btx-Biotin and saturated biotin sites with Streptavidin-Alexa647; three days later, recycled AChRs (bound to free Btx-Biotin – StreptavidinA647 released after the internalization of the receptors) were labelled by adding saturating doses of Streptavidin-Alexa555 [74]. We then compared the population of recycled receptors (pixels positive for A555) to the population of all receptors labelled with Btx-Biotin (pixels labelled with A555 or A647). In these conditions, the proportion of recycled AChRs tends to decrease in muscle from $Mbnl1^{\Delta 3/\Delta 3}$ mice, as compared to controls (Figure 4E, F). Together, these results suggest that AChR turnover is affected at NMJs in DM1 muscle, which may involve perturbation in CaMKII-dependent recycling of the receptors.

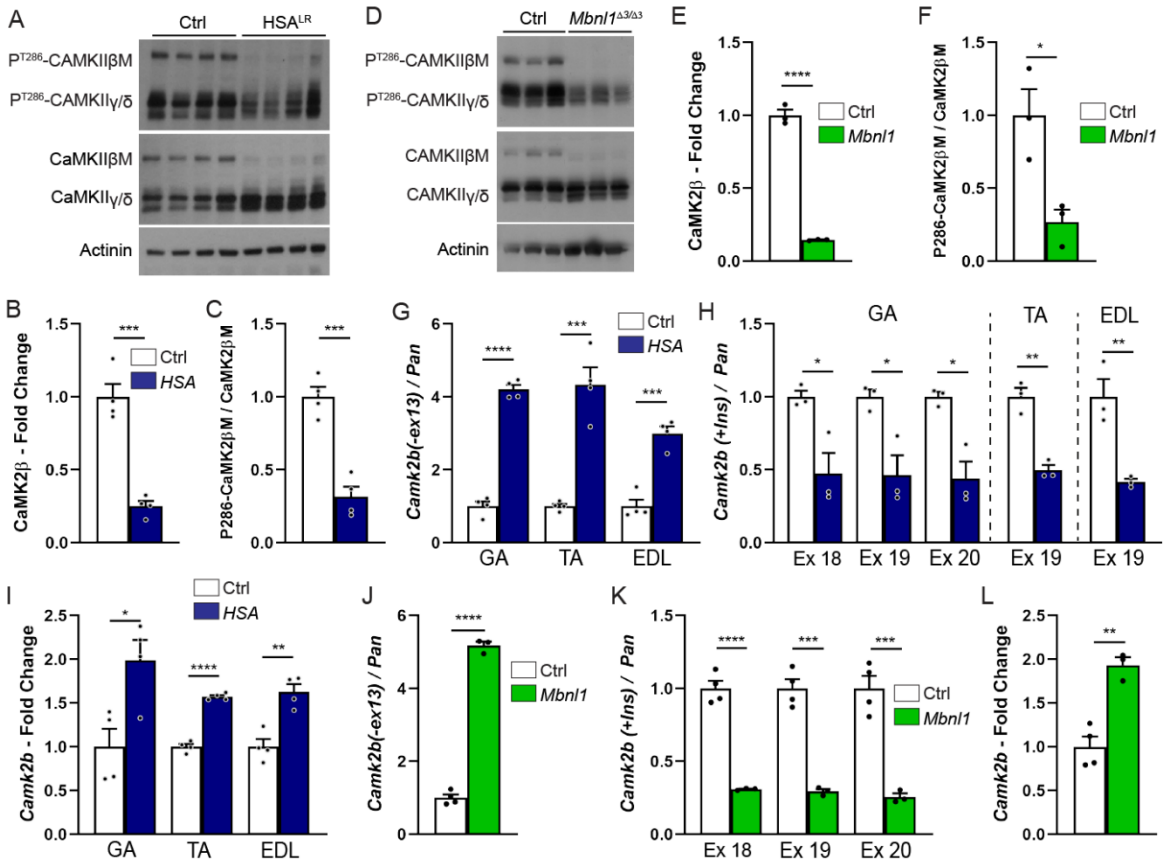

Figure 3: CaMKIIβ deregulation in *Mbnl1*$^{\Delta 3/\Delta 3}$ and *HSA*^{LR} muscles.

A-C) Western blot analysis of CaMKII isoforms in *gastrocnemius* muscle from 3-month-old control and *HSA*^{LR} mice. Quantification of CaMKIIβM levels and of its phosphorylated form is shown in B and C; normalization is made on α-actinin (B) or on total CaMKIIβM (C), relative to control. n=4 per group. D-F) Western blot analysis of CaMKII isoforms in TA muscle from 3-month-old control and *Mbnl1*$^{\Delta 3/\Delta 3}$ mice. Quantification of CaMKIIβM levels and of its phosphorylated form is shown in E and F; normalization is made on α-actinin (E) or on total CaMKIIβM (F), relative to control. n=3 per group. G-I) qPCR analysis of the exclusion of exon 13 (G, n=4 per group), of the inclusion of exons 18-20 (H, n=3 per group), and of total levels of *Camk2b* (I, n=4 per group) in *gastrocnemius*, TA and EDL muscles from *HSA*^{LR} and control mice. Data are normalized on levels of total *Camk2b* transcripts (G, H) or of *Tbp* (I). J-L) qPCR analysis of the exclusion of exon 13 (J), of the inclusion of exons 18-20 (K), and of total levels of *Camk2b* (L) in TA muscle from *Mbnl1*$^{\Delta 3/\Delta 3}$ and control mice. n = 4 Ctrl / 3 KO. Data are normalized on levels of total *Camk2b* transcripts (J, K) or of *Tbp* (L). All data are mean±sem; * p<0.05; ** p<0.01; **** p<0.0001; two-tailed unpaired Student's t-test.

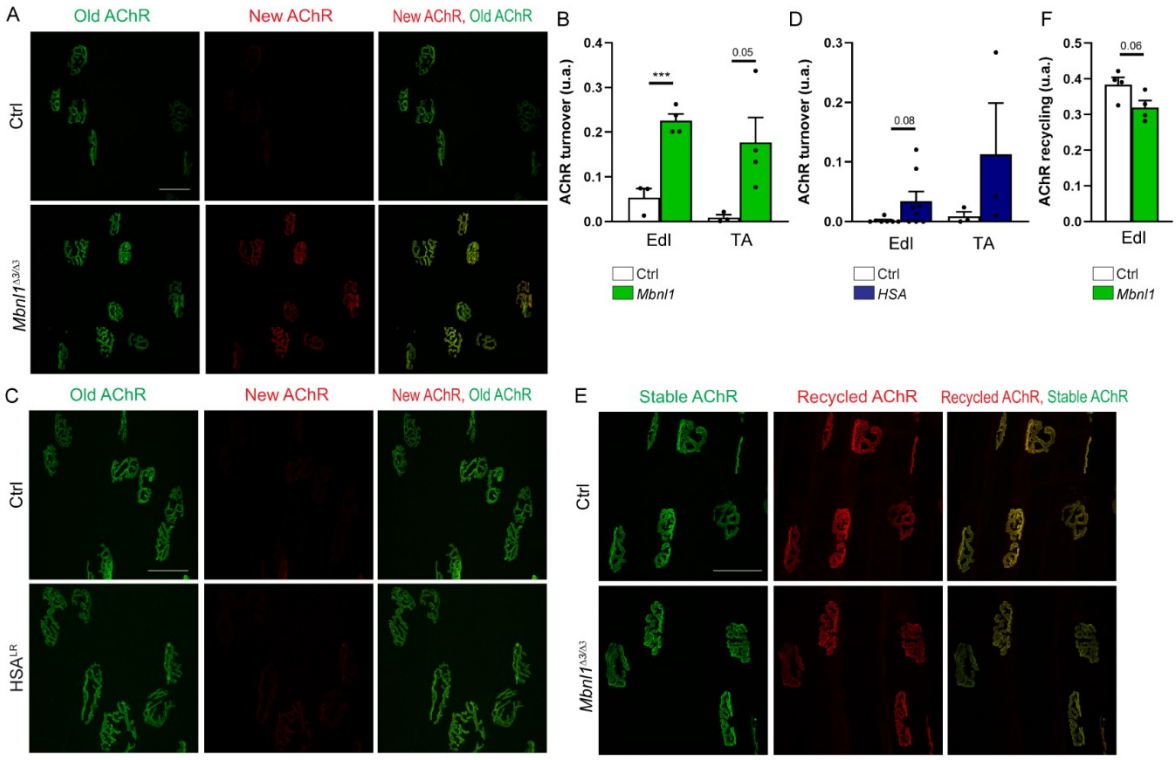

Figure 4: Abnormal AChR dynamics in *Mbnl1*$^{\Delta 3/\Delta 3}$ and *HSA*^{LR} muscles.
A-D) Turnover assay in EDL and TA muscles from *Mbnl1*$^{\Delta 3/\Delta 3}$ and *HSA*^{LR} mice. Fluorescent images show "old" (green) and "new" (red) AChRs in control and *Mbnl1*$^{\Delta 3/\Delta 3}$ (A) and *HSA*^{LR} (C) innervated muscles. Scale bar, 50 µm. Quantification for *Mbnl1*$^{\Delta 3/\Delta 3}$ and *HSA*^{LR} muscles is given in B and D, respectively. n = 3/4 Ctrl/KO (B); 7/8 (EDL) and 3/3 (TA) Ctrl/*HSA*^{LR} (D). E, F) Recycling assay in EDL muscle from *Mbnl1*$^{\Delta 3/\Delta 3}$ mice. Fluorescent images show "stable" (green) and "recycled" (red) AChRs in control and *Mbnl1*$^{\Delta 3/\Delta 3}$ (E) innervated muscles. Scale bar, 50 µm. Quantification is given in F. n = 4 per group (F). Data are mean±sem; *** p<0.001; two-tailed unpaired Student's t-test.

HDAC4 signalling and synaptic gene expression are perturbed in DM1 muscle

As AChR turnover integrates both the fate of the receptors upon internalization (*i.e.* degradation or recycling), and the rate of insertion of new receptors at the sarcolemma, we next considered potential changes in the synthesis of AChRs. CaMKII deficiency may perturb synaptic gene expression, by affecting the activity of histone deacetylases (HDACs), such as HDAC4 [222, 233]. Transcript levels of *Chrna1,* encoding the AChR subunit α, were increased in $Mbnl1^{\Delta 3/\Delta 3}$ muscle (Figure 5A), and in *gastrocnemius* from HSA^{LR} mice (Figure 5B). In contrast, they were unchanged in EDL and TA muscles from HSA^{LR} mice, as compared to controls (Figure 5B). Interestingly, protein levels of HDAC4 tend to increase in muscle of 3-month-old $Mbnl1^{\Delta 3/\Delta 3}$ mice, as compared to controls (Figure 5C, D). In contrast, CaMKII-dependent phosphorylation of HDAC4 (Ser632) remained largely unchanged in mutant muscle (Figure 5E). Interestingly, there was a marked accumulation of HDAC4 in muscle from HSA^{LR} mice (Figure 5F, G). In this case, however, CaMKII-dependent phosphorylation of HDAC4 tended to decrease in mutant muscle, as compared to control (Figure 5H). Consistent with a reduced inhibition of HDAC4 by CaMKIIs, HDAC4 levels were increased in the nuclear fraction of the *gastrocnemius* muscle of HSA^{LR} mice, compared to controls (Figure 5I, J). Notwithstanding, HDAC4 remained barely detectable by immunostaining in muscle from HSA^{LR} mice, as observed for control mice (Figure 5K). In parallel, transcriptional expression of *Hdac4* and *Myog,* two activity-dependent genes indirectly promoted by HDAC4, was unchanged in both *gastrocnemius* (Figure 5L) and TA (Figure 5M) muscles from HSA^{LR} mice. Moreover, transcript levels of direct, repressed targets of HDAC4, *Dach2* and *Mitr* (alternative spliced isoform of HDAC9), were similar in HSA^{LR} and control muscles (Figure 5L, M). This was consistent with the detection of similar levels of acetylated histone H3 in HSA^{LR} and control muscles (Figure 5J). Interestingly, expression of *Myog, Hdac4* and *Dach2* was also unchanged in $Mbnl1^{\Delta 3/\Delta 3}$ muscle. Moreover, despite increased HDAC4 levels, *Mitr* transcript levels were slightly increased in mutant muscle (Figure 5N). Hence, although CaMKII deficiency may promote the accumulation of HDAC4 in DM1 muscle, it is unlikely that HDAC4 is responsible for the up-regulation of synaptic gene expression in DM1 muscle.

Muscle response to denervation is affected in $Mbnl1^{\Delta 3/\Delta 3}$ mice

To understand the mechanisms underlying NMJ deterioration in DM1 context, we challenged 3-month-old $Mbnl1^{\Delta 3/\Delta 3}$ and HSA^{LR} mice by cutting the sciatic nerve to obtain a complete denervation of hind limb muscles. Endplate remodelling upon denervation is dependent on the induction of activity-dependent signalling, such as HDAC4 that allows the up-regulation of synaptic genes throughout the fibre [223, 233]. After 3 weeks of denervation, the loss of muscle mass was significantly less in $Mbnl1^{\Delta 3/\Delta 3}$ mice, as compared to control mice (Figure 6A). In parallel, endplate fragmentation increased and remained higher in $Mbnl1^{\Delta 3/\Delta 3}$ EDL and TA muscles, as compared to controls (Figure 6B, C). To further assess endplate remodelling in denervated conditions, we quantified AChR turnover by labelling "old" receptors at 5 days post nerve injury and assessing their turnover 10 days later.

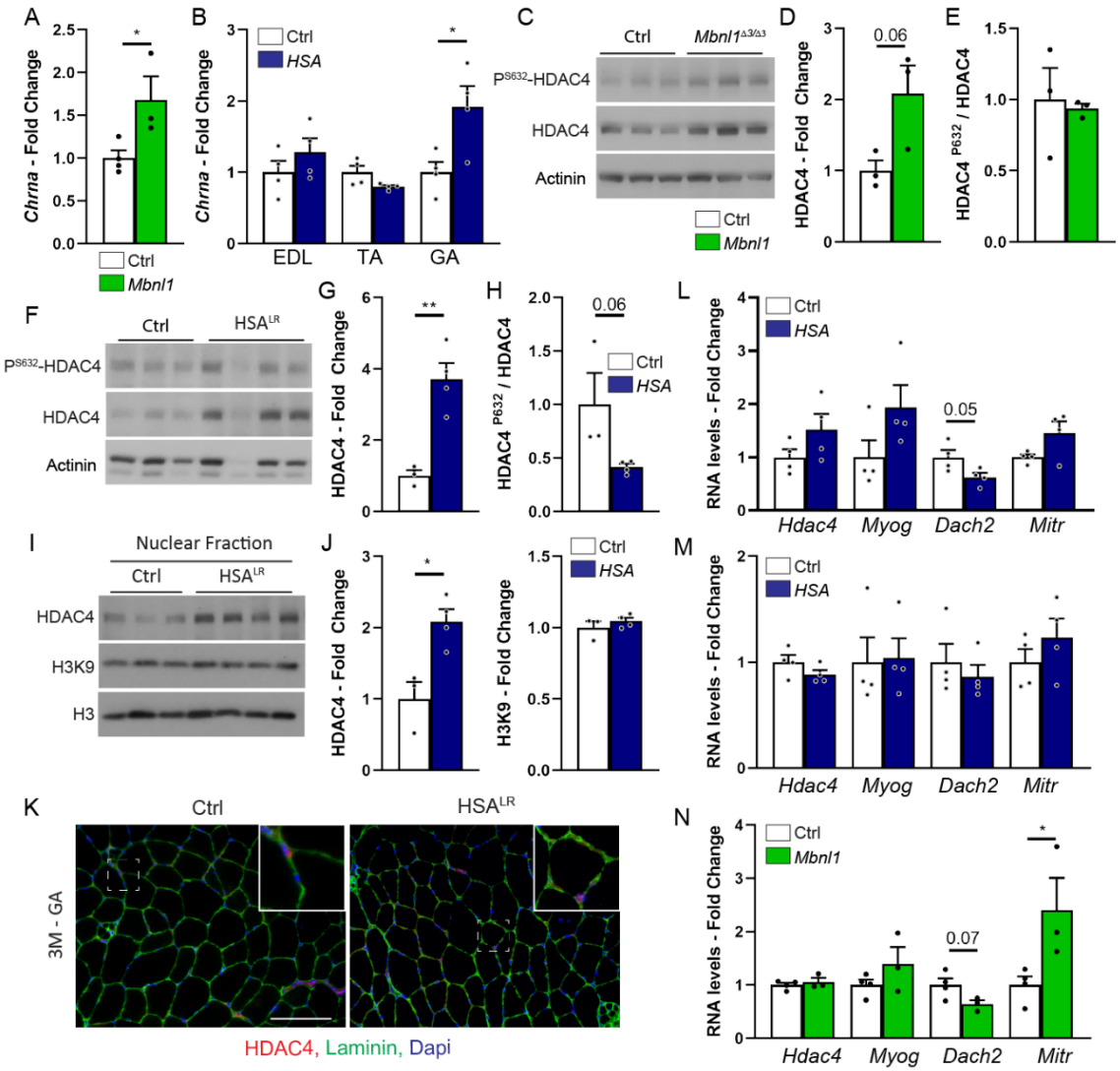

Figure 5: Changes in HDAC4 levels and synaptic gene expression in DM1 muscles.
A,B) Quantitative PCR analysis of *Chrna1* in TA from 3-month-old *Mbnl1*$^{\Delta E3/\Delta E3}$mice (A) and EDL, TA and *gastrocnemius* muscles from 3-month-old *HSA*^{LR} mice (B). Levels are normalized to *Tbp*. n=4/3 Ctrl/KO (A); 4/4 Ctrl/HSA (B). C-H) Western blot analysis of HDAC4 and its phosphorylated form (Ser632) in total protein lysate of TA muscle from *Mbnl1*$^{\Delta E3/\Delta E3}$mice (C) and *HSA*^{LR} mice (F). Quantification of total and phosphorylated levels is given in (D, E) for *Mbnl1*$^{\Delta 3/\Delta 3}$ muscle and (G, H) for *HSA*^{LR} muscle. Total and phosphorylated levels are normalized to α-actinin and total HDAC4, respectively, and relative to control. n = 3 per group (D,E) and 3/4 Ctrl/HSA (G,H). I, J) Western blot analysis of HDAC4 and acetylated histone (H3K9) in nuclear fraction of *gastrocnemius* muscle from control and *HSA*^{LR} mice. Quantification of HDAC4 and H3K9 is given in J. Levels are normalized to histone H3 and relative to control. n = 3/4 Ctrl/HSA (J). K) Fluorescent image of control and *HSA*^{LR} muscles with antibodies against HDAC4 (red), Laminin (green) and Dapi (blue). Scale bar, 100 µm. Higher magnification panel shows HDAC4-positive myonuclei. L-N) qPCR analysis of activity-dependent genes, *i.e. Hdac4, Myog, Dach2* and *Mitr*, in *gastrocnemius* (L) and TA (M) from *HSA*^{LR} mice, and in TA from *Mbnl1*$^{\Delta 3/\Delta 3}$ mice (N). Transcript levels are normalized to *Tbp* and relative to control. n = 4 per group (L, M); 4/3 Ctrl/KO (N). Data are mean±sem; * p<0.05; two-tailed unpaired Student's t-test.

In control, the turnover of AChRs increased drastically upon denervation, as compared to innervated conditions (Figure 6D, E), as previously reported [234]. Importantly, AChR turnover strongly increased and remained higher in *Mbnl1*$^{-/-}$ muscle in denervated conditions, as compared to control denervated muscle (Figure 6D,E). These results indicate that the muscle response to denervation is perturbed in *Mbnl1*$^{\Delta 3/\Delta 3}$ mice, with an altered remodelling of the motor endplate.

To get insights on the response of *Mbnl1*$^{\Delta 3/\Delta 3}$ muscle to denervation, we analysed changes in activity-dependent signalling after 3 days of denervation. The loss of CaMKIIβM persisted upon denervation in *Mbnl1*$^{\Delta 3/\Delta 3}$ muscle (Figure 6F). In parallel, there was an efficient increase in protein levels of HDAC4 in denervated muscle from mutant mice (Figure 6F, G). Accordingly, expression of the direct downstream targets of HDAC4, *Dach2* and *Mitr*, was similarly repressed after denervation in *Mbnl1*$^{\Delta 3/\Delta 3}$ and control muscles (Figure 6H). In contrast and importantly, up-regulation of *Myog*, *Chrna1* and *Chrng (*encoding the AChR γ sub-unit) was hampered in *Mbnl1*$^{\Delta 3/\Delta 3}$ denervated muscle, compared to controls (Figure 6I). Together, these results point to abnormal regulation of the expression and dynamic of synaptic proteins in *Mbnl1*$^{\Delta 3/\Delta 3}$ mice, which may depend on CaMKII but not on HDAC4 deregulation after denervation.

Unexpectedly, we observed that *HSA*^{LR} mice lost the expression of the *HSA* transgene after 3 days denervation (Supplementary Figure 2A). Consistently, accumulation of ribonuclear foci and mis-splicing of *Clcn1* and *Camk2b* were reduced in denervated *HSA*^{LR} muscle, as compared to innervated muscle (Supplementary Figure 2B-D). Thus, analysis of muscle response in *HSA*^{LR} mice upon acute denervation was impossible, as down-regulation of the *HSA* promoter would likely hamper the defects detected in the transgenic line. Interestingly, after prolonged denervation (2-3 weeks), the accumulation of nuclear foci increased to levels similar to innervated muscle (Supplementary Figure 2B). Consistently, expression of the transgene was not significantly different from innervated levels, anymore, in EDL, TA and *gastrocnemius* muscles (Supplementary Figure 2E). Mis-splicing of *Clcn1* and *Camk2b* also turned back to innervated levels (Supplementary Figure 2F, G). In this context, we observed a resistance to denervation-induced atrophy, as in *Mbnl1*$^{\Delta 3/\Delta 3}$ mice (Supplementary Figure 2H). Fragmentation of motor endplates aggravated in *HSA*^{LR} muscle after 3 weeks denervation, and remained higher as compared to controls (Supplementary Figure 2I). Interestingly, after 3 weeks of denervation, transcript levels of *Myog* and *Chrna1*, but not of *Hdac4,* were lower in *gastrocnemius* from *HSA*^{LR} mice, compared to controls (Supplementary Figure 2J). In parallel, expression of *Mitr,* but not of *Dach2,* remained higher in the mutant muscle (Supplementary Figure 2K). In contrast, expression of activity-dependent genes in TA from *HSA*^{LR} mice was similar to controls (Supplementary Figure 2L, M). This confirmed that results obtained in *gastrocnemius* muscle from *HSA*^{LR} mice are closer to those obtained in *Mbnl1*$^{\Delta 3/\Delta 3}$ mice. Together, these results point to an incapacity of DM1 muscle to respond efficiently to nerve injury and to up-regulate synaptic gene expression after acute and prolonged denervation.

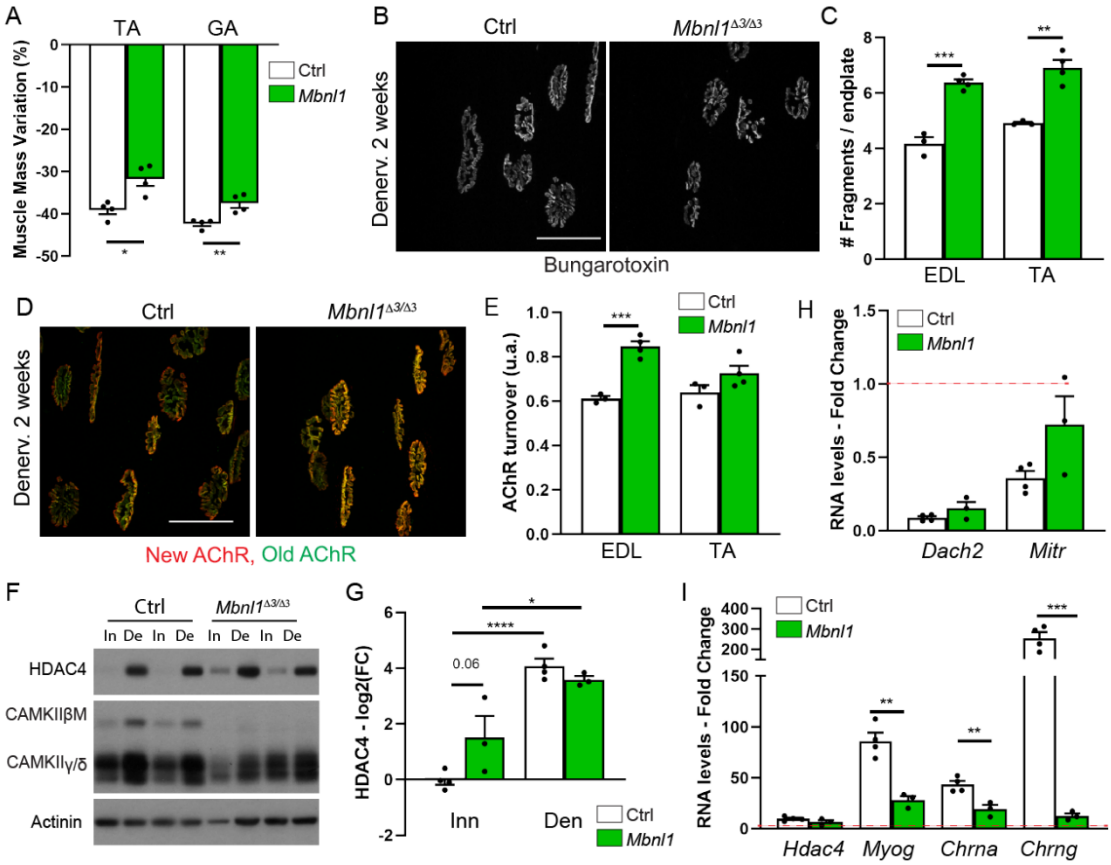

Figure 6: Abnormal response to denervation in *Mbnl1*$^{\Delta 3/\Delta 3}$ mice.

A) Mass variation after 3 weeks of denervation in control and *Mbnl1*$^{\Delta 3/\Delta 3}$ mice, for TA and *gastrocnemius* (GA) muscles. n = 4 per group. B, C) Fluorescent images of control and *Mbnl1*$^{\Delta 3/\Delta 3}$ muscles, after 3 weeks of denervation, showing motor endplates stained with α-bungarotoxin. Scale bar, 50 µm. Quantification of the fragmentation is given in C) for EDL and TA muscles. n = 3/4 Ctrl/KO. D, E) AChR turnover assay in denervated muscle from *Mbnl1*$^{\Delta 3/\Delta 3}$ and control mice. Fluorescent images showing "old" and "new" receptors are shown in (D). Scale bar, 50 µm. Quantification of AChR turnover is given in (E). n = 3/4 Ctrl/KO. F, G) Western blot analysis of HDAC4 and CaMKIIs, in innervated (In) and denervated (De, 3 days) muscles from control and *Mbnl1*$^{\Delta 3/\Delta 3}$ mice. n = 4/3 per group. Levels of HDAC4 are normalized to α-actinin, relative to control and expressed as the log2 (Fold Change) (G). H,I) Quantitative PCR analysis of activity-dependent genes, *i.e. Dach2 and Mitr* (H), *Hdac4, Myog, Chrna1* and *Chrng* (I), at 3 days post-denervation in TA muscle from control and *Mbnl1*$^{\Delta 3/\Delta 3}$ mice. Levels are normalized to *Tbp* and relative to control innervated. n=4 per group. Levels in the innervated control muscle are shown by the red dotted line. Data are mean±sem; ** p<0.01; *** p<0.001; two-tailed unpaired Student's t-test.

Discussion

One key process in DM1 pathogenesis is the mis-splicing of several genes in affected tissues, including skeletal muscle. However, how these changes lead to muscle alterations and myotonia remains unclear. NMJ alterations have been described in muscle biopsies from DM1 patients and in muscle from DM1 mouse models. However, it remains unknown what mechanisms underlie these perturbations and whether these defects arise from DM1-related changes in the muscle or nerve compartments. Here, we showed that NMJ are affected in *Mbnl1*$^{\Delta 3/\Delta 3}$ and *HSA*^{LR} mice, two well-known mouse models for DM1. We established that CaMKIIβ is strongly deregulated in *Mbnl1*$^{\Delta 3/\Delta 3}$ and *HSA*^{LR} muscles, which may contribute to changes in synaptic gene expression and AChR turnover observed in innervated mutant muscle. The response of DM1 muscle to denervation was also changed, with a defective up-regulation of synaptic genes, which may arise from CaMKII-independent mechanisms.

Signs of NMJ deterioration, without denervation of muscle fibres, have been reported in muscle biopsies from DM1 patients, as well as in DMSXL and *Mbnl1/2*-deficient mice [161, 224-227, 235]. As the nerve is also affected in these mouse models, the question whether the defects arise from pre- or post-synaptic perturbations was unsolved. Here, we found major endplate fragmentation in *Mbnl1*$^{\Delta 3/\Delta 3}$ and *HSA*^{LR} mice at different ages. Moreover, NMJ alterations were similar between TA/EDL and *gastrocnemius* muscles, which are affected differentially in *HSA*^{LR} mice. As *HSA*^{LR} mice express the transgene carrying the (CTG)n repeats only in muscle, we unveiled that DM1-associated perturbation in the post-synaptic compartment, *i.e.* muscle, contributes to NMJ deterioration. Although endplate fragmentation may not be a good indicator for impaired neurotransmission [236], it may still be a sign for NMJ deterioration and reduction in AChR density at endplates. Interestingly, recycling of AChRs tended to decrease in *Mbnl1*$^{\Delta 3/\Delta 3}$ muscle, which may contribute to increased AChR turnover. Indeed, upon internalization, receptors are directed for degradation or recycling. Reduced recycling may hence be accompanied by an increased degradation of the receptors, and thereby to their increased turnover. The limited up-regulation of synaptic genes detected in both DM1 mouse models may be an attempt to compensate for the increased degradation of AChRs. Insufficient up-regulation of these genes may actually lead to a reduced density of AChRs at the sarcolemma. Interestingly, NMJ alterations associated with increased turnover and decreased density of AChRs have been reported in other mouse models, such as α-syntrophin-deficient mice [237].

Seeking for pathomechanisms that may compromise NMJ integrity in DM1, we examined the potential role of CaMKII deregulation. Mis-splicing in *Camk2b, 2d* and *2g* has been reported in DM1 patients, as well as in mouse models [177, 198, 199, 221]. In particular, abnormal exclusion of *Camk2b* exon 13 appeared as one of the most important splicing changes detected in DM1 tissues. Although pathophysiological consequences have been investigated in the brain, the consequences of CaMKII deregulation in skeletal muscle have not yet been analysed. We here report for the first time that the three exons specifically included in the CaMKIIβ isoform expressed in muscle, are excluded in *Mbnl1*$^{\Delta 3/\Delta 3}$ and *HSA*^{LR} muscles. Together with the exon 13 and 16, exons 18-20 are part of the highly

variable region of the *Camk2b* gene, which allows the expression of tissue-specific variants. Consistent with the abnormal splicing of *Camk2b* in DM1 muscle, CaMKIIβM was not detected by Western blot in $Mbnl1^{\Delta 3/\Delta 3}$ and HSA^{LR} muscles. Studies on the specific functions of CaMKIIβM in skeletal muscle are missing. As previous reports suggested that CaMKIIβM is the only isoform accumulating at the NMJ, it may ensure the function, ascribed to CaMKIIs, in regulating AChR recycling [77]. Hence, CaMKIIβM deficiency is likely to hamper AChR recycling in DM1 muscle. Furthermore, CaMKIIs have also been shown to contribute to synaptic gene repression in non-synaptic region [86, 222, 233]. We thus hypothesized that increased synaptic gene expression in DM1 mice may arise from CaMKIIβM deficiency. By examining HDAC4 signalling, which is supposed to mediate part of the effect of CaMKIIs on synaptic gene expression, we failed to unveil obvious changes in the pathway. Indeed, although HDAC4 accumulated in DM1 muscle, there was no change in *Myog* expression, which is required for synaptic gene induction in non-synaptic regions. Hence, it is unlikely that CaMKII-dependent induction of HDAC4 contributes to synaptic gene up-regulation in DM1 muscle. Of note, expression of synaptic genes in the sub-synaptic region is not dependent on myogenin in innervated muscle. Changes detected in DM1 muscle may thus be related to stronger changes specifically at the motor endplate.

To get further insights on the capacity of DM1 muscle to regulate activity-dependent signalling and maintain their motor endplates, we challenged $Mbnl1^{\Delta 3/\Delta 3}$ and HSA^{LR} mice with nerve injury. Unexpectedly, transgene expression, associated to *HSA* promoter, was lost in HSA^{LR} muscle upon denervation, which limited the analysis. In this context, we established that AChR turnover is strongly increased in $Mbnl1^{\Delta 3/\Delta 3}$ muscle, which may arise from increased degradation of the receptors, as in innervated conditions. Contrasting with this efficient response to denervation, the up-regulation of synaptic genes was strongly reduced in DM1 muscle. Up-regulation of synaptic genes upon denervation relies on the inhibition of transcription repressors inhibiting *Myog* expression. In particular, induction of HDAC4 is supposed to repress the expression of MITR/HDAC9 and Dach2 [87, 223, 238]. Expression of these two repressors was efficiently reduced upon denervation in DM1 muscle, which was consistent with the major accumulation of HDAC4 in mutant muscle. Hence, although we cannot rule out the contribution of CaMKIIβM deficiency in the defective up-regulation of synaptic genes in DM1 muscle, it is unlikely to occur via deregulation of HDAC4 signalling.

In conclusion, our study identified NMJ deterioration as a major hallmark of muscle affliction in DM1, which likely involves muscle perturbations in activity-dependent pathways. We unveiled that the muscle-specific isoform CaMKIIβM is lost in DM1 muscle and may contribute to NMJ destabilization, especially by affecting synaptic gene expression and AChR recycling. Hence, one should consider NMJ destabilisation as a potential process contributing to muscle atrophy and weakness in DM1, and the deregulation of CaMKII pathway as a key event in DM1 pathogenesis in muscle and non-muscle tissues.

Material and Methods

Mice

Homozygous mice of the mouse line LR20b carrying about 250 (CTG)n repeats within the *HSA* transgene (HSA^{LR}) were obtained from Thornton and colleagues (University of Rochester Medical Center, Rochester, New York, USA) [153]. Mice of the corresponding background strain (FVB/N) were used as control. Mice were genotyped for HSA^{LR} transgenes by quantification of *ACTA1* levels normalized to endogenous actin (mouse *Acta1*) in genomic DNA. Mice from the *Mbnl1ΔE3* line were obtained from Swanson and colleagues (College of Medicine, University of Florida, Gainesville, Florida, USA) [173]. $Mbnl1^{+/+}$ littermates were used as control. Mice from the *Mbnl1ΔE3* line were genotyped for the homozygous exclusion of exon 3 in the *Mbnl1* locus. Mice were maintained in a conventional specific-pathogen–free facility with a fixed light cycle (23°C, 12-hour dark-light cycle). All animal studies were performed in accordance with the European Union guidelines for animal care and approved by the Veterinary Office of the Canton of Basel city (application number 2601).

Muscle force and relaxation

In vitro force measurement of EDL muscle was conducted as previously described [239]. Half- and late relaxation times were calculated according to Moyer et al. (2011) [240].

Western blotting

Muscles powdered in liquid nitrogen were lysed in cold RIPA+ buffer (50 mM Tris-HCl pH 8, 150 mM NaCl, 1% NP-40, 0.5% sodium deoxycholate, 0.1% SDS, 1% Triton X, 10% glycerol, phosphatase and protease inhibitors). Subcellular fractionation was done according to Dimauro et al. (2012) [241]. Following dosage (BCA Protein Assay, Sigma-Aldrich), proteins were separated on SDS-polyacrylamide gels and transferred to nitrocellulose membrane. Blots were blocked in TBS, 3% BSA, 0.1% Tween-20, and incubated overnight at 4°C with primary antibodies, then for 2 hours with HRP-labelled secondary antibodies. Immunoreactivity was detected using the ECL Western blot detection reagent LumiGLO (KPL) and exposed to Super RX-N films (Fujifilm). Protein expression was normalized to α-actinin, or the total protein of the corresponding phosphorylated form. Antobodies are listed in Supplemental Materials.

Polymerase chain reaction

Total RNAs were extracted with the RNeasy Mini Kit (Qiagen), reverse transcribed with the SuperScript III First-Strand Synthesis System (Invitrogen), and amplified with the Power SYBR Green Master Mix (Applied Biosystems). Expression of specific spliced or pan transcripts was analysed by end-point PCR and electrophoresis, or by quantitative PCR with Step One software and normalization to *Tbp* expression. Primers are listed in Supplemental Material, Table S1

Histology and immunofluorescence

Muscles were frozen in liquid nitrogen–cooled isopentane. Eight-micrometer muscle sections were stained with H&E and observed with an upright microscope (Olympus). For immunostaining, sections were fixed with 4% paraformaldehyde (PFA), then blocked in PBS, 3% BSA, incubated sequentially with primary and secondary fluorescent antibodies (Invitrogen), mounted with Vectashield medium (Vector), and observed with a Leica fluorescent microscope. Antibodies are listed in Supplemental Materials.

Fluorescence in situ hybridization

FISH was conducted on muscle cryosections as previously described by Batra et al. (68), using a Cy3-CAG10 DNA probe. Nuclear foci were observed with a Leica confocal microscope.

Staining of muscle bundles

To analyse NMJ organization, muscles were bathed ex vivo (2 µg/ml) with α-bungarotoxin-Alexa555 (Invitrogen) for 30 min, before being washed and fixed with 4% PFA. Muscle bundles were cut, permeabilized in PBS, 1% Triton-X100, and blocked in PBS, 1% BSA, 0.1% Triton-X100. Bundles were then successively incubated with primary antibodies against Neurofilament and Synaptophysin (to stain pre-synaptic compartment), and the corresponding secondary antibodies (Invitrogen) together with bungarotoxin (ThermoFisher). Images were recorded using a Leica confocal microscope with ×40 to ×100 objectives.

AChR turnover and recycling

AChR turnover was assessed by injecting α-bungarotoxin-Alexa647 and -Alexa555 (25 pmoles - Invitrogen) into TA/EDL muscles at days 1 and 10, respectively (5 and 14 days after nerve cut when combined with denervation). AChR recycling was assessed by injecting α-bungarotoxin-Biotin (20 pmoles - Invitrogen) and saturating dose of streptavidin-Alexa555 (40 pmoles - Invitrogen) into TA/EDL muscles at day 1, followed by injection of streptavidin-Alexa488 (40 pmoles - Invitrogen) at day 3. Analysis was conducted with muscle bundles as previously done [232]. For turnover and recycling quantification, images were recorded using a Leica confocal microscope with ×63 objective. Pixel dominance (old *vs.* new or stable *vs.* recycled receptors) was calculated using Fiji and Matlab software.

Statistics

Quantitative data are displayed as mean ± SEM of independent samples, with n (number of individual experiments) ≥ 3. Statistical analysis of values was performed using unpaired Student's t test or 2-way ANOVA test with Tukey's multiple comparisons test correction, with a 0.05 level of confidence accepted for statistical significance.

Acknowledgements

We thank Prof. C. A. Thornton (University of Rochester Medical Center) for the generous gift of *HSA*^{LR} mice, and Prof. M. Swanson (University of Florida) for the generous gift of *Mbnl1*$^{\Delta 3/\Delta 3}$ mice. This work was supported by the University of Basel and University Hospital Basel (MS), the University of Basel–Stadt and Basel-Landschaft (MAR), the Neuromuscular Research Association Basel (MS, PC), the Swiss Foundation for Research on Muscle Diseases (MAR, MS), the Olga Mayenfisch Foundation (PC), and the Swiss National Science Foundation (PC, MS).

Competing interests

There is no conflict of interest.

Supplemental Data

CaMKII deregulation and changes in neuromuscular junctions in Type I Myotonic Dystrophy

Denis Falcetta[1,2], Marine Théodore[1], Shuo Lin[2], Lionel Tintignac[1], Jochen Kinter[1], Markus A. Rüegg[2], Michael Sinnreich[1], Perrine Castets[3]

Supplemental data includes 2 supplemental figures, 1 supplemental Table (List of primers), and supplemental methods.

Supplementary Material

Antibodies

The following antibodies were used for immunoblotting (dilution 1/100) or immunofluorescence: HDAC4 (#15164 and #7628; 1/1000 for IHC), Phospho-HDAC4Ser632 (#3424), Phospho-CaMKIIThr286 (#12716), CaMKII pan (#4436), Acetyl-Histone H3 (Lys9/Lys14) (#9677), Histone H3 (#9717) from Cell Signaling Technology; α-actinin (A5044) and Neurofilament 200 (N4142; 1/2000 for IHC) from Sigma; Laminin (ab11575 and ab11576; 1/300 for IHC) from Abcam; Synaptophysin (A0010; 1/200 for IHC) from Dako.

Supplementary Figure 1

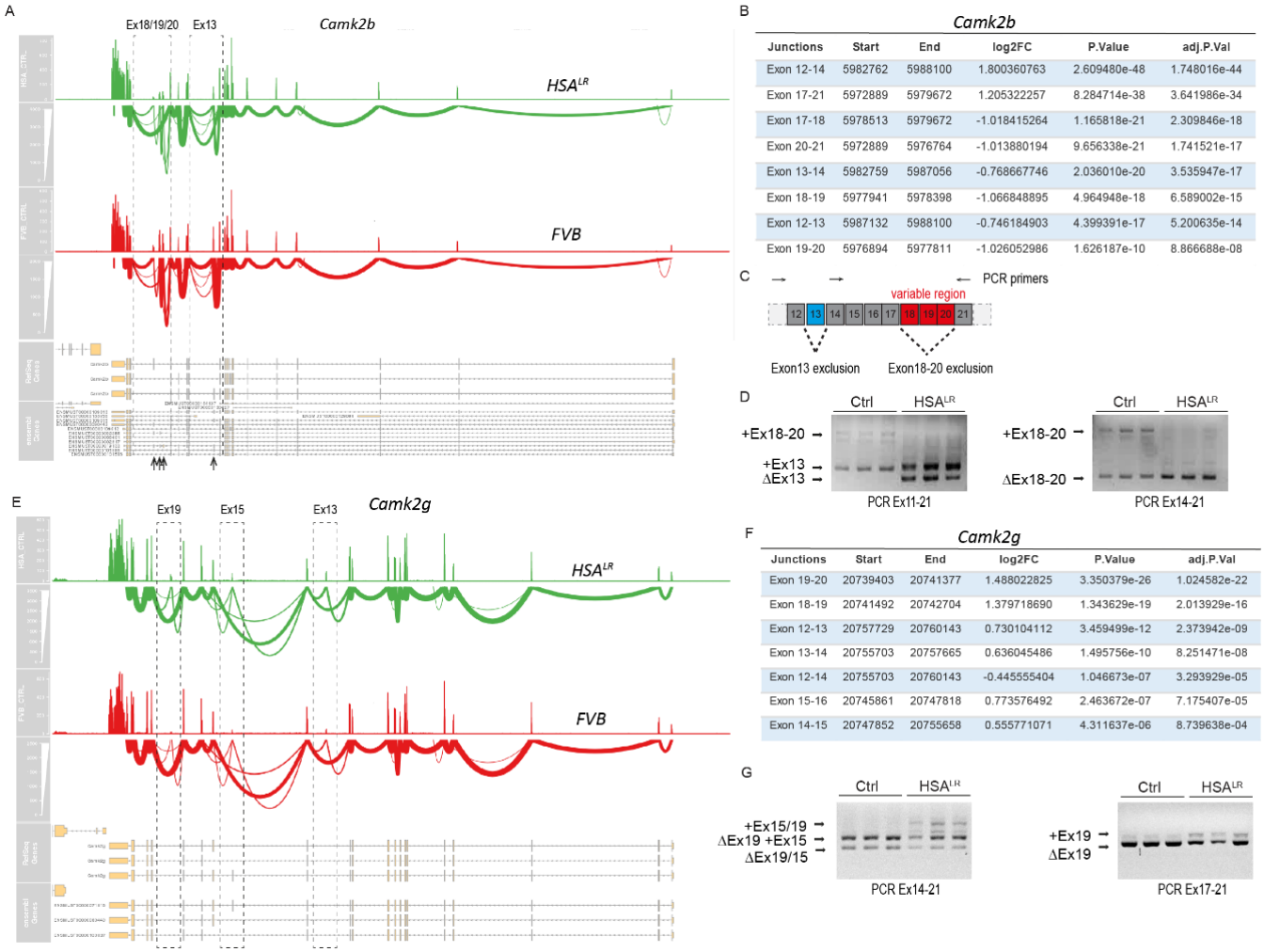

Junctions	Start	End	log2FC	P.Value	adj.P.Val
Exon 12-14	5982762	5988100	1.800360763	2.609480e-48	1.748016e-44
Exon 17-21	5972889	5979672	1.205322257	8.284714e-38	3.641986e-34
Exon 17-18	5978513	5979672	-1.018415264	1.165818e-21	2.309846e-18
Exon 20-21	5972889	5976764	-1.013880194	9.656338e-21	1.741521e-17
Exon 13-14	5982759	5987056	-0.768667746	2.036010e-20	3.535947e-17
Exon 18-19	5977941	5978398	-1.066848895	4.964948e-18	6.589002e-15
Exon 12-13	5987132	5988100	-0.746184903	4.399391e-17	5.200635e-14
Exon 19-20	5976894	5977811	-1.026052986	1.626187e-10	8.866688e-08

Camk2g

Junctions	Start	End	log2FC	P.Value	adj.P.Val
Exon 19-20	20739403	20741377	1.488022825	3.350379e-26	1.024582e-22
Exon 18-19	20741492	20742704	1.379718690	1.343629e-19	2.013929e-16
Exon 12-13	20757729	20760143	0.730104112	3.459499e-12	2.373942e-09
Exon 13-14	20755703	20757665	0.636045486	1.495756e-10	8.251471e-08
Exon 12-14	20755703	20760143	-0.445555404	1.046673e-07	3.293929e-05
Exon 15-16	20745861	20747818	0.773576492	2.463672e-07	7.175407e-05
Exon 14-15	20747852	20755658	0.555771071	4.311637e-06	8.739638e-04

Supplementary Figure 1: Mis-splicing of CaMKIIs in *HSA^{LR}* muscle.
A) RNA-seq results for *Camk2b* showing the mis-spliced regions in *HSA^{LR}* muscle, compared to control. n=4. B) Statistical analysis of RNA-seq for *Camk2b* in *gastrocnemius* control and *HSA^{LR}* muscles. C, D) Splicing analysis of exon 13 and exons 18-20 of *Camk2b* by end-point PCR. Scheme of the gene and primers is given in (C). E, F) RNA-seq results for *Camk2g* showing the mis-spliced region in *HSA^{LR}* muscle, compared to control. Statistical analysis is given in F. n = 4 per group. G) End-point PCR analysis of mis-splicing of exons 15 and 19 of *Camk2g* in *gastrocnemius* from *HSA^{LR}* and control muscles. n=3 per group.

Supplementary Figure 2

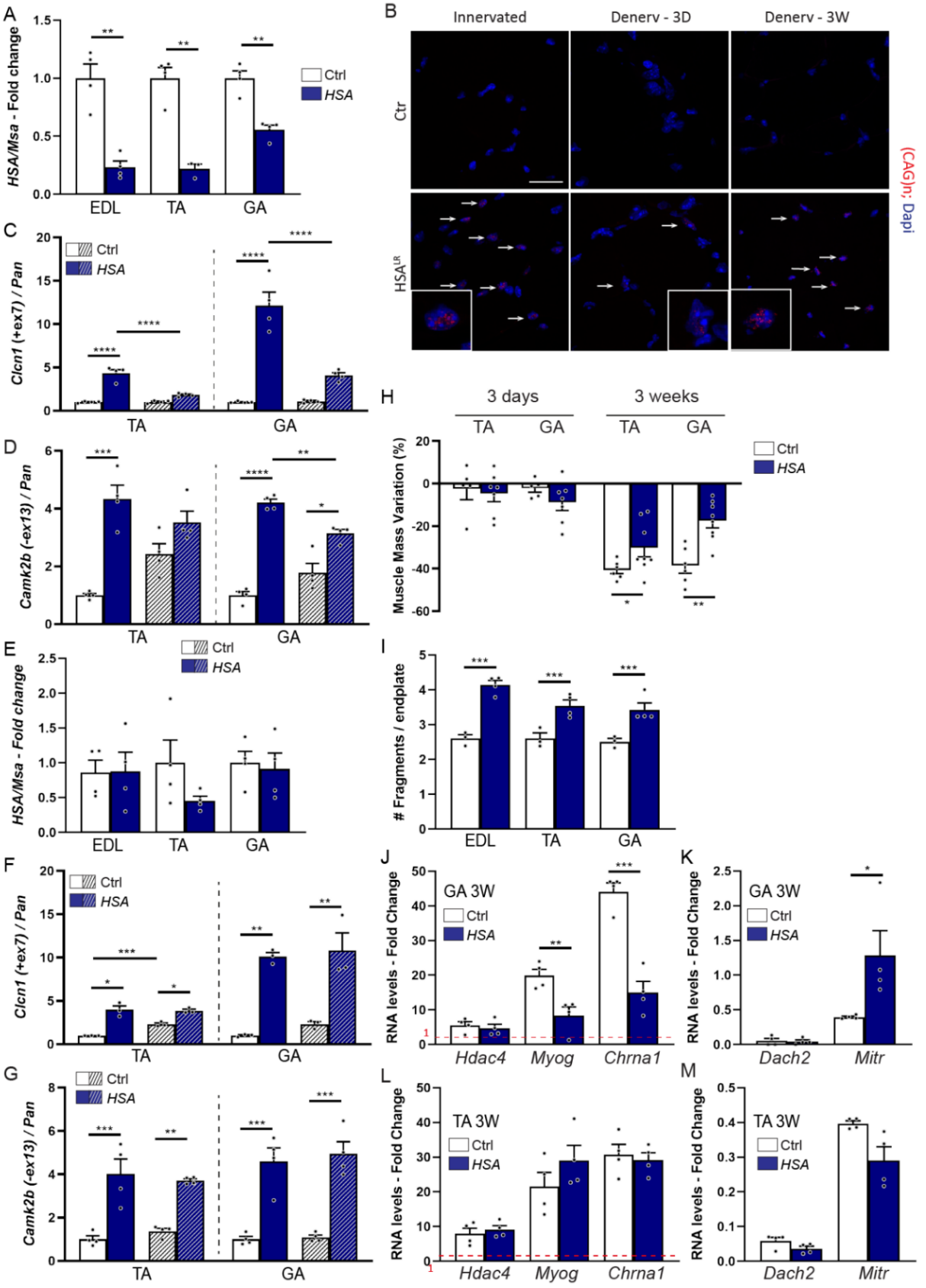

Supplementary Figure 2: Limits of the *HSA^{LR}* mouse model upon nerve injury.
A) qPCR analysis of *ACTA1* expression in EDL, TA and *gastrocnemius* in *HSA^{LR}* innervated muscle after 3 days of denervation. Results are normalized on mouse *Acta1* and relative to innervated *HSA^{LR}* muscle. n=4 per group. B) Fluorescent in situ hybridization with Cy3-CAG_{10} DNA probe, on sections of innervated and denervated (3 days and 3 weeks) muscles from control and *HSA^{LR}* mice. Arrows point to (CAG)n●(CUG)n-positive nuclei. Scale bar, 25 μm. C, D) qPCR analysis of spliced transcript of *Clcn1* (C) and *Camk2b* (D) in TA and *gastrocnemius* muscles from control and *HSA^{LR}* mice after 3 days of denervation. Levels are normalized on total transcript levels and relative to innervated control muscle. n=4 per group. E) qPCR analysis of *ACTA1* expression in EDL, TA and *gastrocnemius* in *HSA^{LR}* innervated muscle after 3 weeks of denervation. Results are normalized on mouse *Acta1* and relative to innervated *HSA^{LR}* muscle. n=4 per group. F, G) qPCR analysis of spliced transcript of *Clcn1* (F, n = 3 per group) and *Camk2b* (G, n = 4 per group) in TA and *gastrocnemius* muscles from control and *HSA^{LR}* mice after 3 weeks of denervation. Levels are normalized on total transcript levels and relative to innervated control muscle. H) Mass variation after 3 weeks of denervation in control and *HSA^{LR}* mice, for TA and *gastrocnemius* (GA) muscles. n = 6/8 Ctrl/HSA. I) Quantification of the number of fragments per motor endplate in EDL, TA and *gastrocnemius* muscles from control and *HSA^{LR}* mice after 3 weeks of denervation. J-M) qPCR analysis of activity-dependent genes in *gastrocnemius* (J,K) and TA (L,M) muscles from control and *HSA^{LR}* mice after 3 weeks of denervation. Levels are normalized to *Tbp* and relative to control innervated muscle (red dotted line). Data are mean±sem; *p<0.05; ** p<0.01; *** p<0.001; ****p<0.0001; two-tailed unpaired Student's t-test.

Supplementary Table 1

Gene	Forward primer	Reverse primer
Acta1 (mouse)	5'-CCGGAAAGAAATCTCAACCA-3'	5'-CCAAGTCCTGCAAGTGAACA-3'
ACTA1 (human)	5'-CGAGACCACCTACAACAGCA-3'	5'-GGCATACAGGTCCTTCCTGA-3'
Atp2a1+ex22	5'- GCCCTGGACTTTACCCAGTG-3'	5'-ACGGTTCAAAGACATGGAGGA-3'
Atp2a1 pan	5'- GCCCTGGACTTTACCCAGTG-3'	5'-CCTCCAGATAGTTCCGAGCA-3'
Camk2b-ex13	5'-TTTCTCAGCAGCCAAGAGTTT-3'	5'-TTCCTTAATCCCGTCCACTG-3'
Camk2b pan	5'-GCACGTCATTGGCGAGGA-3'	5'-ACGGGTCTCTTCGGACTGG-3'
Camk2b-ex18	5'-CCTGATGTCCTGAGCTTGGT-3'	5'-GAACTGGAGATTGGCAGGAG-3’
Camk2b-ex19	5'-TCAGTGAGAAGGGGCTGTG-3'	5'-CTAGGAGACCCGGAGACAAG-3’
Camk2b-ex20	5'-CCCCCAGGATCTCTGACA-3'	5'-TGCTTCCGGGATGGGGTGGGC-3’
Camk2b-ex13 (gel)	5'-GTTCCACCGTGGCCTCTAT-3'	5'-TCGGAAGATTCCAGGGCAGC-3’
Camk2b-ex18-20 (gel)	5'-CCAGACAAACAGCACCAAAA-3'	5'-TGAGCTGCTCTGTGGTCTTG-3’
Camk2g+exon 15/19 (gel)	5'-AGTTCCAGC GTGCACCTAAT-3'	5'-ACGTGGACGTGAGGGTTTAG-3’
Camk2g+exon 19 (gel)	5'-ACACCACTACAGAAGACGAAGA-3'	5'-AACCTCAAACGAACAGGACC-3’
Clcn1+ex7a	5'-GGGCGTGGGATGCTACTTTG-3'	5'- AGGACACGGAACACAAAGGC-3'
Clcn1 pan	5'-CTGACATCCTGACAGTGGGC-3'	5'- AGGACACGGAACACAAAGGC-3'
Chrna1	5'-TCCCTTCGATGAGCAGAACT-3'	5'-GGGCAGCAGGAGTAGAACAC-3'
Chrnag	5'-GTGTCTTCGAGGTGGCTCTC-3'	5'-TCTGGGATTGGAAGATGAGG-3'
Dach2	5'-CCAGCTCAAATCCCAGTCAT-3'	5'-CGCAGTTCCTTCTTTTCCTG-3'
Hdac4	5'-CAGACAGCAAGCCCTCCTAC-3'	5'-AGACCTGTGGTGAACCTTGG-3'
Mitr	5'-CCTGCAGCACCTACTGTTGA-3'	5'-GTACCTCTAATGCCCGGTGA-3'
Myogenin	5'-ACTCCCTTACGTCCATCGTG-3'	5'-CAGGACAGCCCCACTTAAAA-3'
Tbp	5'-CTCAGTTACAGGTGGCAGCA-3'	5'-CAGCACAGAGCAAGCAACTC-3'

Supplementary Table 1: List of primers

3.1.2 Additional results

In the course of our study on NMJs in DM1, we identified changes in *Clcn1* and *Camk2b* expression upon denervation in control mice. At 3 days post-denervation, splicing of exon 7a was unchanged in control denervated muscle (Figure 7A), while there was a drastic reduction in the overall transcript expression of *Clcn1* in both HSA^{LR} and control muscles (Figure 7B). After 3 weeks of denervation, insertion of exon 7a slightly increased in TA denervated muscle from control mice (Figure 7C), while expression of total *Clcn1* transcript remained much lower than in innervated muscle (Figure 7D).

In parallel, the expression pattern of *Camk2b* also changed upon denervation in control mice, with an increased exclusion of exon 13 (Figure 7E, tendency in TA/*gastrocnemius,* significant in EDL) and a strong decrease in exon18-20 inclusion at 3 days (Figure 7F). The total expression of *Camk2b* remained unchanged in the denervated muscle, as compared to innervated muscle, in control mice (Figure 7G). After 3 weeks denervation, splicing of exon 13 turned back to basal levels (Figure 7H), and the expression of total *Camk2b* remained similar to innervated muscle (Figure 7I).

These results suggest that splicing changes towards the DM1 pattern in control denervated muscle, which may be part of the muscle response to nerve injury. This is consistent with the re-induction of the embryonic program in denervated muscle fibres and the expression of embryonic spliced isoforms in DM1 muscle. This leads to the hypothesis that DM1 muscle may be more prone to respond and adapt to nerve injury. Further investigations on these changes will be of interest to better understand the molecular mechanisms underlying the muscle response to denervation or the process of re-innervation.

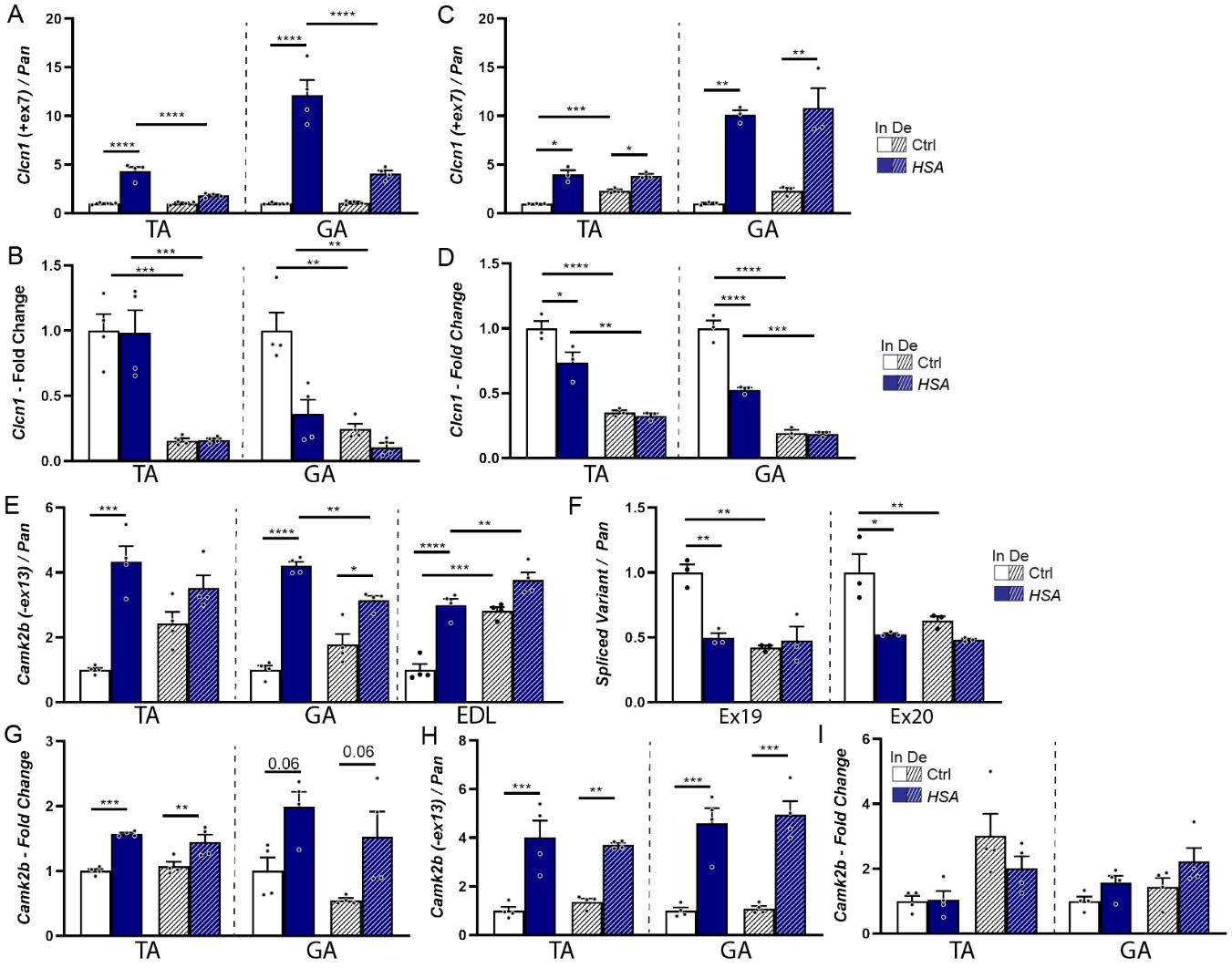

Figure 7: Changes in *Clcn1* and *Camk2b* expression upon denervation.
Quantitative PCR analysis of the splicing (A, C, E, F, H) and of the total expression (B, D, G) of *Clcn1* (A-D; insertion exon 7a) and *Camk2b* (E-I; exclusion exon 13 or insertion exons 19/20) in TA, *gastrocnemius*, and EDL (E) muscles from control and HSA^{LR} mice after 3 days (A, B, E, F, G) or 3 weeks (C, D, H, I) of denervation. Levels are normalized on *Pan* transcript (for spliced variant) or on *Tbp,* and relative to innervated control muscle. n=3/4 per group. Data are mean±sem; * p<0.05; ** p<0.01; *** p<0.001; **** p<0.0001; two-ANOVA with Tukey's post-hoc test. *In: Innervated; De: Denervated.*

3.2 Project 2 – Manuscript

The following manuscript will be completed with two additional experiments, before submission.

Short Report

Altered expression pattern of chloride channel accessory proteins suggests a role in muscle pathophysiology in Myotonic Dystrophy Type I

Denis Falcetta[1,2], Marine Théodore[1], Shuo Lin[2], Lionel Tintignac[1], Jochen Kinter[1], Markus A. Rüegg[2], Michael Sinnreich[1], Perrine Castets[3]

1. Neuromuscular centre, Department of Biomedicine, University Hospital Basel, Klingelbergstrasse 50/70, CH-4056 Basel, Switzerland
2. Biozentrum, University of Basel, Klingelbergstrasse 50/70, CH-4056 Basel, Switzerland
3. Department of Cell Physiology and Metabolism, Faculty of Medicine, University of Geneva, 1 rue Michel Servet, CH-1211 Geneva, Switzerland

* Corresponding author: Perrine Castets, perrine.castets@unige.ch, +41 22 379 52 35

Introduction

Besides muscle atrophy and weakness, patients affected by Myotonic Dystrophy type I (DM1) commonly present with myotonia [118, 242]. Myotonia corresponds to the delayed relaxation of muscle after contraction [120]. In skeletal muscle, chloride conductance (G_{Cl-}) is pivotal to restore the resting membrane potential of skeletal muscle fibers after an action potential. In DM1, myotonia arises from the hyper-excitability of the sarcolemma, due to the loss of the chloride channel ClC-1 (encoded by *Clcn1*), and the consecutive decrease in G_{Cl-} [19, 123, 191, 243].

Since the discovery of *Clcn1* mis-splicing in DM1 muscle, strategies to counteract myotonia have focused on the restauration of ClC-1. Studies in DM1 mouse models, such as HSA^{LR} and $Mbnl1^{\Delta 3/\Delta 3}$ mice, as well as in patient-derived DM1 muscle cells, have demonstrated that correction of *Clcn1* mis-splicing using antisense oligonucleotides is sufficient to reduce DM1-associated myotonia [191, 244, 245]. These studies hence established that aberrant splicing of *Clcn1* is required for DM1-associated myotonia. However, whether *Clcn1* mis-splicing is sufficient to drive myotonia remains unknown. Indeed, although *Clcn1* knock-out mice (*adr* mice) display myotonia, there is no mouse model reproducing ClC-1 deficiency associated to *Clcn1* mis-splicing. Moreover, there is evidence that other pathomechanisms contribute to myotonia. Electrophysiological investigations showed a G_{Cl-}-independent pattern in the myotonic discharges measured in DM1 patients and in muscle fibers, which suggested the involvement of calcium-activated potassium channels and voltage-gated sodium (Na_v) channels [123, 246, 247]. Na_v channels are essential for the initiation and propagation of the action potential in excitable cells [14]. Mice harboring mutations in *Scn4a* (encoding Nav1.4) found in channelopathies, display progressive myopathy and myotonia [248]. The mechanisms contributing or liable to limit myotonia in DM1, hence, remain to be further investigated.

Here, we examined the potential role of chloride channel accessory proteins (CLCA) in the pathophysiology of DM1. We found increased levels of CLCA1 and CLCA4 in muscle from HSA^{LR} mice, a DM1 mouse model. Moreover, we identified that inbreed HSA^{LR} lose myotonia, which did not correlated with the progressive shortening of the (CTG)n repeats in the mouse line. Loss of myotonia was associated with only mild reduction in *Clcn1* mis-splicing. Moreover, levels of *Clca1/4* transcripts inversely correlated with late relaxation time. Although endogenous CLCA1/4 proteins were not detectable in muscle, their overexpression confirmed that the protein is cleaved into a secreted N-term peptide and a cellular C-term product, which may both contribute to the beneficial effect on membrane relaxation in DM1 muscle.

Results

Inbreed *HSA^{LR}* mice lose myotonia

The *HSA^{LR}* mouse line has been developed by the group of Thornton (University of Rochester Medical Center) and provided the first evidence of the pathological cause of DM1, by carrying in the *HSA* (*Human Skeletal Actin*) transgene, abnormal (CTG)n repeats, found in patients in the *DMPK* gene [153]. *HSA^{LR}* mice reproduce the typical myotonia found in patients, which can be evaluated using *ex vivo* muscle force measurement upon tetanic stimulation [216, 240]. Myotonia assessment revealed an attenuation and eventually a loss of the myotonic phenotype in inbreed *HSA^{LR}* mice (Figure 1A). In parallel, we identified a shift in the genomic transgene size, with some *HSA^{LR}* mice harboring a shorter CTG expansion (Figure 1B). From the 220 (CTG) triplets initially present in the *HSA^{LR}* line (noted [L], for *Long*) [153, 249], we evaluated that these mice (referred to as [S], for *Short*) lose around 20-30 (CTG). Mice showing intermediate size of band or two bands at different size were grouped as "*intermediate*". To determine if this shortening was responsible for the loss of myotonia, we measured the late relaxation time of EDL muscle, after tetanic stimulation, in [L], [S] or intermediate mice. Mice were grouped dependent on their age, as late relaxation time tends to decrease with age in *HSA^{LR}* mice. Interestingly, there was a significant effect of the size of the repeat on the relaxation time, in 3-5-month-old *HSA^{LR}* mice (Figure 1C) and in 6-9-month-old mutant mice (Figure 1D). In both groups, the relaxation time significantly decreased in intermediate and [S] mice, as compared to [L] mice. Notwithstanding, at both ages, there were some non-myotonic [L] mice, as well as some myotonic [S] mice (Figure 1C, D). Surprisingly, specific tetanic force (sP0) was also slightly reduced in [S] mice, as compared to [L]. However, this was only observed at 3-5 months of age (Figure 1E, F).

Although triplet repeat extension and contraction are known phenomenon in the DM1 context [119, 249], these results point to the importance of refreshing inbred mouse lines regularly. They also gave the opportunity to analyze the mechanisms liable to reduce or eliminate myotonia in DM1.

Non-myotonic *HSA^{LR}* mice show limited reduction in mis-splicing events

As the shortening of the repeats was minor, we wondered whether this corresponds to a size threshold, below which myotonia is abrogated. We defined mice as myotonic and non-myotonic when late relaxation time of EDL muscle was more than 500 ms and less than 50 ms, respectively. To get further insights on the changes associated to myotonia loss, we first evaluated the expression of the *HSA* transgene in muscle from myotonic and non-myotonic *HSA^{LR}* mice by quantitative PCR, but did not detect significant difference (Figure 2A). Similarly, the accumulation of ribonuclear foci was observed in *gastrocnemius* muscle, as well as in less affected *tibialis anterior* (TA) muscle, from both myotonic and non-myotonic *HSA^{LR}* mice (Figure 2B). We next evaluated DM1-associated mis-splicing events in myotonic and non-myotonic *HSA^{LR}* mice. Importantly quantitative analysis and myotonia evaluation were done in EDL muscle from the same mice. Inclusion of exon 7a in *Clcn1,* evaluated by quantitative PCR, was strongly increased in myotonic and non-myotonic *HSA^{LR}* mice, as compared to control.

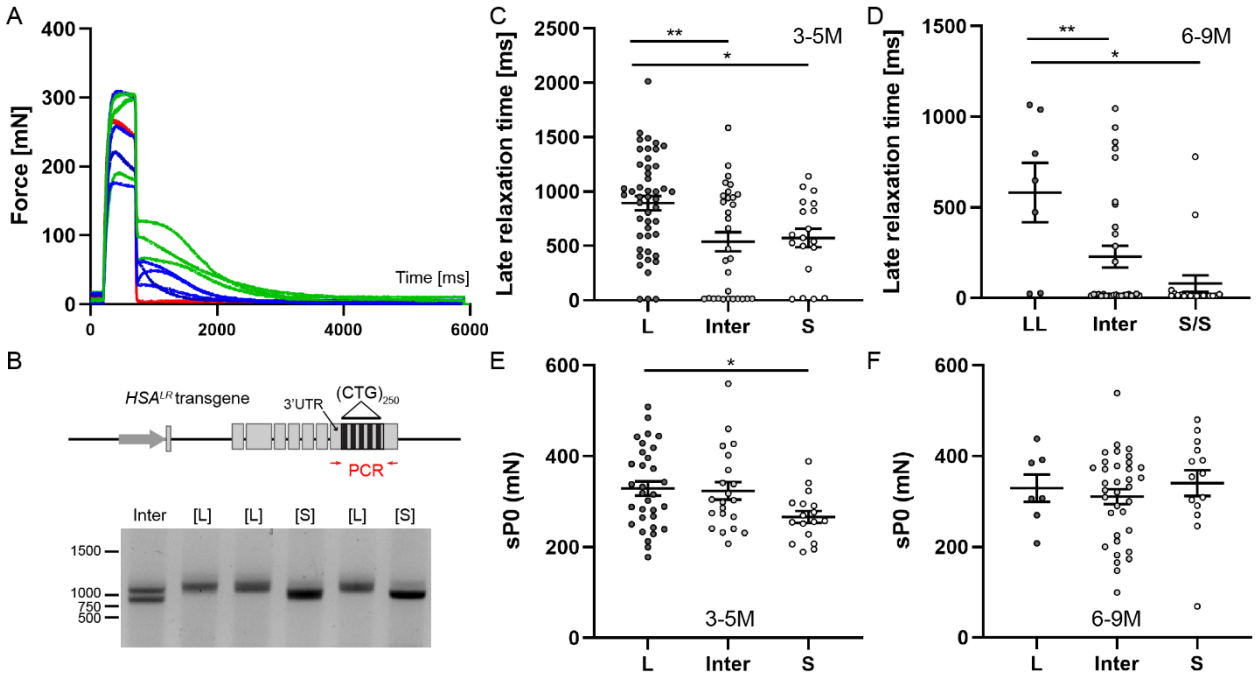

Figure 1: Loss of myotonia correlates with minor shortening of (CTG)n repeat.

A) Variable late relaxation time upon tetanic stimulation in EDL muscle from 3-month-old *HSA*^{LR} mice. Green, blue and red force measurement correspond to myotonic (relaxation time > 500 ms), mildly myotonic (relaxation time between 50 and 500 ms) and non-myotonic (<50 ms) response, respectively. B) Shortening of the (CTG)n repeat within the *HSA* transgene is visible by end-point PCR. [L] and [S] correspond to long and shorter repeats, respectively. Inter: intermediate. C, D) Late relaxation time upon EDL stimulation in 3-5- (C) and 6-9- (D) month-old *HSA*^{LR} mice, with long [L], intermediate or short repeat [S]. N=47 [L], 31 Inter, 19 [S] (C); N= 7 [L], 31 [Inter], 19 [S] (D). E, F) Specific tetanic force (sP0) of EDL muscle in 3-5 (E) and 6-9 (F) -month-old *HSA*^{LR} mice. N=31 [L], 21 Inter, 17 [S] (E); N= 7 [L], 35 [Inter], 14 [S] (F). Data are mean ± SEM. *p<0.05, **p<0.01, one-way ANOVA with a Tukey's post-hoc analysis.

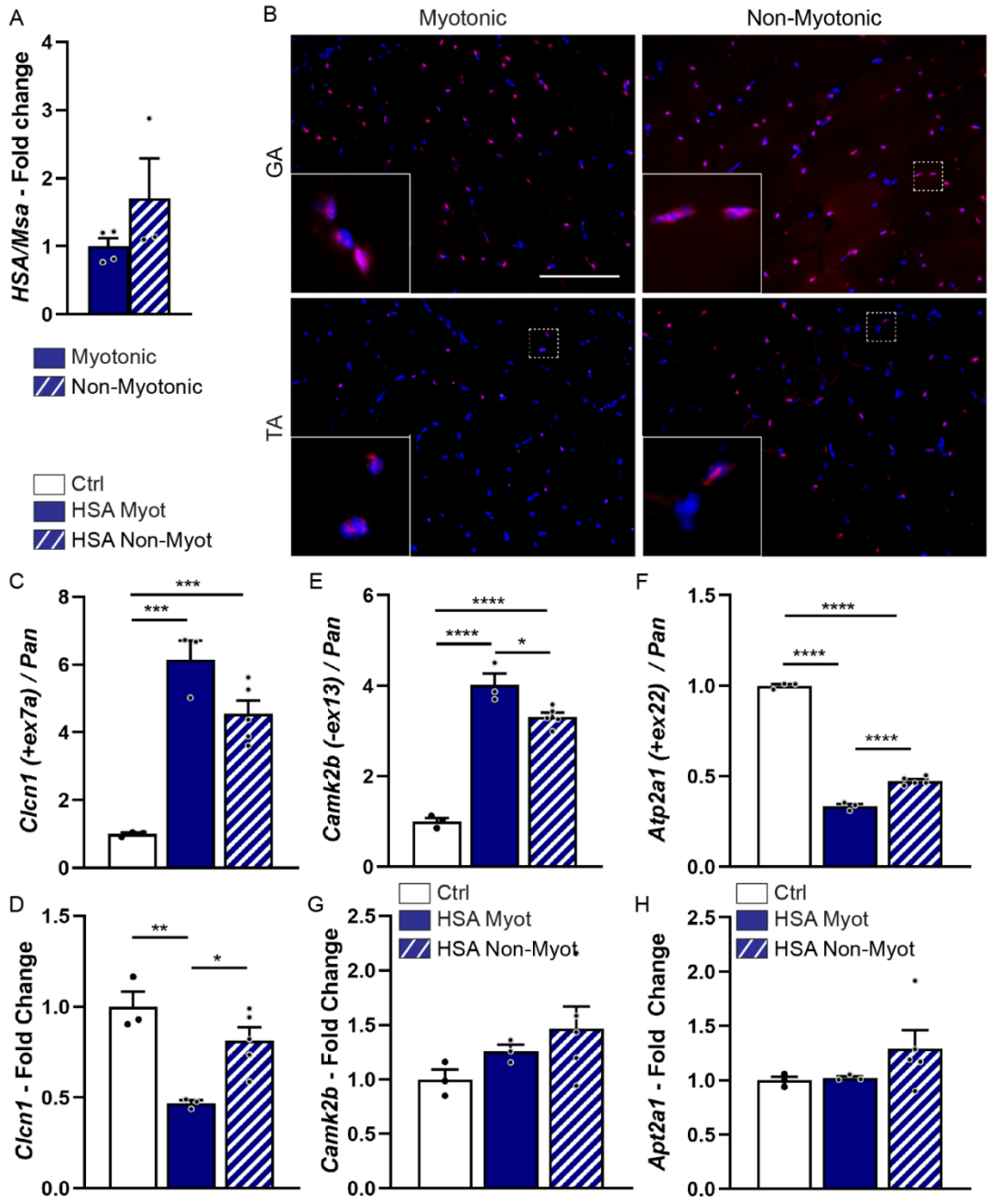

Figure 2: DM1-associated mis-splicing are slightly changed in non-myotonic *HSA^{LR}* mice.

A) Quantification of the expression of the *HSA* transgene in muscle from myotonic and non-myotonic *HSA^{LR}* mice. N=4 myotonic, 3 non-myotonic. B) Ribonuclear foci staining on TA and GA muscles from myotonic and non-myotonic *HSA^{LR}* mice. Scale bar, 100µm. C-H) Quantitative PCR analysis of the splicing (C, E, F) and of the total expression (D, G, H) of the *Clcn1* (inclusion exon 7a), *Camk2b* (exclusion exon 13) and *Atp2a1* (inclusion exon 22) genes in EDL muscle from *HSA^{LR}* mice (N=3 Ctrl, 3 myotonic, 5 non-myotonic). Expression of spliced variants is normalized on total expression. Total expression is normalized on *Tbp* expression. Data represent mean ± SEM. *p<0.05, **p<0.01, ***p<0.001, ****p<0.0001, one-way ANOVA with a Tukey's post-hoc analysis.

There was no significant difference between myotonic and non-myotonic mutant mice (Figure 2C). In contrast, the total transcriptional expression of *Clcn1* was reduced only in myotonic HSA^{LR} mice (Figure 2D). Although *Clcn1* mis-splicing persisted in non-myotonic mice, the overall increase in *Clcn1* expression, as compared to myotonic mice, likely contributes to the amelioration of muscle relaxation (Figure 2D). In parallel, mis-splicing of *Camk2b* (exclusion of exon 13) and of *Atp2a1* (exclusion of exon 22) was slightly reduced in non-myotonic HSA^{LR} mice, as compared to myotonic mice (Figure 2E, F). However, these mis-splicing events remained major, as compared to control mice (Figure 2E, F). Total expression of *Camk2b* and *Atp2a1* was not different between the three groups of mice (Figure 2G, H). Altogether, these results indicate that minor changes in the splicing or expression of DM1-affected genes are sufficient to abrogate some pathological features affecting muscle, such as myotonia.

Expression of *Clca1/4* is strongly increased in DM1 muscle

Taking advantage of RNAseq data obtained with *gastrocnemius* from HSA^{LR} and control mice, we searched for candidate genes that are differentially expressed in mutant muscle and may contribute to myotonia modulation. We identified major changes in the expression of members of the Chloride Channel Accessory (CLCA) family (Table 1), which has been shown to regulate chloride channels in different tissues [250-254]. RNAseq results suggested that expression of *Clca1, Clca3b* and *Clca4a1* was strongly increased in mutant muscle, compared to control (Table 1). To confirm these results, we quantified their expression by qRT-PCR in *gastrocnemius*, TA and EDL muscle from HSA^{LR} and control mice. For both *Clca1* and *Clca4a1*, transcript levels were drastically increased in all muscles from HSA^{LR} mice when compared to control (Figure 3A, B). Proper evaluation of *Clca3b* expression was impossible in muscle, probably because of a too low expression of the gene in the tissue (*not shown*). As there was a high variability in gene expression within the group of HSA^{LR} mice, we hypothesized that *Clca1* and *Clca4a1* expression may vary dependent on the myotonic phenotype of the mice. We hence quantified their expression in EDL muscle, dependent on the late relaxation time measured in the corresponding muscle in mutant mice (*i.e.* myotonic if > 500 ms, non-myotonic if < 50 ms). Expression of *Clca1* and *Clca4a1* indeed tended to be higher in non-myotonic mice, as compared to myotonic mutant mice (Figure 3C, D). When using linear regression, we observed that expression of *Clca* genes tends to inversely correlates with late relaxation time, with a stronger effect detected for *Clca4a1* (Figure 3E, F). This suggested that up-regulation of *Clca1/4a1* may constitute a compensatory mechanism and limit myotonia in HSA^{LR} mice. Antibodies available for CLCA1/4 did not allow to confirm these changes at protein levels, which may also arise from the low expression of the genes in muscles tissues.

Table 1

Gene Id	Symbol	Gene name	Log2(FC)	P. Value	Adj. P. Value
23844	*Clca1*	*chloride channel accessory 1*	4.1832	1.50E-20	2.89E-18
99663	*Clca4a*	*chloride channel accessory 4a*	4.9746	1.84E-20	3.48E-18
229927	*Clca3b*	*chloride channel accessory 3b*	3.5783	2.28E-12	1.53E-10
99709	*Clca4b*	*chloride channel accessory 4b*	0.3228	0.00291	0.01965
229933	*Clca2*	*chloride channel accessory 2*	0.5657	0.15751	0.367
80797	*Clca3a2*	*chloride channel accessory 3a2*	0.5856	0.65152	0.82422
12722	*Clca3a1*	*chloride channel accessory 3a1*	0.0528	0.83037	0.93604

Table 1: RNA-seq results for *Clca* genes

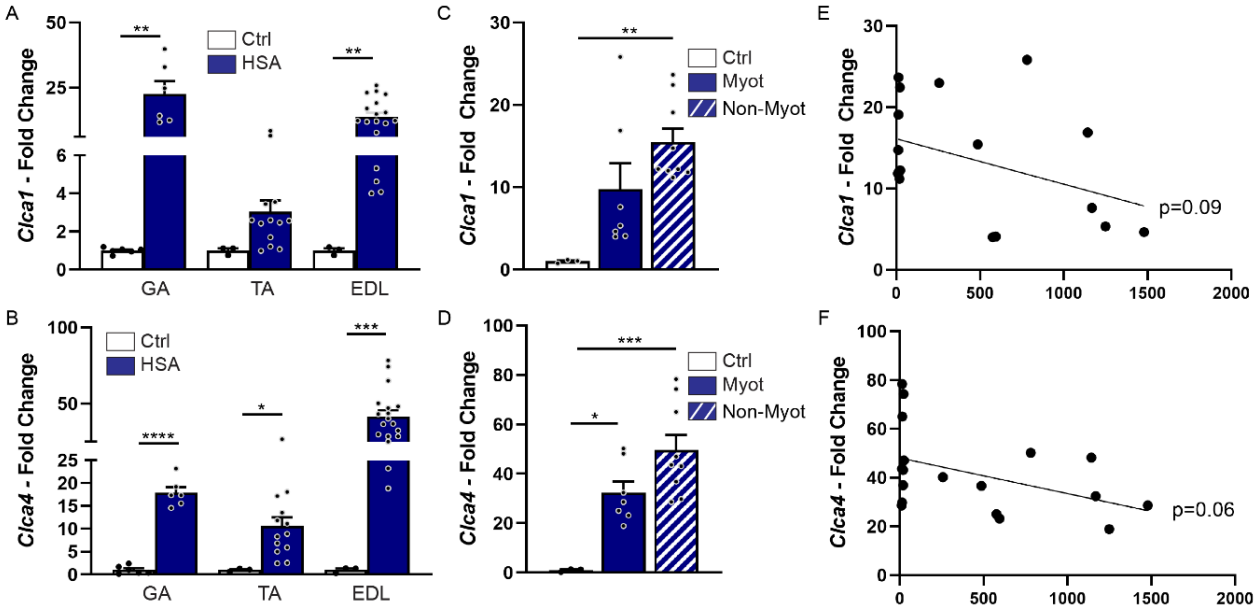

Figure 3: Expression of CLCAs is increased in *HSA^{LR}* mice.

A, B) Quantitative PCR analysis of the expression of the *Clca1* (A) and *Clca4a* (B) in GA, TA and EDL muscles from *HSA^{LR}* mice. N=6 (GA), 3 Ctrl and 13 HSA (TA), 3 Ctrl and 18 HSA (EDL). Expression is normalized on *Tbp* expression. C, D) Quantitative PCR analysis of *Clca1* (C) and *Clca4a1* (D) in EDL muscle from control mice and non-myotonic and myotonic *HSA^{LR}* mice. N=3 Ctrl, 7 myotonic, 9 non-myotonic. Expression is normalized on *Tbp* expression. E, F) Linear regression between *Clca1* (E) or *Clca4* (F) expression and the late relaxation time of EDL muscle from *HSA^{LR}* mice. Data represent mean ± SEM. *p<0.05, **p<0.01, ***p<0.001, ****p<0.0001, unpaired 2-tailed Student's t test (A, B) and one-way ANOVA with a Tukey's post-hoc analysis (C-F).

N-terminal cleaved product of CLCA1/4 is secreted in muscle cells

To get further insights on the role of CLCAs in skeletal muscle, we assessed the expression pattern of CLCA1 and CLCA4. As the detection of endogeneous proteins was impossible, we first validated plasmids encoding CLCA1/4 tagged with Myc-DDK in HEK293 cells. As previous reports suggested that CLCAs are cleaved, with a secretion of the obtained N-term peptide, we tested the expression of CLCAs by analyzing the N- and C-terminal parts of the protein with an antibody targeting CLCAs (epitope in the N-term) and Myc (tag fused in C-term). Following their overexpression, we detected the full-length protein of both CLCA1 and CLCA4 using anti-Myc (Figure 4A, B). The small peptide corresponding to the C-terminal part of the proteins was detected in both the cell lysate and the medium of the cells, suggesting that part of the C-term peptide is secreted (Figure 4A, B). Using anti-CLCA1, the peptide corresponding to the N-terminal part of the protein was detected most predominantly in the medium of the cells, and to a minor extent in the cell lysate (Figure 4A, B). In contrast, the N-terminal peptide of CLCA4 was barely detectable in the medium, but present in cell lysates (Figure 4A, B). These results validated the cleavage of CLCAs and suggested different processing and function of CLCA1 and CLCA4.

To go further, we applied similar analysis to C2C12 cells transfected with either *Clca1* or *Clca4* plasmids. As observed in HEK293 cells, we identified the full-length protein of CLCA1, as well as the C-terminal peptide mainly in cell lysates (Figure 4C). In contrast, the N-terminal peptide was detected both in cell lysate and the medium (Figure 4C). By treating cells with brefeldin A, to block the ER-to-Golgi trafficking, and thereby secretion of the protein, there was an additional band detected for the C-terminal peptide, and an enrichment of the N-terminal peptide in the cell lysate (Figure 4C). This suggested that post-translational modification of CLCAs peptides may occur in the Golgi and regulate the secretion of peptides. When CLCA4 was overexpressed in C2C12 cells, the full-length, the C-terminal and the N-terminal peptides were all detected in cell lysates (Figure 4D). Interestingly, contrasting with CLCA1, the N-terminal peptide was undetectable in the medium of the cells (Figure 4E). Of note, immunostaining against the Myc flag revealed a diffuse staining in C2C12 cells, with focal points of enrichment at the membrane (Figure 4F), suggesting that the full-length and/or the C-term peptide may play specific function at the plasma membrane. To validate these observations in mature muscle, we co-electroporated TA muscle from control mice with CLCA1 and GFP encoding plasmids. Western blot analysis 7 days after the electroporation allowed the detection of the full-length protein, as well as the C-terminal and N-terminal peptides in the electroporated muscle, while there were not detected in the contralateral non-electroporated muscle (Figure 4G). Immunostaining with the anti-CLCA1 and anti-Myc showed that a large proportion of fibers expressed CLCA1, with a diffuse staining observed with both staining (Figure 4H). Of note, as detected in C2C12 cells, the detection of the C-terminal part of the protein gave locally stronger signal, underneath the membrane, that remains to be further investigated (Figure 4H).

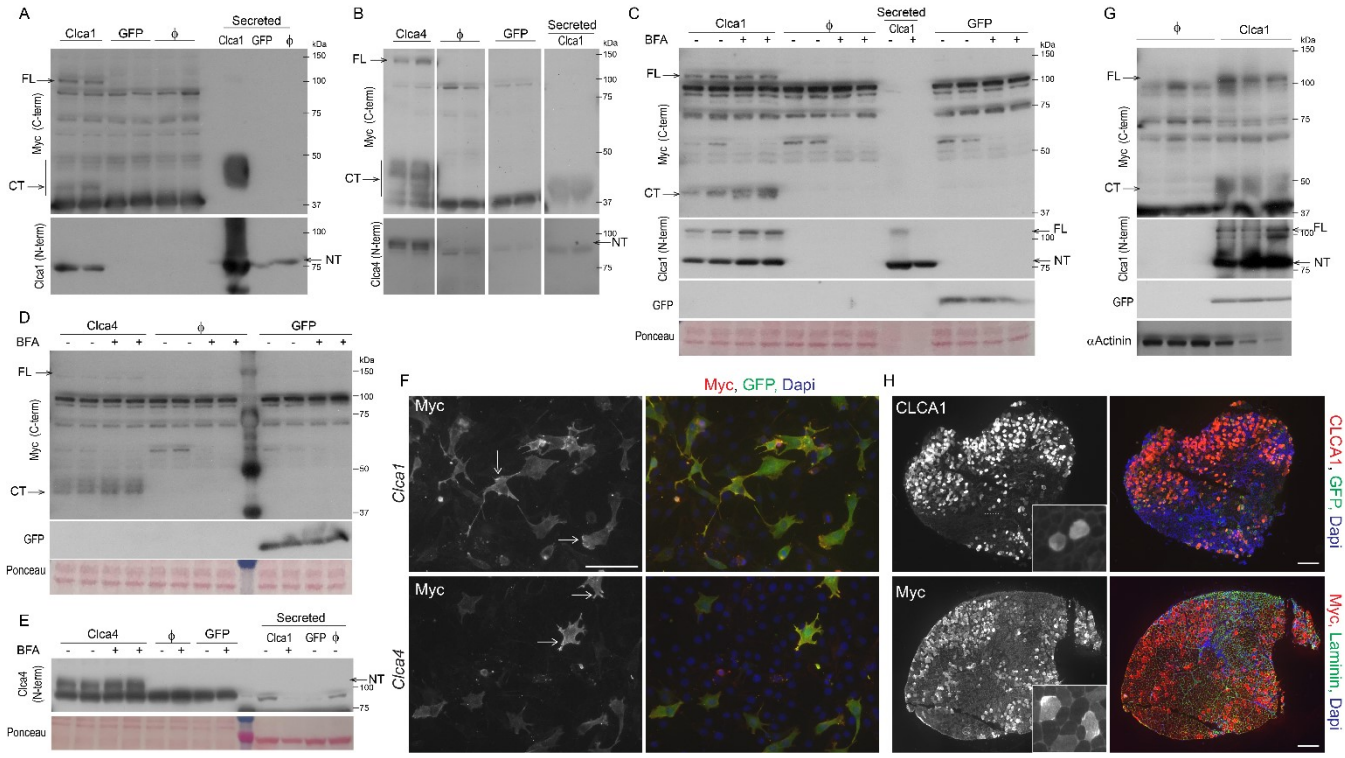

Figure 4: CLCA1/4 are cleaved in muscle cells.

A, B) Western blot analysis of CLCA1 (A) and CLCA4 (B) in the culture medium (secreted) and lysate from HEK293 transfected with overexpressing plasmids for *Clca1* (A), *Clca4* (B) or GFP (A, B). Full-length (FL) and C-terminal (CT) proteins are detected with anti-Myc. The N-terminal (NT) protein is detected with anti-CLCA1 (A) or CLCA4 (B). ∅: non-transfected cells. C-E) Western blot analysis of CLCA1 (C) and CLCA4 (D, E) in the culture medium (secreted) and lysate from C2C12 cells transfected with overexpressing plasmids for *Clca1* (C), *Clca4* (D, E), GFP (C-E) or not transfected (∅, C-E). Full-length (FL) and C-terminal (CT) proteins are detected with anti-Myc. The N-terminal (NT) protein is detected with anti-CLCA1 (C) or CLCA4 (D, E). BFA: brefeldin A. F) Immunofluorescent staining using anti-Myc in muscle cells co-transfected for *Clca1* (upper panel) or *Clca4* (down panel), and GFP. Arrows point to local accumulation. Scale bar, 100 µm. G) Western blot analysis of CLCA1 in lysate from TA muscle electroporated with overexpressing plasmids for *Clca1* or not electroporated (∅). Full-length (FL) is detected with both anti-Myc and anti-CLCA1. The C-terminal (CT) and N-terminal (NT) proteins are detected with anti-Myc and anti-CLCA1, respectively. H) Immunofluorescent staining using anti-CLCA1 (upper panel) or anti-Myc (lower panel) antibodies in TA/EDL muscles electroporated with *Clca1* overexpressing plasmids. Scale bar, 500 µm.

Together these results indicate that CLCA1/4 are cleaved in skeletal muscle, as observed in other cell types, and they suggest that the N- and C-terminal peptides generated likely play differential function in cells. Investigations on the effect of the overexpression of CLCA1/4 in DM1 muscle will be of major interest to assess their role in myotonia.

Expression of anoctamin and voltage-gated sodium channel is not affected in non-myotonic *HSA^{LR}* mice

As CLCAs have been involved in the regulation of chloride channels, in particular of the Anoctamin family, we checked whether expression of Anoctamins was changed in *HSA^{LR}* mice. Interestingly, the expression of *Ano1* was slightly reduced in myotonic *HSA^{LR}* mice, although with no difference between myotonic and non-myotonic mice (Figure 5A). Expression of *Ano5* and *Ano6* was also unchanged in mutant mice (Figure 5A). As splicing of *Ano1* has been reported to influence its function, we then evaluated splicing changes focusing on the exon 6b, 13 and 14 [255, 256]. By qPCR, there was no difference in the splicing of these exons between control, myotonic and non-myotonic mutant mice (Figure 5B). These results suggest that deregulation of CLCAs in *HSA^{LR}* muscle is not related to changes in Anoctamin expression, although one cannot rule out that the protein levels and/or the activity of Anoctamins may be affected in mutant muscle.

Lastly, as changes in voltage-gated sodium channels have also been suggested to contribute to myotonia in DM1 muscle, we determined if the loss of myotonia in some *HSA^{LR}* mice may correlate with changes in their expression. However, expression of *Scn1, Scn4a* and *Scn5a* remained unchanged in control, myotonic and non-myotonic mice. Moreover, splicing of the exon 6b of *Snc5a*, which has been shown to be abnormally excluded in heart from myotonic dystrophy patients [257], was not affected in *HSA^{LR}* mice. Hence, changes in the expression and known splicing of *Scn* genes is unlikely to contribute to the loss of myotonia in *HSA^{LR}* mice.

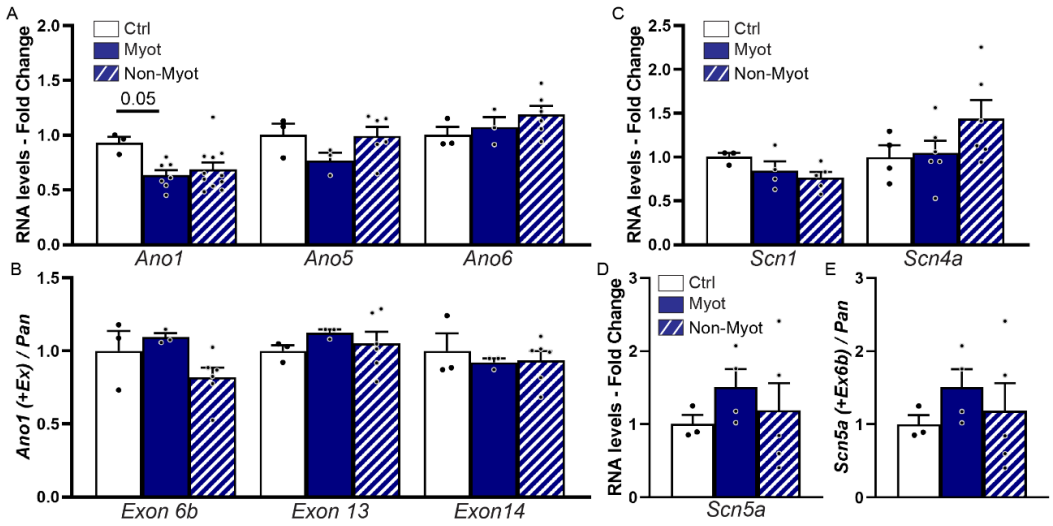

Figure 5: Expression of *Ano1/5/6* and *Scn1/4a/5a* is not altered in *HSA^{LR}* mice.

Quantitative PCR analysis of the total expression (A, C, D) and the splicing of the *Ano1* (B; inclusion of exon 6b/13/14, B), *Ano5 and 6* (A), *Scn1* and *4a* (C), and *Scn5a* (D; inclusion exon 6b, E) genes in EDL muscle from control mice, and myotonic and non-myotonic *HSA^{LR}* mice. N=3 Ctrl; 7 (A, *Ano1*), 3 (A, *Ano5/6*; B), 4 (C, *Scn1*; D,E), 6 (C, *Scn4a*) myotonic; 11 (A, *Ano1*), 6 (A, *Ano5/6*; B), 5 (C, *Scn1*; D,E), 6 (C, *Scn4a*) non-myotonic. Data represent mean ± SEM, one-way ANOVA with a Tukey's post-hoc analysis.

Discussion and outlook

CLCAs have been shown to regulate inhibitory chloride currents important for stabilization of membrane potential, as well as store-operated calcium entry (SOCE) through modulation of Ca^{2+}-activated chloride channels in several tissues [250-252]. Evidence suggests that activation of Ca^{2+}-activated chloride channels occurs via secretion of the N-terminal fragment after auto-proteolytic cleavage, whereas the function of the C-terminal fragment remains obscure [250, 258-260]. Albeit reports have suggested CLCA1-dependent regulation of Ca^{2+}-activated chloride channels also expressed in skeletal muscle, such as ANO1, their function in muscle tissue remain largely unknown [253, 254]. Here, we investigated whether CLCAs may contribute to the modulation of myotonia in DM1 muscle. Indeed, we identified that some inbred HSA^{LR} mice, a well-characterized model for DM1, lost their myotonic phenotype. The drastic improvement in muscle relaxation was associated with a minor shortening of the (CTG)n repeat present in the *HSA* transgene in HSA^{LR} mice. Such shortening is well-known in the context of DM1, and has actually already been reported in the initial HSA^{LR} line (20b), which went from 250 to 220 (CTG) repeats [249]. Here, we estimated that around 30 (CTG) were lost in some mice. Although there was a correlation between the repeat size and the late relaxation time of HSA^{LR} muscle, there were still non-myotonic mice exhibiting long repeat and myotonic mice with short repeat. This suggested that alternative mechanisms may modulate myotonia in the mutant mice.

In this context, we identified that CLCAs are up-regulated in HSA^{LR} mice, compared to controls. Expression of Clca1/4 tended to inversely correlate with the myotonia of the mice, prompting us to further investigate the expression and role of CLCAs in DM1. As the role of CLCAs in skeletal muscle remains largely unknown, we investigated whether results obtained in other cell types regarding CLCA1/4 expression is also observed in muscle. By overexpression of CLCA1/4 in C2C12 cells and in muscle in vivo, we found that CLCA1 self-cleavage occurs also in skeletal muscle with subsequent secretion of its N-terminal fragment. In contrast, although CLCA4 was also cleaved in muscle cells, the N-terminal peptide remained largely inside the cells.

To get further insights on the role of CLCAs in skeletal muscle, immunoprecipitation of the N- and C-terminal peptides, followed by proteomics analysis will help to identify specific interaction partners. Electrophysiological measurement of chloride fluxes in isolated and electrically stimulated muscle fibers upon CLCA overexpression or knockdown may further help to delineate its contribution to membrane potential and to chloride channel regulation. In a recent report, CLCA1 has been shown to interact and regulate the chloride channel ANO1 [254], but whether CLCAs may also modulate the activity of other chloride channel, including ClC-1 remains to be determined.

Whether CLCAs play a role in DM1-associated myotonia also remains an open question. Our findings suggest compensatory up-regulation of CLCA1/4 to counteract myotonic discharges. However, further studies are needed to verify this hypothesis. Evaluation of the late relaxation time in EDL and TA muscles that overexpress *Clca1/4* in muscle from HSA^{LR} mice, as well as in other DM1 mouse models, like $Mbnl1^{\Delta 3/\Delta 3}$ mice, will be of major interest. To this end, I showed that the overexpression of

CLCA1 is feasible in control muscle by electroporation. Although it allowed efficient detection of the full-length protein, as well well as the cleaved N-terminal and C-terminal fragments, electroporation brings the concern of potential damaging the muscle. In this context, freshly formed myotonic myofibers in HSA^{LR} muscle may exert milder phenotype, which may artificially affect the late relaxation time. AAV-mediated delivery may minimize this risk. In addition, the loss of the active and secreted N-terminal fragment in solution during the *ex-vivo* force measurement may also create a bias. *In situ* assessment of myotonia in TA muscle may represent an alternative. As we failed to detect myotonia in TA from HSA^{LR} mice using *in situ* measurement (data not shown), the use of another model for DM1, such as $Mbnl1^{\Delta 3/\Delta 3}$ mice, in which strong relaxation delay was detected *in situ* (data not shown), will be necessary. Inversely, *in vivo* shRNA-mediated knockdown of *Clca1/4* and/or of their potential targets (*i.e. Ano1*) may be used to verify that the loss of CLCA1/4 in DM1 muscle aggravates myotonia, and constitutes therefore an adaptive protective mechanism in the context of DM1. Evaluation of their expression in muscle biopsies from patients will be as well of major interest.

In conclusion, our study points to interesting effectors, which may be involved in the modulation of myotonia in DM1 or liable to improve muscle relaxation in DM1 muscle by regulating the activity of different chloride channels. Further investigations will be essential to validate their pathophysiological role in DM1.

Material and Methods

Mice

Homozygous mice of the mouse line LR20b carrying about 250 (CTG) repeats within the *HSA* transgene (HSA^{LR}) were obtained from Thornton and colleagues (University of Rochester Medical Centre, Rochester, New York, USA) [153]. Mice of the corresponding background strain (FVB/N) were used as control. Mice were genotyped for HSA^{LR} transgenes by quantification of *ACTA1* levels normalized to endogenous actin (mouse *Acta1*) in genomic DNA. Mice were maintained in a conventional specific-pathogen–free facility with a fixed light cycle (23°C, 12-hour dark-light cycle). All animal studies were performed in accordance with the European Union guidelines for animal care and approved by the Veterinary Office of the Canton of Basel city (application number 2601).

Muscle force and relaxation

In vitro force measurement of EDL muscle was conducted as previously described [239]. Half- and late relaxation times were calculated according to Moyer et al. (2011) [240].

Western blotting

Muscles powdered in liquid nitrogen were lysed in cold RIPA+ buffer (50 mM Tris-HCl pH 8, 150 mM NaCl, 1% NP-40, 0.5% sodium deoxycholate, 0.1% SDS, 1% Triton X, 10% glycerol, phosphatase and protease inhibitors). Following dosage (BCA Protein Assay, Sigma-Aldrich), proteins were separated on SDS-polyacrylamide gels and transferred to nitrocellulose membrane. Blots were blocked in TBS, 3% BSA, 0.1% Tween-20, and incubated overnight at 4°C with primary antibodies, then for 2 hours with HRP-labelled secondary antibodies. Immunoreactivity was detected using the ECL Western blot detection reagent LumiGLO (KPL) and exposed to Super RX-N films (Fujifilm). Protein expression was normalized to α-actinin.

Electroporation of muscle

Mice were anesthetized by isoflurane inhalation (3 %, 2.5% oxygen flow) and TA muscles injected with 8 U of hyaluronidase (SIGMA M7167) for 1h. Plasmids were injected into TA muscles at concentration of 1µg/ul and electroporated with the Nepa21 electroporator.

Cell culture

HEK293 and C2C12 cells were cultured in growth medium (DMEM, 10% FBS, 1% Penicillin-Streptomycin. Plasmids were transfected with lipofectamin 2000/3000 from Invitrogen, according to the protocol of the manufacturer. Cells were treated with brefeldin A (SIGMA) at a concentration of 2µg/mL. For protein extraction, cells were lysed in cold RIPA+ buffer (50 mM Tris-HCl pH 8, 150 mM NaCl, 1% NP-40, 0.5% sodium deoxycholate, 0.1% SDS, 1% Triton X, 10% glycerol, phosphatase and

protease inhibitors). For concentration and recovery of proteins in cell media, Amicon ultra filters were used according to the manufacturer's protocol.

Plasmids

Plasmids encoding CLCA1 (NM_017474) and CLCA4 (NM_207208) tagged with Myc-DDK were obtained from Origen (MR211160 and MR217842). They were amplified with NucleoBond Xtra Maxi endotoxin-free plasmid kit (Macherey-Nagel).

Antibodies

All primary antibodies were used at 1/1000 for Western blot; when the antibody was used for IHC, the dilution is indicated in the list. The following antibodies were used: α-actinin (A5044) from Sigma; Laminin (ab11575 and ab11576; 1/300 for IHC), anti-MYC (ab9132), CLCA1 (ab180851; 1/200 for IHC) from Abcam; CLCA4 (c400662) from LSBio, GFP (A10262; 1/200 for IHC) from ThermoFisher.

Polymerase chain reaction

Total RNAs were extracted with the RNeasy Mini Kit (Qiagen), reverse transcribed with the SuperScript III First-Strand Synthesis System (Invitrogen), and amplified with the Power SYBR Green Master Mix (Applied Biosystems) or the Hot FirePol EvaGreen qPCR Mix (Solis BioDyne). Expression of specific spliced or pan transcripts was analysed by quantitative PCR with StepOne software and normalization to *Tbp* expression. Primers are listed in Table 2.

Histology and immunofluorescence

Muscles were frozen in liquid nitrogen–cooled isopentane. For immunostaining, eight micrometer sections were fixed with 4% paraformaldehyde (PFA), then blocked in PBS, 3% BSA, incubated sequentially with primary and secondary fluorescent antibodies (Invitrogen), mounted with Vectashield medium (Vector), and observed with a Olympus fluorescent microscope.

For immunostaining on muscle cells, cells were cultured on gelatin-coated coverslips in 24 well plates. Coverslips were fixed with 4% PFA/2% sucrose, incubated in 0.1M glycine/PBS, blocked with 3% IgG free BSA 0.5% triton for 1.5h, incubated sequentially with primary and secondary fluorescent antibodies, mounted with Vectashield medium (Vector), and observed with a Leica fluorescent microscope. Images were acquired using an Olympus microscope.

Fluorescence *in situ* hybridization

FISH was conducted on muscle cryosections as previously described by Batra et al. (68), using a Cy3-CAG10 DNA probe. Nuclear foci were observed with a Leica confocal microscope.

Statistics

Quantitative data are displayed as mean ± SEM of independent samples, with n (number of individual experiments) ≥ 3. Statistical analysis of values was performed using unpaired Student's t test or 2-way ANOVA test with Tukey's multiple comparisons test correction, with a 0.05 level of confidence accepted for statistical significance.

Acknowledgements

We thank Prof. C. A. Thornton (University of Rochester Medical Centre) for the generous gift of HSA^{LR} mice. This work was supported by the University of Basel and University Hospital Basel (MS), the University of Basel–Stadt and Basel-Landschaft (MAR), the Neuromuscular Research Association Basel (MS, PC), the Swiss Foundation for Research on Muscle Diseases (MAR, MS), the Olga Mayenfisch Foundation (PC), and the Swiss National Science Foundation (PC, MS).

Competing interests

There is no conflict of interest.

Table 2

Gene	Forward primer	Reverse primer
Atp2a1 +ex22	5'- GCCCTGGACTTTACCCAGTG-3'	5'-ACGGTTCAAAGACATGGAGGA-3'
Atp2a1 pan	5'- GCCCTGGACTTTACCCAGTG-3'	5'-CCTCCAGATAGTTCCGAGCA-3'
Camk2b -ex13	5'-TTTCTCAGCAGCCAAGAGTTT-3’	5'-TTCCTTAATCCCGTCCACTG-3'
Camk2b pan	5'-GCACGTCATTGGCGAGGA-3'	5'-ACGGGTCTCTTCGGACTGG-3'
Clca1	5'--AGTATGGGCCACAAGACAGG-3'	5'--AAAGGAAAACCCCAAGCAGT-3’
Clcn1 +ex7a	5'-GGGCGTGGGATGCTACTTTG-3'	5'- AGGACACGGAACACAAAGGC-3'
Clcn1 pan	5'-CTGACATCCTGACAGTGGGC-3'	5'- AGGACACGGAACACAAAGGC-3'
Scn1b	5'-ATACCGAGGCTGTGTATGGG-3'	5'-CAAAGCGCTCATCTTCCTCC-3'
Scn4a	5'-AAAGGCCATCTTCCGATTCT-3'	5'-CGTGGATGAGCACCTTGATA-3'
Scn5a pan	5'-ACAATCGTGGGAGCCCTAAT-3'	5'-GGTCCATTGACTCAGTAAA-3'
Scn5a +ex6b	5'-CATGGCGTATGTATCAGAGAA-3'	5'-CAGGCCTGAAATGACCGATA-3'
Ano1 pan	5'-CGCCCTGCTAAACAACATCA-3'	5'-CACGTCTGACTTCATCCCTCG-3'
Ano1 +ex6b	5'-CAGCATGGGTATCACCAGCCTCCTG-3'	5'-TTCCTGACCAGGTCAATGGGCTGG-3'
Ano1 +ex13	5'-CCCTGCCACCGTCTTCTTCTCTGTG-3'	5'-TGCTCTGGGATGATCCTCCTCCTCC3’
Ano1 +ex15	5'-AGAGACCGACAAGGTGAAGCTGACC-3'	5'-CGTCAGTGTACCCCGGATGTTGGA-3'
Ano5	5'-GATGCCTGGAAGCTGACAAC-3'	5'-CGAATTCCACAGAGCCCTTG-3'
Ano6	5'-AGTTGTCCTAGCGAGCGTTA-3'	5'-GCTTGGCTGGGCTATTACAC-3'
Tbp	5'-CTCAGTTACAGGTGGCAGCA-3'	5'-CAGCACAGAGCAAGCAACTC-3'

Table 2: List of primers

4. Discussion and Outlook

Since the postulation of the paradigm of an RNA-induced toxicity in DM1, research and therapeutic approaches have predominantly focused on counteracting the spliceopathic nature of the disease. Although efforts have been made to identify cellular processes that are deregulated in DM1, a detailed understanding of their contribution to DM1 muscle pathology is still missing. During my PhD, I investigated whether NMJ alterations contribute to DM1 muscle pathology, using two mouse models for the disease. I established that DM1 associates with structural alterations of the motor endplates, which was accompanied by changes in synaptic gene expression and AChR dynamics. Moreover, I confirmed that CaMKIIs are deregulated in DM1 muscle and I identified, in particular, the loss of the muscle-specific and NMJ-associated CaMKIIβ isoform (CaMKIIβM). Lastly, I showed that the muscle response to nerve injury is perturbed in DM1 muscle. These results indicate that defective NMJ maintenance may contribute DM1 pathophysiology, and may involve deregulation of CaMKII-dependent mechanisms. In the following, results obtained in the project 1 will be further discussed. Discussion and outlook for the project 2 are included in the part 3.2.

4.1 NMJ deterioration in DM1: *contribution to DM1-related muscle pathology?*

One aspect that has been under debate for decades in the DM1 field is the potential involvement of NMJ alterations in muscle pathophysiology. Studies have reported changes at the NMJs in muscle from DM1 patients and DM1 mouse models, but it is unknown what mechanisms underlie these perturbations and whether these stem from the muscle or the nerve.

4.1a NMJ alterations: comparison between mouse models and patients

- *Signs of NMJ deterioration in DM1 patients*

Early studies have implicated NMJ-associated alterations in DM1. In some reports, muscle biopsies from DM1 patient show multiple and abnormally large endplates on the same muscle fiber [224, 225]. Moreover, pre-synaptic changes, such as axon swelling and sprouting, are consistent with peripheral neuropathy [225]. Accordingly, neurophysiological studies revealed abnormal neuromuscular transmission in DM1 patients, which suggested that NMJ impairments contribute to DM1 muscle weakness and fatigue [261]. Of note, the presence of ribonuclear foci and MBNL1 sequestration in sub-synaptic myonuclei of DM1 muscle biopsies suggests potential DM1-associated mis-splicing of genes important for NMJ maintenance [230]. Although the mechanisms and specific molecules contributing to these changes remain unknown, these observations point to NMJ-associated alterations as a common feature in DM1 muscle pathology.

- *NMJ alterations in mouse models for DM1*

Studies conducted in DM1 mouse models provided further support for NMJ alterations in DM1. DMSXL mice showed partially denervated endplates and morphological changes, such as a reduction in the number of myelinated motor neurons and in AChR density [161, 262]. Moreover, sciatic nerves of DMSXL mice exhibit structural alterations reminiscent of an axonopathy [262]. Similarly, muscle of *Mbnl1/2* compound knockout mice exhibited an increased loss of mature NMJs, which was accompanied by an abnormal increased incidence of premature NMJs [235]. Hence, besides skeletal muscle itself, the development and maintenance of NMJs may be affected in DM1.

During my PhD study, I investigated and compared NMJ perturbations in two DM1 mouse models. I first showed that $Mbnl1^{\Delta 3/\Delta 3}$ mice have an increased fragmentation of the endplates in different muscles at different ages. In accordance with previous results obtained in muscle biopsies from DM1 patients, $Mbnl1^{\Delta 3/\Delta 3}$ muscle did not show signs of functional denervation, such as extra-synaptic clusters, overt axon sprouting or degenerated fiber segments. As *Mbnl1* is knocked out in both muscle and motor neurons, this raised the question if the observed alterations arise from pre-or- post-synaptic changes. Secondly, using the HSA^{LR} mice, I also observed higher fragmentation of endplates, at different ages without any signs of denervation. As expression of pathological (CUG)n repeats is restricted to muscle fibers in these mice, these results nicely highlight the contribution of DM1-associated perturbations in muscle to NMJ alteration [230]. I included in the study a comparison between three distinct muscles, which have been shown to be differently affected in HSA^{LR} mice. Interestingly, I observed strong endplate fragmentation in the affected *gastrocnemius* muscle, but also in the less affected muscles EDL and TA.

Endplate fragmentation has been observed in context of muscular dystrophies, such as Duchenne Muscular Dystrophy, but the origin of this phenomenon is still not fully understood [263-265]. Degeneration of muscle fiber segments underneath postsynaptic sites, as well as to the deterioration of the pre-synaptic motor neurons followed by denervation/re-innervation cycles may contribute to this fragmentation [266]. As HSA^{LR} and $Mbnl1^{\Delta 3/\Delta 3}$ mice only show minor muscle degeneration/regeneration or pre-synaptic alterations, these events are unlikely to cause the deterioration of the endplates. Hence, other changes in signaling pathway or cellular processes in muscle are likely to contribute to the observed degeneration of the endplates.

4.1b Changes associated to NMJ perturbations

- <u>*Changes in synaptic gene expression*</u>

In innervated active muscle, expression of synaptic genes, such as *Chrn* and *MuSK*, is maintained in sub-synaptic myonuclei and suppressed at extra-synaptic sites [49, 267]. This is ensured on the one hand, by permissive regulations at sub-synaptic sites, and on the other hand, by the repressive action of different effectors, such as MITR and DACH2, in extra-synaptic nuclei. In contrast, in the absence of electrical activity, nuclear import of HDAC4 represses MITR and DACH2 expression, leading to up-regulation of *Myog*, and in turn of synaptic genes [83, 84, 233, 238].

HSA^{LR} and Mbnl1$^{\Delta 3/\Delta 3}$ muscles showed similar changes in the expression pattern of activity-dependent genes. Interestingly, expression of *Dach2* tended to decrease, while *Chrna1* expression (encoding AChR α-subunit) was increased under basal conditions. As there was no sign of denervation in innervated *HSA*^{LR} and *Mbnl1*$^{\Delta 3/\Delta 3}$ muscles, such as extra-synaptic AChR clusters, the increased expression of *Chrn* subunits may rather relate to an abnormal regulation of activity-dependent genes, and in particular to an abnormal switch to the developmental expression program. Considering the fact that I used cDNA from total muscle lysate, changes in expression may predominately reflect altered expression pattern in extra-synaptic regions. Still, major changes specifically in sub-synaptic nuclei may be detectable. In this context, RNA *in situ* hybridization may help to evaluate expression of synaptic genes at specific sites in DM1 muscle. Moreover, laser capture microdissection (LCM) and subsequent gene enrichment analysis (GO ontology), and/or single-nucleus RNA-sequencing (snRNA-seq), may give further insights into the transcriptional heterogeneity of extra- and sub-synaptic regions in DM1 muscle. In particular, ribonuclear inclusions were detected in both extra- and sub-synaptic myonuclei. Whether genes important for NMJ maintenance, especially in sub-synaptic nuclei, are directly affected by their presence, remains unknown [120, 230]. To our knowledge, investigations in the field are scarce and predominantly relate to the potential contribution of defective post-transcriptional processing of synaptic molecules to the neurological phenotype of DM1 patients [163]. Hence, future studies on genes affected in sub-synaptic regions in DM1 muscle may be warranted.

- *Changes in synaptic protein dynamics*

The post-synaptic apparatus of skeletal muscle fibers is characterized by the selective aggregation of specific cytoskeletal and membrane proteins, including AChRs, rapsyn, and MuSK. To ensure maintenance of the post-synaptic structure upon different functional demands, correct expression, adequate supply and precise localization of synaptic proteins has to be warranted. Proper AChR subunit composition, localization, and density are essential for normal neuromuscular transmission and therefore muscle activity. AChR turnover comprises AChRs biosynthesis, delivery to the membrane, as well as their recycling and degradation after endocytic internalization.

In this study, I showed that AChR turnover is increased in innervated muscle from *Mbnl1*$^{\Delta 3/\Delta 3}$ mice. Similarly, AChR turnover tended to be higher in *HSA*^{LR} muscle under basal conditions compared to control muscles. Of note, *gastrocnemius* muscle cannot be tested for AChR turnover, as the assay was not optimized for large tissue. As *gastrocnemius* shows in general stronger changes in *HSA*^{LR} mice, than EDL/TA muscles, increase in AChR turnover in this muscle may be significant and more similar to changes observed in *Mbnl1*$^{\Delta 3/\Delta 3}$ mice. The increase in synaptic gene expression detected in both models under basal conditions may contribute to the increase in AChR turnover. In parallel, I found that AChR recycling tends to decrease in *Mbnl1*$^{\Delta 3/\Delta 3}$ muscle. Reduced recycling of AChRs may lead to the re-routing of the receptors to the degradative route in mutant muscle, and thereby to their increased turnover. Optimization of the recycling assay will help to identify more precisely changes or defects in

the AChR recycling in DM1 muscle. This may be obtained in particular by reducing the period between the injection of the bungarotoxin coupled with biotin (followed by immediate injection of the first streptavidin) and the injection of the second streptavidin used to mark recycled receptors at the membrane. Adjustment of the procedure for *gastrocnemius* may also reveal more important changes in HSA^{LR} muscle.

Interestingly, similar changes have been observed in α-syntrophin deficient mice and α-dystrobrevin null mice, which exhibit decreased AChR recycling, as well as an increase in AChR turnover. This ultimately leads to a decrease in AChR density at the membrane surface [237, 268]. Hence, reduced recycling may well contribute to the increased endplate fragmentation observed in innervated mutant muscle. Of note, the increased expression of synaptic gene may be a compensatory mechanism induced at the NMJ to cope with the increased degradation of the receptors. Analyses of the rates of internalization and degradation of AChRs at the endplates in DM1 mice will bring further insights on the existing perturbations. Overall, these findings suggest that processes associated with AChR turnover are perturbed in DM1, which may lead to alterations in NMJ maintenance.

- *Contribution of pre-synaptic perturbation on NMJ deterioration?*

As mentioned above, DM1 patients and mouse models show signs of both pre- and post-synaptic alterations. MBNL1 is depleted in muscle and in motor neurons of $Mbnl1^{\Delta 3/\Delta 3}$ mice. In contrast, HSA^{LR} mice express the pathological (CUG)n only in muscle tissue. It is hence unlikely that pre-synaptic perturbations primarily contribute to the observed NMJ deterioration. Moreover, NMJs of both HSA^{LR} and $Mbnl1^{\Delta 3/\Delta 3}$ mice did not exhibit obvious changes in the pre-synaptic compartments under basal conditions. These findings do not exclude a contribution of pre-synaptic alterations to DM1 muscle pathology, but they suggest that changes in muscle contribute to NMJ deterioration. Of note, studies conducted in $Mbnl1^{-/-}$; $Mbnl2^{+/-}$ compound knockout mice suggest that MBNL2 up-regulation in $Mbnl1^{\Delta 3/\Delta 3}$ mice may compensate for the loss of MBNL1 in muscle but also in motor neuron [235]. Consequently, one could envisage that the observed effects in $Mbnl1^{\Delta 3/\Delta 3}$ muscle are limited by this compensatory mechanism. Reduction of MBNL2 especially in motor neuron in $Mbnl1^{\Delta 3/\Delta 3}$ mice, may lead to severe aggravation of the phenotype observed at the NMJ, by combining deleterious changes in both the pre- and post-synaptic compartments. Since homozygous genetic ablation of MBNL1/2 is embryonically lethal, it would be interesting to analyze NMJs and changes in NMJ-associated signaling in $Mbnl1^{\Delta 3/\Delta 3}$; $Mbnl2^{+/-}$ compound mice.

4.1c Contribution to DM1-associated muscle pathology

- *NMJ fragmentation: an indicator for NMJ dysfunction?*

Endplate fragmentation is often used as an indicator for defective NMJ maintenance and function. However, in the last years, a novel debate on the correlation between endplate fragmentation and NMJ dysfunction opened in the aging field. Indeed, a study from Willadt et al. (2016) suggested that increased

endplate fragmentation does not correlate with reduced neurotransmission efficiency or decline in NMJ function [236]. Hence, evaluation of endplate fragmentation may not be relevant enough to conclude on functional changes at NMJs. Still, fragmentation is thought to happen upon destabilization of the motor endplate, which may be accompanied by a reduced density of synaptic proteins aggregated at the membrane. It may hence precede degeneration of the endplate, and the induction of dying back process of the motor neurons. In our models, extensive characterization of the NMJs, with novel tools like the NMJ-morph software developed by the group of Gillingwater [269] may be of interest to complement the fragmentation results. Evaluation of the density of AChRs at the sarcolemma in the NMJ region would also bring complementary insights.

- *Comparison with aging – DM1 as a model for muscle aging?*

Several reports have pointed to similarities between DM1 and aging, leading to the idea that DM1 may be considered as a syndrome of premature aging [270-272]. Similarities include in particular the appearance of cataracts and cognitive decline in patients, as well as muscle affliction. Aging is associated with gradual loss of muscle strength and mass (referred to as sarcopenia) [273, 274]. Interestingly, structural changes in pre- and post-synaptic compartments of NMJs are hallmarks of sarcopenia, and are likely to contribute to age-related muscle weakness. Upon aging, the frequency of denervation events increases; abnormalities such as axonal sprouting, AChRs at extra-synaptic sites, and endplate fragmentation are also observed [274-276]. In this context, changes in the expression of synaptic genes, including the up-regulation of *Chrna1* and *Chrng* have been reported *[277, 278].* However, in contrast to DM1, these changes are likely associated to the increased incidence of fiber denervation and the induction of the associated gene expression program. Hence, NMJ deterioration in DM1 and aging may not be comparable processes. Notwithstanding, perturbations in common cellular processes may still be involved in NMJ changes in both pathological conditions. In particular, impaired autophagy has been shown in DM1 and aging muscles [216, 279, 280]. Blockage in autophagic flux is associated with endplate degeneration in *Atg7*$^{-/-}$ mice, which involves impaired autophagy-mediated degradation of AChRs [79]. Interestingly, AChR turnover was increased in these conditions, although the underlying mechanisms remain unknown. Hence, one can hypothesize that in both DM1 and aging, altered autophagic flux may contribute to increased AChR turnover (as shown in my work), which may ultimately lead to NMJ fragmentation and degeneration. Another process that may contribute to NMJ deterioration in DM1 and aging is the dysfunction or loss of muscle stem cells (MuSC). Indeed, a recent study has established that deficiency in MuSCs in adult mice precipitates NMJ degeneration. MuSCs would be required to support nuclei turnover in the sub-synaptic region [281]. Reduced MuSC proliferation capacity has been reported in DM1 patients and mouse models [281, 282]. MuSC dysfunction is suggested to contribute to muscle atrophy and to limit the regenerative capacity of DM1 muscle. Reduction in MuSC proliferative capacity may also contribute to NMJ deterioration. Further

investigations in this direction would be of major interest to complement the comparison between DM1 and aging, and unveil mechanisms involved in DM1-associated muscle pathology.

4.2 Pathomechanisms underlying NMJ deterioration in DM1

4.2a Deficiency in CaMKIIs is a hallmark of DM1

In DM1, aberrant splicing of CaMKII isoforms is considered as a main mis-splicing event in multiple tissues, including brain and skeletal muscle [199]. However, how these splicing changes affect the expression and function of CaMKII isoforms, and how these deregulations contribute to DM1 pathogenesis, especially in muscle, remain unclear.

- *Mis-splicing affecting Camk2b*

Mis-splicing of *CAMK2B* has been described in DM1 patients; the abnormal exclusion of the variable exons 13 and 16/17 has been reported in some studies [198, 221, 283]. Here, I confirmed that *Camk2b* is mis-spliced in both HSA^{LR} and $Mbnl1^{\Delta 3/\Delta 3}$ mice by exclusion of exon 13. In parallel, using RNA-seq results obtained in the group with HSA^{LR} mice, I identified another predominant splicing change in HSA^{LR} muscle, with the exclusion of the exons 18-20. Exclusion of these exons was confirmed by qPCR in both HSA^{LR} and $Mbnl1^{\Delta 3/\Delta 3}$ mice. Moreover, exclusion of these exons explained the loss of the muscle-specific isoform of CaMKIIβM detected by Western blot in HSA^{LR} and $Mbnl1^{\Delta 3/\Delta 3}$ mice. To our knowledge, the abnormal splicing of exons 18/19/20 has not yet been described. Exons 18 to 20 reside in the variable region inside the linker domain of *Camk2b* and encode an additional 12kDa peptide. Of note, it may be that the splice variant specific for muscle is expressed only in mature myofibers, as we observed a shift in splicing towards the loss of the variable inserts (encoded by exons 18-20) upon denervation in control mice (Figure 7). However, studies on the developmental regulation and function of the different isoforms of CaMKIIβ in muscle have not been conducted. Interestingly, CaMKIIβM does not migrate at the expected size on western blot (around 70 kDa, when planned at around 60). To confirm that the band lost in DM1 mice corresponds to CaMKIIβM, I conducted mass spectrometry analysis. Peptides corresponding to the common region of CaMKIIβ isoform were found in excess in HSA^{LR} mice, while peptides corresponding to the variable inserts were less abundant, as compared to control muscle. This confirmed that the CaMKIIβM isoform is specifically lost in DM1 muscle. Because antibodies against CaMKIIs are not specific enough, it was difficult to characterize more precisely the changes in DM1 muscle. In particular, other abnormal bands are observed around the size of non-muscle CaMKIIβ (similar to CaMKIIγ/δ) in DM1 muscle: identification of the corresponding products would require mass spectrometry analysis following extraction of the band. Expression of the different products identified in muscle from DM1 mouse models would also need to be confirmed in muscle biopsies from DM1 patients. The potential functional consequences of CaMKIIβM mis-splicing will be discussed below.

- *Mis-splicing affecting other Camk2 genes*

Investigations conducted in DM1 brain tissue reported the mis-splicing of CaMKIIδ by increased inclusion of exons 14–15 (exons 14–16 in mice). This leads to an enhanced expression of fetal CaMKIIδ isoforms [177, 199]. Of note, using RNA-seq results obtained for HSA^{LR} mice, I did not detect changes in the expression pattern of CaMKIIδ. This suggests that this mis-splicing event may be limited to specific tissues, such as brain. In parallel, changes affecting splicing of *CAMK2G* have been reported in muscle from DM1 patients, with an increased retention of intron 18-19 and exon 18 [221, 283]. In this study, I showed that inclusion of exons 13, 15 and 19 of *Camk2g* is increased HSA^{LR} muscle. These changes were overall less important as compared to the changes detected in *Camk2b*. As CaMKIIα isoforms are predominantly expressed in brain tissue, information on potential deregulations of CaMKIIα in DM1 muscle is rather scarce. As muscle expresses a non-kinase variant of CaMKIIα (α-kap), which anchors CaMKIIβM to specific subcellular sites, including NMJs, analysis of α-kap expression in DM1 muscle would be of major interest [77, 112].

4.2b Pathophysiological role of CaMKII deficiency

- *Prediction and models for CaMKII deficiency*

The consequences of the genetic ablation of CaMKIIs have been mainly described in the brain. In particular, deficits in learning and memory have been reported for $Camk2a^{-/-}$, $Camk2b^{-/-}$, $Camk2d^{-/-}$ and $Camk2g^{-/-}$ mice [284-288]. The importance of CaMKIIδ isoforms has also been established in the heart, where it may associate with α-kap to regulate cardiac relaxation *via* interaction with SERCA2 [289]. For most isoforms, further investigations using tissue-specific knockout models, to address their function remain to be conducted [290].

Global genetic ablation of CaMKIIβ ($Camk2b^{-/-}$ mice) leads to developmental delay, cognitive defects, altered body composition, reduced muscle strength, and impaired motor coordination [291]. Studies in the brain pointed to a major role of CaMKIIβ in synaptic plasticity, as well as structural organization. In contrast, the physiological roles of CaMKIIβM in skeletal muscle remain ill-known. CaMKIIβ isoforms contain a F-actin binding domain allowing binding to the cytoskeleton of muscle fibers and brain [285, 292]. In brain, cytoskeletal-targeting of CaMKIIβ isoforms is involved in the regulation of the structure of dendrites. Interestingly, the F-actin domain is encoded by the exon 13 of *Camk2b*, which is retained in only some CaMKIIβ isoforms, including CaMKIIβM. Abnormal exclusion of exon 13 in DM1 muscle may hence affect actin cytoskeleton organization. In parallel, evidence suggests that the longer linker domain of CaMKIIβM (*i.e.* encoded by exons 18-20) modulates its affinity and sensitivity for CaM, and facilitates relative positioning of the kinase domains within the holoenzyme. Consequently, CaMKIIβM exhibits higher autonomous activity and a broader frequency response to Ca^{2+} oscillations than other CaMKIIβ isoforms [112, 114]. *In-vitro* studies using Drosophila CaMKII homologs also suggested that the variable domain of CaMKIIs modulates the affinity and specificity of their kinase domain [293]. Of note, the 12kDA insert of CaMKIIβM consists of three

proline-rich repeats containing a putative binding site for proteins that harbor a SH3-domain [294]. Therefore, exclusion of this insert may compromise the activity of CaMKIIβM, but also specific protein-protein interactions, which may contribute to its proper localization at subcellular sites. CaMKIIβM is targeted to the membrane of the SR via α-kap. There, CaMKII-mediated phosphorylation of RyR1, phospholamban and SERCA directly regulates activity-induced Ca^{2+} release and uptake [107-111]. Although it remains unclear which CaMKII isoform is involved in these phosphorylation, CaMKIIβM deficiency may affect muscle contractility and relaxation by affecting the release of Ca^{2+}. In addition, CaMKIIβM is the only isoform expressed at post-synaptic sites, where it co-localizes with AChRs [77]. In this context, studies have reported that α-kap associates with AChRs and promotes AChR stability at mature NMJs [295]. As CaMKIIs are players in regulating AChR recycling *in-vivo*, CaMKIIβM deficiency may lead to changes in AChR turnover and therefore NMJ maintenance. As CaMKIIβM is the only isoform containing these three inserts, it is likely that it plays specific roles in the physiology of skeletal muscle and that its loss, in DM1, contributes to the deterioration of muscle maintenance and/or function.

- <u>*CaMKII deficiency: Contribution to NMJ deterioration by affecting synaptic genes*</u>

CaMKIIs are thought to play a determinant role in the regulation of synaptic gene expression. CaMKIIs would suppress the expression of AChRs in non-synaptic regions by direct phosphorylation of myogenin and by inhibiting the nuclear import of HDAC4 [86, 90, 101]. HDAC4 inhibition would allow the expression of DACH2 and MITR responsible for the repression of myogenin and synaptic gene expression in innervated muscle [101, 223, 233, 238]. Therefore, Ca^{2+}-mediated activation of CaMKIIs indirectly participates in inhibiting synaptic gene expression in extra-synaptic nuclei.

Innervated HSA^{LR} and $Mbnl1^{\Delta 3/\Delta 3}$ muscles both showed an increase in total HDAC4 protein levels. Moreover, subcellular fractionation of HSA^{LR} muscle suggested higher HDAC4 levels in the nuclear compartment. Hence, one hypothesis is that CaMKII deficiency releases its inhibition on HDAC4 and promotes HDAC4 nuclear import. Accordingly, the phosphorylation of HDAC4 at one site targeted by CaMKII was reduced in HSA^{LR} muscle, while it was unchanged in $Mbnl1^{\Delta 3/\Delta 3}$ muscle. However, as CaMKIIs are known to inhibit HDACs by phosphorylating at least three different sites, analysis of the phosphorylation levels at these other sites may be needed.

Importantly, HDAC4 is supposed to indirectly induce synaptic gene expression by allowing the up-regulation of *Myog*. Although the expression of Chrna1 was increased in HSA^{LR} and $Mbnl1^{\Delta 3/\Delta 3}$ muscles, there was no change in *Myog* expression in the different muscles tested from the two mouse models. Moreover, only mild changes were detected in the expression of *Dach2* and *Mitr*, two direct targets repressed by HDAC4. Hence, the contribution of HDAC4 signaling to the up-regulation of synaptic genes in DM1 muscle is uncertain. Future experiments may include the analysis of HDAC4 localization and signaling in cytosolic and nuclear fractions of $Mbnl1^{\Delta 3/\Delta 3}$ muscle. In addition, HDAC4 staining on muscle biopsies from DM1 patients, as well as quantification of the expression of HDAC4 targets, would

be essential. Moreover, CaMKII deficiency may also affect other HDACs. In particular, HDAC5 has been shown to acquire responsiveness to CaMKII signaling through oligomerization with HDAC4 [102] HDAC9 (or its spliced variant MITR) also belongs to the class II of HDACs and may thus be a target of CaMKIIs as well. It still remains unclear how CaMKIIs allow the balanced regulation of HDAC4/5 and HDAC9 in innervated *vs.* denervated muscles. As CaMKIIs are supposed to inhibit all class II HDACs, the mechanisms ensuring the opposite activity of HDAC4/5 and HDAC9 (*e.g.* active HDAC9 and inhibited HDAC4/5 in innervated muscle) are still unknown. One may hypothesize that different isoforms or spliced variants of CaMKIIs may regulate distinct HDACs. Of note, CaMKIIs have also been shown to promote the activity of class I HDACs. In particular, cardiac overexpression of CaMKII in mice increases expression of HDAC1/3 and promotes their deacetylase activity [296]. As HDAC9-dependent repression of *Myog* is mediated by HDAC1 and HDAC3 [87], CaMKII deficiency may also alleviate synaptic gene repression by affecting HDAC1/HDAC3. Analysis of their expression, localization and DNA binding may be of interest in the DM1 context. Of note, studies have demonstrated that treatment of DM1 cells with HDAC inhibitor increases MBNL1 protein levels and ameliorates *Clcn1* splicing. Hence, further investigations on the role of HDACs in DM1 pathogenesis or as potential therapeutic targets are certainly of interest.

- <u>*CaMKII deficiency: Contribution to NMJ deterioration by affecting AChR dynamics*</u>

CaMKIIs promote AChR recycling at the sarcolemma upon their internalization and contribute to the maintenance of a high post-synaptic AChRs density [77]. This function may be ensured specifically by CaMKIIβM, as it was suggested to be the only CaMKII isoform accumulating at the motor endplate [77]. How CaMKIIs modulate AChRs stability is still unclear. It is possible that CaMKIIs modulate AChR dynamics through direct phosphorylation of AChRs and/or by regulating proteins involved in the trafficking of AChRs-containing vesicles. In central synapses, CaMKIIs have been shown to interact with multiple postsynaptic proteins, including NMDA receptors and voltage-sensitive calcium channels [297]. Furthermore, CaMKIIβM was found to co-localize with AChRs at the NMJ, suggesting potential direct interactions [77]. In this context, future studies assessing the capacity of different CaMKII isoforms to phosphorylate AChRs may help to uncover novel regulatory mechanisms involved in AChR trafficking and stability.

Here, I revealed that AChR turnover is increased in HSA^{LR} and $Mbnl1^{\Delta 3/\Delta 3}$ muscles, which may mainly arise from a reduced recycling and increased degradation rates of AChRs. CaMKIIβM deficiency may directly affect AChR recycling, although additional experiments remain to be conducted to confirm this hypothesis. In particular, overexpression of CaMKIIβM in HSA^{LR} and/or $Mbnl1^{\Delta 3/\Delta 3}$ muscles will be essential to conclude on its role in the increase AChR turnover and/or in synaptic gene perturbations. Testing the consequences of its restauration on muscle force and muscle relaxation will be also of major interest. In parallel, the potential deregulation of the non-kinase variant of CaMK2α, α-kap (non-kinase anchoring protein) in DM1 muscle needs to be investigated. CaMKIIβM and α-kap associate and interact

at the NMJ [77, 112]. Knockdown of α-kap in murine muscle leads to a decreased insertion rate at the membrane of newly synthesized and recycled AChRs [298]. Interestingly, CaMKII localization changes dependent on the expression of the fetal (α-kapA) or adult (α-kapB) isoforms [299]. Abnormal switch in the expression of the fetal / adult isoforms of α-kap in DM1 may hence further perturb CaMKII signaling, and thereby alter AChR dynamics.

Although our main interest in the study was the potential impact of CaMKII deficiency on NMJs, it is evident, based on the large range of functions of CaMKIIs in skeletal muscle, as well as in non-muscle tissues, that the deregulation of CaMKII signaling likely contributes to different aspects of DM1 pathogenesis. In muscle, CaMKII deficiency may affect the expression of various target genes, alter the contractile and metabolic properties of the fibers, and contribute to the fiber type switch described in DM1 muscle. Changes in CaMKII signaling may also have a strong impact on the heart and brain, which are two strongly affected tissues in DM1 patients.

4.2c CaMKII-independent mechanisms with potential impact on NMJs in DM1

- *PKC signaling: deregulation in DM1 and role in NMJs*

In DM1 tissues, pathological (CUG)n transcripts activate PKCα and βII, which leads to increased CUGBP1 stability and phosphorylation [181]. Further investigations on the consequences of DM1-associated PKC hyper-activation are scarce. PKC signaling is involved in multiple processes in muscle tissue, including activity-dependent AChRs expression and recycling [76, 84]. While PKA decreases the removal rate of pre-existing AChRs at the membrane and promotes recycling, PKC accelerates the removal and prevents AChR recycling [76]. Therefore, evaluation of PKC signaling pathway in HSA^{LR} muscle (expression of (CUG)n repeats) and of the consequences of its inhibition on muscle phenotype, including NMJ deterioration and AChR dynamics, would give further insights on the role of PKC in DM1-associated muscle pathology.

- *Impact of autophagy and proteasome deregulation on NMJ*

Autophagy plays a critical role in the turnover of AChRs [63]. Once, internalized, AChRs are either recycled back to the membrane surface or degraded via the autophagosomal system. In HSA^{LR} mice, the group has previously shown that autophagy is perturbed in catabolic conditions [216]. Interestingly, innervated muscles from Atg7-deficient mice exhibit similar NMJ changes as observed in HSA^{LR} and $Mbnl1^{\Delta 3/\Delta 3}$ mice, including increased AChR turnover and higher fragmentation of endplates. Administration of the autophagy-promoting agent Trolox ameliorated AChR turnover in $Atg7^{-/-}$ mice. In parallel, studies have demonstrated that genetic ablation of Murf1 ($Murf1^{-/-}$ mice) partially rescued the decrease in AChRs stability upon denervation. The authors hypothesized that Murf1 may play a key role in the endo/lysosomal progression of AChRs under catabolic conditions [80]. Therefore, deregulations of autophagy and atrogene-related degradation pathways may affect muscle response and AChR

turnover in DM1 muscle. Hence, further assessment of autophagy dynamics and degradation pathways locally at the NMJ, as well as closer analysis of internalized AChRs (*i.e.* whether they accumulate underneath the membrane) would be of interest.

- *Role of the deregulation of DGC proteins*

Components of the DGC have been shown to affect AChR turnover: NMJs from α-syntrophin-deficient mice and α-dystrobrevin null mice show decreased AChR density and recycling, as well as an increase in AChR turnover [237, 268]. Interestingly, α-dystrobrevin, which binds to α-syntrophin, is mis-spliced in DM1 muscle cells [203]. Hence, changes in the components of the DGC complex may contribute to alterations in AChR dynamics in DM1 context.

4.3 Altered muscle response to nerve injury in DM1

To get further insights on the mechanisms underlying NMJ alterations in DM1, I investigated the muscle response of HSA^{LR} and $Mbnl1^{\Delta 3/\Delta 3}$ mice after different time-points of denervation.

4.3a Abnormal response to denervation in DM1 mice

- *Limitations of HSA^{LR} mice*

During the course of my project, I first assessed the muscle response to nerve injury in HSA^{LR} mice. Unexpectedly, I detected that transgene expression decreases in HSA^{LR} muscle upon acute denervation. Consequently, HSA^{LR} muscles showed a reduction in the number of DM1-associated ribonuclear foci. Consistent with this, I observed that splicing defects of well-known target genes, such as *Clcn1*, decreased during the first days after denervation. Interestingly, transgene expression, the number of ribonuclear foci, as well as splicing defects were back to "innervated" levels after prolonged denervation. Based on these observations, I suspect that some of the results obtained, and especially the difference observed between HSA^{LR} muscle and controls, were restrained by the loss of the transgene expression. The loss of expression of the *HSA* promoter, used in HSA^{LR} mice, was actually unexpected and has not been reported before. This setback significantly delayed the progress of my PhD and led me to characterize the response to denervation in another mouse model for DM1. $Mbnl1^{\Delta 3/\Delta 3}$ mice were chosen, as MBNL1 is constitutively ablated in these mice.

- *Catabolic response to denervation*

$Mbnl1^{\Delta 3/\Delta 3}$ mice showed a decrease in muscle weight loss upon prolonged denervation. Interestingly, previous studies have demonstrated the potential role of CaMKIIβ as a catabolic regulator in skeletal muscle. In particular, inhibition of CaMKIIβ limits denervation-induced atrophy by suppressing the transcriptional expression of Murf1 and Atrogin1 in a FOXO3A-dependent manner [300]. Hence, CaMKII deficiency may limit protein degradation upon denervation in DM1 muscle, and thereby protect

the muscle from atrophy. Further analysis on the expression of atrogenes upon denervation, as well as its restoration upon CaMKIIβ overexpression will be of interest.

In this context, the group has previously showed that the AMPK and mTORC1 are abnormally inhibited and active, respectively in HSA^{LR} muscle under fasted conditions [216, 301]. As AMPK promotes the expression of FOXO3A, defective activation of AMPK upon denervation may also limit the expression of atrogenes in mutant muscle [302]. Evaluation of these metabolic pathways upon nerve injury will help to elucidate mechanisms conveying a potential protection against denervation-induced atrophy in the DM1 context.

- *Changes in the synaptic response in $Mbnl1^{\Delta 3/\Delta 3}$ mice*

When challenged with nerve injury, fragmentation of the endplates increased and remained higher in $Mbnl1^{\Delta 3/\Delta 3}$ mice, compared to controls. Moreover, I unveiled that denervation-induced increase in AChR turnover is further increased in mutant mice, as compared to controls, while there was no detectable changes in AChR recycling. Moreover, $Mbnl1^{\Delta 3/\Delta 3}$ muscle showed a limited capacity to up-regulate synaptic gene expression. Indeed, mutant muscle showed a more than 50% reduction in the expression of *Myog, Chrna1* and *Chrng* after denervation.

The overall interpretation of the results is delicate. Increased turnover suggests that the degradation of AChRs and/or their synthesis and insertion may be increased. As synaptic gene up-regulation was hampered upon denervation in mutant mice, it is unlikely that synthesis and insertion of new receptors are increased. Although I did not detect changes in AChR recycling, the main hypothesis remains that internalization and degradation of the receptors are increased in $Mbnl1^{\Delta 3/\Delta 3}$ muscle. As mentioned before, one may further optimize the recycling assay in order to adapt to instable receptors (*i.e.* with short half-life). It may be that the injections conducted in this specific time interval did not allow proper detection of AChR recycling and of abnormal dynamics in the mutant muscle.

The limited up-regulation of synaptic genes in the mutant denervated muscle is also of interest. So far, the role of CaMKIIs in the context of denervation remains unclear. Findings, including my own observations, suggest that CaMKIIβM expression increases upon nerve injury. Due to the proposed inhibitory function of CaMKIIs on synaptic gene expression, CaMKIIβM deficiency in mutant muscles was expected to further promote HDAC4 induction and increase expression levels of synaptic genes upon denervation (as seen in the innervated conditions). In contrast, synaptic genes up-regulation was strongly hampered in mutant muscle. Of note, similar observations have been made in TSCmKO mice, which exhibited defects in HDAC4 activity and reduced synaptic gene expression, while CaMKIIβM expression was abrogated [232]. Hence, there are likely other mechanisms, which may lead to the altered expression of synaptic gene in $Mbnl1^{\Delta 3/\Delta 3}$ mice.

4.3b Similarities between muscle response to denervation and DM1-associated muscle perturbations: *role of ClC-1 in the response to denervation?*

- *Comparison between DM1-related changes and the denervation context*

When considering denervation and DM1 contexts, interesting similarities emerge. Studies have demonstrated the presence of fibrillation potentials, *i.e.* spontaneous contractions, in denervated murine muscles [303, 304]. These fibrillations are actually one of the first changes detected in denervated muscle following nerve injury. Interestingly, these fibrillations have been related to a decrease in the resting membrane potential caused by an increase in sodium concentration and permeability, together with a reduction in ClC-1 levels [303, 305]. Similarly, DM1-associated myotonic discharges relate to perturbations in the sarcolemmal resting potential, which arises from a decrease in Cl^- conductance due to the loss of ClC-1 [143, 191, 230]. In the course of my study, I confirmed that denervated control muscle showed a decrease in total *Clcn1* transcript levels (see Figure 7), which was accompanied by an increase in *Clcn1* mis-splicing. Moreover, denervated muscle acquired similar expression pattern as in innervated HSA^{LR} / $Mbnl1^{\Delta 3/\Delta 3}$ muscles, for some DM1-altered genes. In particular, I detected an increase in the exclusion of exon 13 and of the muscle-specific exons of *Camk2b* upon denervation (see Figure 7). This observation is in accordance with the switch from adult to fetal expression pattern of multiple transcripts upon denervation, which is one of the hallmark of DM1 pathophysiology [306, 307]. Hence, one may argue that DM1 muscle is already engaged in a "denervation-like" pattern, which may lead to a quicker response to nerve injury.

Inversely, if these changes, in particular the sarcolemmal hyper-excitability, is part of the mechanisms allowing muscle to sense the loss of innervation, DM1 muscle may not react as strongly as a control muscle to nerve injury. In a similar way, a previous report from Klocke et al. (1994) has suggested that spontaneous myotonic discharges may actually substitute for the lack of electrical activity in denervated muscle [308]. Indeed, in non-synaptic region of an innervated muscle, the electrical activity has been demonstrated to be responsible for the suppression of synaptic gene expression and AChR synthesis, which would involve specific flux of Ca^{2+} [84, 309, 310]. In this hypothesis, the response of DM1 muscle may be hampered because the remaining electrical discharges may still be sufficient to repress myogenic and synaptic genes. As proper evaluation of myotonic discharges requires the use of needles for the EMG, which *per se* would induce discharges, it remains delicate to conclude on the persistence of myotonic discharges and their contribution as compensatory "electrical activity" in the context of denervation. Moreover, as fibrillations are observed in the primary stages following denervation, one may doubt that these spontaneous electrical discharges actually block muscle response.

- *Opening thoughts: role of chloride flux in initiating the response to denervation*

An interesting hypothesis actually emerged from the study of Klocke et al., which suggested that spontaneous electrical activity in DM1 muscle may confer a compensatory mechanism upon nerve injury. This conclusion was based on results obtained in *adr* mice, which are depleted for ClC-1. The

up-regulation in the expression of activity-dependent genes, such as *Myog*, *MyoD* and *Chrna1,* was strongly attenuated in denervated muscles from myotonic *adr* mice [308]. The authors hypothesized that myotonic discharges were sufficient to compensate for the loss of electrical activity. Another tempting hypothesis based on the results obtained would be that chloride fluxes driven by ClC-1 may be part of the initial sensing and response of the muscle to nerve injury. Previous studies have clearly established that electrical activity in innervated muscle leads to the repression of myogenic and synaptic genes in non-synaptic region. Ca^{2+} flux through the DHPR channel has been suggested to confer this effect, rather than Ca^{2+} fluxes through RyR1 upon contraction. By extrapolation, loss of Ca^{2+} flux and inhibition of CaMKIIs upon denervation would constitute the initial trigger leading to the re-expression of myogenic and synaptic genes upon nerve injury. However, there was no clear *in vivo* study demonstrating their primary involvement in the muscle response to denervation. Based on the results obtained in *adr* mice, one may hypothesize that changes in chloride fluxes, through the ClC-1 channel, may actually be an initially signal upon nerve injury. This would explain why *adr* mice do not respond to denervation, in terms of synaptic gene expression. This would as well explain why *Mbnl1*$^{\Delta 3/\Delta 3}$ mice do not show efficient up-regulation of synaptic genes upon denervation. How denervation would induce change in chloride fluxes, and how these fluxes may trigger signaling cascade ultimately allowing synaptic gene up-regulation, remain to be investigated. Similarly, whether a limited capacity to respond and adapt to neural inactivity may contribute to NMJ deterioration in DM1 remains an open question.

5. Conclusion

During my PhD, I got the opportunity to work on two mouse models of the neuromuscular disorder Myotonic Dystrophy Type 1. In addition, I complemented my studies with investigations in cell culture. This allowed me to apply different methodologies and techniques and, to explore pathomechanisms, which may contribute to DM1 muscle pathogenesis. Granted by my affiliation to two research groups, I could greatly benefit from a vast scientific expertise, infrastructure and platform.

Thanks to this, I brought new insights into the role of NMJ in DM1 muscle. I showed that NMJs are affected in DM1 muscle, which possibly relates to CaMKII deregulation. In addition, I identified novel effectors (CLCAs) that may be considered further in DM1 pathophysiology.

During my work, I encountered several difficulties that limited my progress. Over the course of my studies, we observed a gradual loss of HSA^{LR} phenotype in inbred mice. On the bright side, this incidence opened new avenues of my research and allowed me to investigate and compare strongly affected and non-affected mice. Fortunately, we were able to refresh the HSA^{LR} mouse line and restore the phenotype in due time. The second major obstacle that I faced was the loss of *HSA* transgene expression in HSA^{LR} mice upon denervation. This obligated me to repeat and confirm most of the experiments performed in the first two years in $Mbnl1^{\Delta 3/\Delta 3}$ mice.

Hence, some of the initially planned experiments could not be performed. Short-term goals will comprise to delineate the interactome of CaMK2β *vs.* $CaMK2\beta_M$, as well as to validate the functional importance of $CaMK2\beta_M$ and CLCAs in DM1 muscle pathogenesis. These data will likely strengthen the results obtained so far and should open new perspective in the field of DM1. In conclusion, the results obtained during my PhD helped to further understand the mechanisms underlying the multisystemic DM1 pathology, and should pave the way for new investigations of the pathophysiology of DM1 and novel potent therapeutic strategies.

References

1. Janssen, I., et al., *Skeletal muscle mass and distribution in 468 men and women aged 18–88 yr.* Journal of Applied Physiology, 2000. **89**(1): p. 81-88.
2. Frontera, W.R. and J. Ochala, *Skeletal Muscle: A Brief Review of Structure and Function.* Calcified Tissue International, 2015. **96**(3): p. 183-195.
3. Lee, J.H. and H.-S. Jun, *Role of Myokines in Regulating Skeletal Muscle Mass and Function.* Frontiers in Physiology, 2019. **10**(42).
4. McDonald, C.M., *Clinical approach to the diagnostic evaluation of hereditary and acquired neuromuscular diseases.* Physical medicine and rehabilitation clinics of North America, 2012. **23**(3): p. 495-563.
5. Morrison, B.M., *Neuromuscular Diseases.* Seminars Neurology, 2016. **36**(05): p. 409-418.
6. Mary, P., L. Servais, and R. Vialle, *Neuromuscular diseases: Diagnosis and management.* Orthopaedics & Traumatology: Surgery & Research, 2018. **104**(1, Supplement): p. S89-S95.
7. Schweitzer, R., E. Zelzer, and T. Volk, *Connecting muscles to tendons: tendons and musculoskeletal development in flies and vertebrates.* Development (Cambridge, England), 2010. **137**(17): p. 2807-2817.
8. Gunning, P.W., et al., *Tropomyosin – master regulator of actin filament function in the cytoskeleton.* Journal of Cell Science, 2015. **128**(16): p. 2965-2974.
9. Ömeroğlu, H. and S. Ömeroğlu, *Skeletal Muscle; Structure, Function, and Repair*, in *Musculoskeletal Research and Basic Science*, F. Korkusuz, Editor. 2016, Springer International Publishing: Cham. p. 443-451.
10. Craig, R. and R. Padrón, *Chapter 7 Molecular Structure of the Sarcomere*. 2004. p. 129-166.
11. Hodgkin, A.L. and P. Horowicz, *The influence of potassium and chloride ions on the membrane potential of single muscle fibres.* The Journal of physiology, 1959. **148**(1): p. 127-160.
12. Unwin, N., *Nicotinic acetylcholine receptor and the structural basis of neuromuscular transmission: insights from Torpedo postsynaptic membranes.* Quarterly reviews of biophysics, 2013. **46**(4): p. 283-322.
13. Hodgkin, A.L. and A.F. Huxley, *A quantitative description of membrane current and its application to conduction and excitation in nerve.* The Journal of physiology, 1952. **117**(4): p. 500-544.
14. Yu, F.H. and W.A. Catterall, *Overview of the voltage-gated sodium channel family.* Genome biology, 2003. **4**(3): p. 207-207.
15. Luff, A.R. and H.L. Atwood, *Membrane properties and contraction of single muscle fibers in the mouse.* The American journal of physiology, 1972. **222**(6): p. 1435-40.
16. Goodman, B.E., *Channels active in the excitability of nerves and skeletal muscles across the neuromuscular junction: basic function and pathophysiology.* Advances in Physiology Education, 2008. **32**(2): p. 127-135.
17. Edwards, J.N., et al., *Longitudinal and transversal propagation of excitation along the tubular system of rat fast-twitch muscle fibres studied by high speed confocal microscopy.* The Journal of physiology, 2012. **590**(3): p. 475-492.
18. Fraser, J.A., C.L.H. Huang, and T.H. Pedersen, *Relationships between resting conductances, excitability, and t-system ionic homeostasis in skeletal muscle.* The Journal of general physiology, 2011. **138**(1): p. 95-116.
19. Altamura, C., et al., *Skeletal muscle ClC-1 chloride channels in health and diseases.* Pflügers Archiv - European Journal of Physiology, 2020. **472**(7): p. 961-975.
20. Fahlke, C., *Chloride channels take center stage in a muscular drama.* The Journal of general physiology, 2011. **137**(1): p. 17-19.
21. Aromataris, E.C. and G.Y. Rychkov, *ClC-1 chloride channel: Matching its properties to a role in skeletal muscle.* Clinical and Experimental Pharmacology and Physiology, 2006. **33**(11): p. 1118-1123.
22. Adrian, R.H., L.L. Costantin, and L.D. Peachey, *Radial spread of contraction in frog muscle fibres.* The Journal of physiology, 1969. **204**(1): p. 231-57.

23. Porter, K.R. and G.E. Palade, *Studies on the endoplasmic reticulum. III. Its form and distribution in striated muscle cells.* The Journal of biophysical and biochemical cytology, 1957. **3**(2): p. 269-300.
24. Barone, V., et al., *Organization of junctional sarcoplasmic reticulum proteins in skeletal muscle fibers.* Journal of muscle research and cell motility, 2015. **36**(6): p. 501-15.
25. Franzini-Armstrong, C., *The sarcoplasmic reticulum and the control of muscle contraction.* Faseb j, 1999. **13 Suppl 2**: p. S266-70.
26. Franzini-Armstrong, C., *Functional implications of RyR-dHPR relationships in skeletal and cardiac muscles.* Biological research, 2004. **37**(4): p. 507-12.
27. Beard, N.A., D.R. Laver, and A.F. Dulhunty, *Calsequestrin and the calcium release channel of skeletal and cardiac muscle.* Progress in biophysics and molecular biology, 2004. **85**(1): p. 33-69.
28. Mukund, K. and S. Subramaniam, *Skeletal muscle: A review of molecular structure and function, in health and disease.* Wiley interdisciplinary reviews. Systems biology and medicine, 2020. **12**(1): p. e1462-e1462.
29. Huxley, H.E., *The mechanism of muscular contraction.* Science, 1969. **164**(3886): p. 1356-65.
30. Huxley, H.E. and M. Kress, *Crossbridge behaviour during muscle contraction.* Journal of muscle research and cell motility, 1985. **6**(2): p. 153-61.
31. Periasamy, M. and A. Kalyanasundaram, *SERCA pump isoforms: their role in calcium transport and disease.* Muscle Nerve, 2007. **35**(4): p. 430-42.
32. Calderon, J.C., P. Bolanos, and C. Caputo, *The excitation-contraction coupling mechanism in skeletal muscle.* Biophysical Reviews and Letters, 2014. **6**(1): p. 133-160.
33. Shishmarev, D., *Excitation-contraction coupling in skeletal muscle: recent progress and unanswered questions.* Biophysical Reviews, 2020. **12**(1): p. 143-153.
34. Heiny, J.A. and G. Meissner, *Chapter 45 - Excitation—Contraction Coupling in Skeletal Muscle*, in *Cell Physiology Source Book (Fourth Edition)*, N. Sperelakis, Editor. 2012, Academic Press: San Diego. p. 783-800.
35. Slater, C., *The Structure of Human Neuromuscular Junctions: Some Unanswered Molecular Questions.* International Journal of Molecular Sciences, 2017. **18**: p. 2183.
36. Stifani, N., *Motor neurons and the generation of spinal motor neurons diversity.* Frontiers in Cellular Neuroscience, 2014. **8**(293).
37. Wu, H., W.C. Xiong, and L. Mei, *To build a synapse: signaling pathways in neuromuscular junction assembly.* Development, 2010. **137**(7): p. 1017-33.
38. Sugiura, Y. and W. Lin, *Neuron-glia interactions: the roles of Schwann cells in neuromuscular synapse formation and function.* Bioscience reports, 2011. **31**(5): p. 295-302.
39. Court, F., et al., *Identity, developmental restriction and reactivity of extralaminar cells capping mammalian neuromuscular junctions.* Journal of cell science, 2009. **121**: p. 3901-11.
40. Li, L., W.C. Xiong, and L. Mei, *Neuromuscular Junction Formation, Aging, and Disorders.* Annual Review of Physiology, 2018. **80**: p. 159-188.
41. Sanes, J.R., *The basement membrane/basal lamina of skeletal muscle.* The Journal of biological chemistry, 2003. **278**(15): p. 12601-4.
42. Anglister, L. and U.J. McMahan, *Basal lamina directs acetylcholinesterase accumulation at synaptic sites in regenerating muscle.* Journal of Cell Biology, 1985. **101**(3): p. 735-743.
43. Rotundo, R.L., et al., *Targeting acetylcholinesterase to the neuromuscular synapse.* Chemico-Biological Interactions, 2005. **157-158**: p. 15-21.
44. Cartaud, A., et al., *MuSK is required for anchoring acetylcholinesterase at the neuromuscular junction.* The Journal of cell biology, 2004. **165**: p. 505-15.
45. Martin, A.R., *Amplification of neuromuscular transmission by postjunctional folds.* Proceedings. Biological sciences, 1994. **258**(1353): p. 321-6.
46. Yakel, J., *Advances and hold-ups in the study of structure, function and regulation of Cys-loop ligand-gated ion channels and receptors.* The Journal of physiology, 2010. **588**(Pt 4): p. 555-556.
47. Kruse, A.C., et al., *Muscarinic acetylcholine receptors: novel opportunities for drug development.* Nature Reviews Drug Discovery, 2014. **13**(7): p. 549-560.
48. Kalamida, D., et al., *Muscle and neuronal nicotinic acetylcholine receptors.* FEBS J, 2007. **274**(15): p. 3799-3845.

49. Tintignac, L.A., H.R. Brenner, and M.A. Ruegg, *Mechanisms Regulating Neuromuscular Junction Development and Function and Causes of Muscle Wasting.* Physiological reviews, 2015. **95**(3): p. 809-52.
50. Wood, S.J. and C. R. Slater, *Safety factor at the neuromuscular junction.* Progress in Neurobiology, 2001. **64**(4): p. 393-429.
51. Albuquerque, E.X., et al., *Mammalian Nicotinic Acetylcholine Receptors: From Structure to Function.* Physiological Reviews, 2009. **89**(1): p. 73-120.
52. Barrantes, F.J., *Cell-surface translational dynamics of nicotinic acetylcholine receptors.* Frontiers in Synaptic Neuroscience, 2014. **6**(25).
53. Mazhar, S. and R. Herbst, *The formation of complex acetylcholine receptor clusters requires MuSK kinase activity and structural information from the MuSK extracellular domain.* Molecular and cellular neurosciences, 2012. **49**(4): p. 475-486.
54. Maconochie, D.J. and J.H. Steinbach, *The channel opening rate of adult- and fetal-type mouse muscle nicotinic receptors activated by acetylcholine.* The Journal of physiology, 1998. **506 (Pt 1)**(Pt 1): p. 53-72.
55. Witzemann, V., et al., *Differential regulation of muscle acetylcholine receptor γ-and ϵ-subunit mRNAs.* FEBS Letters, 1987. **223**(1): p. 104-112.
56. Gu, Y. and Z.W. Hall, *Characterization of acetylcholine receptor subunits in developing and in denervated mammalian muscle.* Journal of Biological Chemistry, 1988. **263**(26): p. 12878-12885.
57. Goldman, D., H.R. Brenner, and S. Heinemann, *Acetylcholine receptor alpha-, beta-, gamma-, and delta-subunit mRNA levels are regulated by muscle activity.* Neuron, 1988. **1**(4): p. 329-33.
58. Levitt, T.A. and M.M. Salpeter, *Denervated endplates have a dual population of junctional acetylcholine receptors.* Nature, 1981. **291**(5812): p. 239-241.
59. Levitt, T.A., R.H. Loring, and M.M. Salpeter, *Neuronal control of acetylcholine receptor turnover rate at a vertebrate neuromuscular junction.* Science, 1980. **210**(4469): p. 550-1.
60. Stanley, E.F. and D.B. Drachman, *Denervation accelerates the degradation of junctional acetylcholine receptors.* Experimental Neurology, 1981. **73**(2): p. 390-6.
61. Yampolsky, P., et al., *AChR channel conversion and AChR-adjusted neuronal survival during embryonic development.* Molecular and Cellular Neuroscience, 2008. **37**(3): p. 634-645.
62. Yampolsky, P., et al., *Time lapse in vivo visualization of developmental stabilization of synaptic receptors at neuromuscular junctions.* The Journal of biological chemistry, 2010. **285**(45): p. 34589-96.
63. Rudolf, R. and T. Straka, *Nicotinic acetylcholine receptor at vertebrate motor endplates: Endocytosis, recycling, and degradation.* Neuroscience Letters, 2019. **711**: p. 134434.
64. Gilhus, N.E., et al., *Myasthenia gravis.* Nature Reviews Disease Primers, 2019. **5**(1): p. 30.
65. Kordas, G., et al., *Direct proof of the in vivo pathogenic role of the AChR autoantibodies from myasthenia gravis patients.* PLoS One, 2014. **9**(9): p. e108327.
66. Fumagalli, G., A.G. Engel, and J. Lindstrom, *Ultrastructural Aspects of Acetylcholine Receptor Turnover at the Normal End-plate and in Autoimmune Myasthenia Gravis.* Journal of Neuropathology & Experimental Neurology, 1982. **41**(6): p. 567-579.
67. Gautam, M., et al., *Failure of postsynaptic specialization to develop at neuromuscular junctions of rapsyn-deficient mice.* Nature, 1995. **377**(6546): p. 232-6.
68. Bartoli, M., M.K. Ramarao, and J.B. Cohen, *Interactions of the rapsyn RING-H2 domain with dystroglycan.* The Journal of biological chemistry, 2001. **276**(27): p. 24911-7.
69. Drachman, D.B., et al., *Mechanisms of acetylcholine receptor loss in myasthenia gravis.* Journal of neurology, neurosurgery, and psychiatry, 1980. **43**(7): p. 601-10.
70. ENGEL, A.G., et al., *Ultrastructural localization of the acetylcholine receptor in myasthenia gravis and in its experimental autoimmune model.* Neurology, 1977. **27**(4): p. 307-307.
71. Du, A., et al., *Suppression of CHRN endocytosis by carbonic anhydrase CAR3 in the pathogenesis of myasthenia gravis.* Autophagy, 2017. **13**(11): p. 1981-1994.
72. Lee, C.W., et al., *Crosslinking-Induced Endocytosis of Acetylcholine Receptors by Quantum Dots.* PloS one, 2014. **9**: p. e90187.
73. Khan, M.M., et al., *Role of autophagy, SQSTM1, SH3GLB1, and TRIM63 in the turnover of nicotinic acetylcholine receptors.* Autophagy, 2014. **10**(1).

74. Bruneau, E., et al., *Identification of nicotinic acetylcholine receptor recycling and its role in maintaining receptor density at the neuromuscular junction in vivo.* The Journal of neuroscience, 2005. **25**(43): p. 9949-59.
75. Bruneau, E.G. and M. Akaaboune, *The dynamics of recycled acetylcholine receptors at the neuromuscular junction in vivo.* Development, 2006. **133**(22): p. 4485-93.
76. Martinez-Pena y Valenzuela, I., M. Pires-Oliveira, and M. Akaaboune, *PKC and PKA regulate AChR dynamics at the neuromuscular junction of living mice.* PLoS One, 2013. **8**(11): p. e81311.
77. Martinez-Pena y Valenzuela, I., C. Mouslim, and M. Akaaboune, *Calcium/calmodulin kinase II-dependent acetylcholine receptor cycling at the mammalian neuromuscular junction in vivo.* The Journal of neuroscience : the official journal of the Society for Neuroscience, 2010. **30**(37): p. 12455-65.
78. Shyng, S. and M. Salpeter, *Effect of reinnervation on the degradation rate of junctional acetylcholine receptors synthesized in denervated skeletal muscles.* Journal of Neurosciences, 1990. **10**(12): p. 3905-3915.
79. Carnio, S., et al., *Autophagy impairment in muscle induces neuromuscular junction degeneration and precocious aging.* Cell reports, 2014. **8**(5): p. 1509-21.
80. Rudolf, R., et al., *Regulation of nicotinic acetylcholine receptor turnover by MuRF1 connects muscle activity to endo/lysosomal and atrophy pathways.* Age (Dordr), 2013. **35**(5): p. 1663-74.
81. Schaeffer, L., A. de Kerchove d'Exaerde, and J.-P. Changeux, *Targeting Transcription to the Neuromuscular Synapse.* Neuron, 2001. **31**(1): p. 15-22.
82. MÉJAT, A., et al., *Synapse-Specific Gene Expression at the Neuromuscular Junction.* Annals of the New York Academy of Sciences, 2003. **998**(1): p. 53-65.
83. Blagden, C.S., L. Fromm, and S.J. Burden, *Accelerated response of the myogenin gene to denervation in mutant mice lacking phosphorylation of myogenin at threonine 87.* Molecular and cellular biology, 2004. **24**(5): p. 1983-9.
84. Klarsfeld, A., et al., *Regulation of muscle AChR alpha subunit gene expression by electrical activity: involvement of protein kinase C and Ca2+.* Neuron, 1989. **2**(3): p. 1229-36.
85. Tang, H., Z. Sun, and D. Goldman, *CaM kinase II-dependent suppression of nicotinic acetylcholine receptor delta-subunit promoter activity.* The Journal of biological chemistry, 2001. **276**(28): p. 26057-65.
86. Macpherson, P., et al., *Protein kinase C and calcium/calmodulin-activated protein kinase II (CaMK II) suppress nicotinic acetylcholine receptor gene expression in mammalian muscle. A specific role for CaMK II in activity-dependent gene expression.* The Journal of biological chemistry, 2002. **277**(18): p. 15638-46.
87. Mejat, A., et al., *Histone deacetylase 9 couples neuronal activity to muscle chromatin acetylation and gene expression.* Nature Neurosciences, 2005. **8**(3): p. 313-21.
88. Thomas, J.L., et al., *PAK1 and CtBP1 Regulate the Coupling of Neuronal Activity to Muscle Chromatin and Gene Expression.* Molecular and cellular biology, 2015. **35**(24): p. 4110-20.
89. Berghella, L., et al., *A highly conserved molecular switch binds MSY-3 to regulate myogenin repression in postnatal muscle.* Genes Development, 2008. **22**(15): p. 2125-38.
90. Tang, H., et al., *CaM kinase II-dependent phosphorylation of myogenin contributes to activity-dependent suppression of nAChR gene expression in developing rat myotubes.* Cellular signalling, 2004. **16**(5): p. 551-63.
91. Klionsky, D.J., et al., *Guidelines for the use and interpretation of assays for monitoring autophagy (3rd edition).* Autophagy, 2016. **12**(1): p. 1-222.
92. Eftimie, R., H.R. Brenner, and A. Buonanno, *Myogenin and MyoD join a family of skeletal muscle genes regulated by electrical activity.* Proceedings of the National Academy of Sciences of the United States of America, 1991. **88**(4): p. 1349-1353.
93. Merlie, J., et al., *Myogenin and acetylcholine receptor alpha gene promoters mediate transcriptional regulation in response to motor innervation.* The Journal of biological chemistry, 1994. **269**: p. 2461-7.
94. Tang, H. and D. Goldman, *Activity-dependent gene regulation in skeletal muscle is mediated by a histone deacetylase (HDAC)-Dach2-myogenin signal transduction cascade.* Proceedings of the National Academy of Sciences, 2006. **103**(45): p. 16977-82.

95. Chin, E.R., *The role of calcium and calcium/calmodulin-dependent kinases in skeletal muscle plasticity and mitochondrial biogenesis.* Proceedings of the National Academy of Sciences, 2004. **63**(2): p. 279-86.
96. Bayer, K.U. and H. Schulman, *CaM Kinase: Still Inspiring at 40.* Neuron, 2019. **103**(3): p. 380-394.
97. Dupont, G. and A. Goldbeter, *CaM kinase II as frequency decoder of Ca2+ oscillations.* Bioessays : News and Reviews in Molecular, Cellular and Developmental Biology, 1998. **20**(8): p. 607-610.
98. Flück, M., et al., *Skeletal muscle Ca(2+)-independent kinase activity increases during either hypertrophy or running.* Journal of applied physiology, 2000. **88**(1): p. 352-8.
99. Eilers, W., et al., *Muscle-Type Specific Autophosphorylation of CaMKII Isoforms after Paced Contractions.* BioMed Research International, 2014. **2014**: p. 943806.
100. Ojuka, E.O., V. Goyaram, and J.A.H. Smith, *The role of CaMKII in regulating GLUT4 expression in skeletal muscle.* American Journal of Physiology-Endocrinology and Metabolism, 2012. **303**(3): p. E322-E331.
101. Backs, J., et al., *CaM kinase II selectively signals to histone deacetylase 4 during cardiomyocyte hypertrophy.* The Journal of clinical investigation, 2006. **116**(7): p. 1853-1864.
102. Backs, J., et al., *Histone Deacetylase 5 Acquires Calcium/Calmodulin-Dependent Kinase II Responsiveness by Oligomerization with Histone Deacetylase 4.* Molecular and Cellular Biology, 2008. **28**(10): p. 3437-3445.
103. Tavi, P. and H. Westerblad, *The role of in vivo Ca^{2+} signals acting on Ca^{2+}-calmodulin-dependent proteins for skeletal muscle plasticity.* The Journal of physiology, 2011. **589**(Pt 21): p. 5021-5031.
104. Abraham, S.T. and C. Shaw, *Increased expression of deltaCaMKII isoforms in skeletal muscle regeneration: Implications in dystrophic muscle disease.* Journal of cellular biochemistry, 2006. **97**(3): p. 621-32.
105. Gray, C. and J. Heller Brown, *CaMKIIdelta subtypes: localization and function.* Frontiers in Pharmacology, 2014. **5**(15).
106. Li, C., et al., *The δA isoform of calmodulin kinase II mediates pathological cardiac hypertrophy by interfering with the HDAC4-MEF2 signaling pathway.* Biochemical and biophysical research communications, 2011. **409**(1): p. 125-130.
107. Witcher, D.R., et al., *Unique phosphorylation site on the cardiac ryanodine receptor regulates calcium channel activity.* The Journal of biological chemistry, 1991. **266**(17): p. 11144-52.
108. Wang, J. and P.M. Best, *Inactivation of the sarcoplasmic reticulum calcium channel by protein kinase.* Nature, 1992. **359**(6397): p. 739-741.
109. Wegener, A.D., et al., *Phospholamban phosphorylation in intact ventricles. Phosphorylation of serine 16 and threonine 17 in response to beta-adrenergic stimulation.* The Journal of biological chemistry, 1989. **264**(19): p. 11468-74.
110. Xu, A., C. Hawkins, and N. Narayanan, *Phosphorylation and activation of the Ca(2+)-pumping ATPase of cardiac sarcoplasmic reticulum by Ca2+/calmodulin-dependent protein kinase.* The Journal of biological chemistry, 1993. **268**(12): p. 8394-7.
111. Hawkins, C., A. Xu, and N. Narayanan, *Sarcoplasmic reticulum calcium pump in cardiac and slow twitch skeletal muscle but not fast twitch skeletal muscle undergoes phosphorylation by endogenous and exogenous Ca2+/calmodulin-dependent protein kinase. Characterization of optimal conditions for calcium pump phosphorylation.* The Journal of biological chemistry, 1994. **269**(49): p. 31198-206.
112. Bayer, K.U., K. Harbers, and H. Schulman, *alphaKAP is an anchoring protein for a novel CaM kinase II isoform in skeletal muscle.* The EMBO journal, 1998. **17**(19): p. 5598-605.
113. Schworer, C.M., et al., *Identification of novel isoforms of the delta subunit of Ca2+/calmodulin-dependent protein kinase II. Differential expression in rat brain and aorta.* The Journal of biological chemistry, 1993. **268**(19): p. 14443-9.
114. Bayer, K.U., P. De Koninck, and H. Schulman, *Alternative splicing modulates the frequency-dependent response of CaMKII to Ca(2+) oscillations.* The EMBO journal, 2002. **21**(14): p. 3590-7.
115. Roder, I.V., et al., *Myosin Va cooperates with PKA RIalpha to mediate maintenance of the endplate in vivo.* Proceedings of the National Academy of Sciences, 2010. **107**(5): p. 2031-6.

116. Costa, M.C.R., et al., *Brain Myosin-V, a Calmodulin-carrying Myosin, Binds to Calmodulin-dependent Protein Kinase II and Activates Its Kinase Activity.* The Journal of Biological Chemistry, 1999. **274**(22): p. 15811-15819.
117. Theadom, A., et al., *Prevalence of muscular dystrophies: a systematic literature review.* Neuroepidemiology, 2014. **43**(3-4): p. 259-68.
118. Turner, C. and D. Hilton-Jones, *Myotonic dystrophy: diagnosis, management and new therapies.* Current opinion in neurology, 2014. **27**(5): p. 599-606.
119. Tome, S. and G. Gourdon, *DM1 Phenotype Variability and Triplet Repeat Instability: Challenges in the Development of New Therapies.* International Journal of Molecular Sciences, 2020. **21**(2).
120. Hahn, C. and M.K. Salajegheh, *Myotonic disorders: A review article.* Iranian journal of neurology, 2016. **15**(1): p. 46-53.
121. Meola, G. and R. Cardani, *Myotonic dystrophies: An update on clinical aspects, genetic, pathology, and molecular pathomechanisms.* Biochimica et biophysica acta, 2015. **1852**(4): p. 594-606.
122. Thornton, C.A., *Myotonic dystrophy.* Neurologic Clinics, 2014. **32**(3): p. 705-19, viii.
123. Adrian, R.H. and S.H. Bryant, *On the repetitive discharge in myotonic muscle fibres.* The Journal of physiology, 1974. **240**(2): p. 505-515.
124. Hehir, M.K. and E.L. Logigian, *Electrodiagnosis of myotonic disorders.* Physical medicine and rehabilitation clinics of North America, 2013. **24**(1): p. 209-20.
125. Ghosh, P.S. and E.J. Sorenson, *Use of Clinical and Electrical Myotonia to Differentiate Childhood Myopathies.* Journal of Child Neurology, 2015. **30**(10): p. 1300-1306.
126. Acket, B., et al., *Chloride channel dysfunction study in myotonic dystrophy type 1 using repeated short exercise tests.* Muscle Nerve, 2016. **54**(1): p. 104-109.
127. Fournier, E., et al., *Cold extends electromyography distinction between ion channel mutations causing myotonia.* Annals of Neurology, 2006. **60**(3): p. 356-365.
128. Franke, C., et al., *Characteristics of Na+ channels and Cl- conductance in resealed muscle fibre segments from patients with myotonic dystrophy.* Journal of Physiology, 1990. **425**: p. 391-405.
129. Boerio, D., et al., *Neuromuscular excitability properties in myotonic dystrophy type 1.* Clinical neurophysiology : official journal of the International Federation of Clinical Neurophysiology, 2007. **118**(11): p. 2375-82.
130. Benders, A.A., et al., *Myotonic dystrophy protein kinase is involved in the modulation of the Ca2+ homeostasis in skeletal muscle cells.* The Journal of clinical investigation, 1997. **100**(6): p. 1440-7.
131. Kimura, T., et al., *Expression and distribution of a small-conductance calcium-activated potassium channel (SK3) protein in skeletal muscles from myotonic muscular dystrophy patients and congenital myotonic mice.* Neuroscience letters, 2003. **347**(3): p. 191-5.
132. Gagnon, C., et al., *Towards an integrative approach to the management of myotonic dystrophy type 1.* Journal of neurology, neurosurgery, and psychiatry, 2007. **78**(8): p. 800-806.
133. Witting, N., L.K. Andersen, and J. Vissing, *Axial myopathy: an overlooked feature of muscle diseases.* Brain, 2015. **139**(1): p. 13-22.
134. Solbakken, G., et al., *Major involvement of trunk muscles in myotonic dystrophy type 1.* Acta neurologica Scandinavica, 2016. **134**(6): p. 467-473.
135. Hammarén, E., G. Kjellby-Wendt, and C. Lindberg, *Muscle force and other factors for falls in myotonic dystrophy type 1: studies of persons with a rare disease.* European Journal of Physiotherapy, 2017. **19**(sup1): p. 66-67.
136. Vihola, A., et al., *Histopathological differences of myotonic dystrophy type 1 (DM1) and PROMM/DM2.* Neurology, 2003. **60**(11): p. 1854-7.
137. Tohgi, H., et al., *Muscle histopathology in myotonic dystrophy in relation to age and muscular weakness.* Muscle Nerve, 1994. **17**(9): p. 1037-1043.
138. Pelargonio, G., et al., *Myotonic dystrophy and the heart.* Heart (British Cardiac Society), 2002. **88**(6): p. 665-670.
139. Gourdon, G. and G. Meola, *Myotonic Dystrophies: State of the Art of New Therapeutic Developments for the CNS.* Frontiers in Cellular Neuroscience, 2017. **11**(101).
140. Mishra, S.K., et al., *"Dystrophia Myotonica" and the Legacy of Hans Gustav Wilhelm Steinert.* Annals of Indian Academy of Neurology, 2018. **21**(2): p. 116-118.

141. Mahadevan, M., et al., *Myotonic dystrophy mutation: an unstable CTG repeat in the 3' untranslated region of the gene.* Science, 1992. **255**(5049): p. 1253-5.
142. Fu, Y.H., et al., *An unstable triplet repeat in a gene related to myotonic muscular dystrophy.* Science, 1992. **255**(5049): p. 1256-8.
143. Brook, J.D., et al., *Molecular basis of myotonic dystrophy: expansion of a trinucleotide (CTG) repeat at the 3' end of a transcript encoding a protein kinase family member.* Cell, 1992. **69**(2): p. 385.
144. Reddy, S., et al., *Mice lacking the myotonic dystrophy protein kinase develop a late onset progressive myopathy.* Nature Genetics, 1996. **13**(3): p. 325-335.
145. Jansen, G., et al., *Abnormal myotonic dystrophy protein kinase levels produce only mild myopathy in mice.* Nature Genetics, 1996. **13**(3): p. 316-324.
146. Carrell, S.T., et al., *Dmpk gene deletion or antisense knockdown does not compromise cardiac or skeletal muscle function in mice.* Human Molecular Genetics, 2016. **25**(19): p. 4328-4338.
147. Thornton, C.A., et al., *Expansion of the myotonic dystrophy CTG repeat reduces expression of the flanking DMAHP gene.* Nature Genetics, 1997. **16**(4): p. 407-409.
148. Klesert, T.R., et al., *Trinucleotide repeat expansion at the myotonic dystrophy locus reduces expression of DMAHP.* Nature Genetics, 1997. **16**(4): p. 402-406.
149. Sarkar, P.S., et al., *Heterozygous loss of Six5 in mice is sufficient to cause ocular cataracts.* Nature Genetics, 2000. **25**(1): p. 110-114.
150. Klesert, T.R., et al., *Mice deficient in Six5 develop cataracts: implications for myotonic dystrophy.* Nature genetics, 2000. **25**(1): p. 105-9.
151. Sarkar, P.S., et al., *Six5 is required for spermatogenic cell survival and spermiogenesis.* Human molecular genetics, 2004. **13**(14): p. 1421-31.
152. Wakimoto, H., et al., *Characterization of cardiac conduction system abnormalities in mice with targeted disruption of Six5 gene.* Journal of interventional cardiac electrophysiology : an international journal of arrhythmias and pacing, 2002. **7**(2): p. 127-35.
153. Mankodi, A., et al., *Myotonic dystrophy in transgenic mice expressing an expanded CUG repeat.* Science, 2000. **289**(5485): p. 1769-73.
154. Mankodi, A., et al., *Expanded CUG repeats trigger aberrant splicing of ClC-1 chloride channel pre-mRNA and hyperexcitability of skeletal muscle in myotonic dystrophy.* Molecular Cell, 2002. **10**: p. 35-44.
155. Seznec, H., et al., *Mice transgenic for the human myotonic dystrophy region with expanded CTG repeats display muscular and brain abnormalities.* Human molecular genetics, 2001. **10**(23): p. 2717-26.
156. Guiraud-Dogan, C., et al., *DM1 CTG expansions affect insulin receptor isoforms expression in various tissues of transgenic mice.* Biochimica et Biophysica Acta, 2007. **1772**(11-12): p. 1183-91.
157. Vignaud, A., et al., *Progressive skeletal muscle weakness in transgenic mice expressing CTG expansions is associated with the activation of the ubiquitin-proteasome pathway.* Neuromuscular Disorders, 2010. **20**(5): p. 319-25.
158. Seznec, H., et al., *Transgenic mice carrying large human genomic sequences with expanded CTG repeat mimic closely the DM CTG repeat intergenerational and somatic instability.* Human Molecular Genetics, 2000. **9**(8): p. 1185-1194.
159. Gomes-Pereira, M., et al., *CTG trinucleotide repeat "big jumps": large expansions, small mice.* PLoS Genetics, 2007. **3**(4): p. e52.
160. Huguet, A., et al., *Molecular, physiological, and motor performance defects in DMSXL mice carrying >1,000 CTG repeats from the human DM1 locus.* PLoS genetics, 2012. **8**(11): p. e1003043.
161. Panaite, P.A., et al., *Functional and histopathological identification of the respiratory failure in a DMSXL transgenic mouse model of myotonic dystrophy.* Disease models & mechanisms, 2013. **6**(3): p. 622-31.
162. Algalarrondo, V., et al., *Abnormal sodium current properties contribute to cardiac electrical and contractile dysfunction in a mouse model of myotonic dystrophy type 1.* Neuromuscular disorders : NMD, 2015. **25**(4): p. 308-20.
163. Hernandez-Hernandez, O., et al., *Myotonic dystrophy CTG expansion affects synaptic vesicle proteins, neurotransmission and mouse behaviour.* Brain, 2013. **136**(Pt 3): p. 957-70.

164. Mahadevan, M.S., et al., *Reversible model of RNA toxicity and cardiac conduction defects in myotonic dystrophy.* Nature genetics, 2006. **38**(9): p. 1066-70.
165. Ranum, L.P.W. and J.W. Day, *Myotonic Dystrophy: RNA Pathogenesis Comes into Focus.* The American Journal of Human Genetics, 2004. **74**(5): p. 793-804.
166. Ho, T.H., et al., *Muscleblind proteins regulate alternative splicing.* The EMBO journal, 2004. **23**(15): p. 3103-3112.
167. Miller, J.W., et al., *Recruitment of human muscleblind proteins to (CUG)(n) expansions associated with myotonic dystrophy.* The EMBO journal, 2000. **19**(17): p. 4439-48.
168. Paul, S., et al., *Interaction of muscleblind, CUG-BP1 and hnRNP H proteins in DM1-associated aberrant IR splicing.* Embo j, 2006. **25**(18): p. 4271-83.
169. Timchenko, L.T., et al., *Identification of a (CUG)n triplet repeat RNA-binding protein and its expression in myotonic dystrophy.* Nucleic acids research, 1996. **24**(22): p. 4407-14.
170. Lin, X., et al., *Failure of MBNL1-dependent post-natal splicing transitions in myotonic dystrophy.* Human molecular genetics, 2006. **15**(13): p. 2087-97.
171. Mankodi, A., et al., *Muscleblind localizes to nuclear foci of aberrant RNA in myotonic dystrophy types 1 and 2.* Human molecular genetics, 2001. **10**(19): p. 2165-70.
172. Kino, Y., et al., *Muscleblind protein, MBNL1/EXP, binds specifically to CHHG repeats.* Human Molecular Genetics, 2004. **13**(5): p. 495-507.
173. Kanadia, R.N., et al., *A muscleblind knockout model for myotonic dystrophy.* Science, 2003. **302**(5652): p. 1978-80.
174. Matynia, A., et al., *Muscleblind1, but Not Dmpk or Six5, Contributes to a Complex Phenotype of Muscular and Motivational Deficits in Mouse Models of Myotonic Dystrophy.* PLOS ONE, 2010. **5**(3): p. e9857.
175. Kimura, T., et al., *Altered mRNA splicing of the skeletal muscle ryanodine receptor and sarcoplasmic/endoplasmic reticulum Ca2+-ATPase in myotonic dystrophy type 1.* Human Molecular Genetics, 2005. **14**(15): p. 2189-200.
176. Lueck , J.D., et al., *Muscle Chloride Channel Dysfunction in Two Mouse Models of Myotonic Dystrophy.* Journal of General Physiology, 2006. **129**(1): p. 79-94.
177. Du, H., et al., *Aberrant alternative splicing and extracellular matrix gene expression in mouse models of myotonic dystrophy.* Nature Structural & Molecular Biology, 2010. **17**(2): p. 187-93.
178. Timchenko, N.A., et al., *RNA CUG repeats sequester CUGBP1 and alter protein levels and activity of CUGBP1.* The Journal of biological chemistry, 2001. **276**(11): p. 7820-6.
179. Dansithong, W., et al., *MBNL1 is the primary determinant of focus formation and aberrant insulin receptor splicing in DM1.* The Journal of Biological Chemistry, 2005. **280**(7): p. 5773-80.
180. Savkur, R.S., A.V. Philips, and T.A. Cooper, *Aberrant regulation of insulin receptor alternative splicing is associated with insulin resistance in myotonic dystrophy.* Nature Genetics, 2001. **29**(1): p. 40-7.
181. Kuyumcu-Martinez, N.M., G.S. Wang, and T.A. Cooper, *Increased steady-state levels of CUGBP1 in myotonic dystrophy 1 are due to PKC-mediated hyperphosphorylation.* Molecular cell, 2007. **28**(1): p. 68-78.
182. Timchenko, N.A., et al., *Overexpression of CUG triplet repeat-binding protein, CUGBP1, in mice inhibits myogenesis.* The Journal of biological chemistry, 2004. **279**(13): p. 13129-39.
183. Ho, T.H., et al., *Transgenic mice expressing CUG-BP1 reproduce splicing mis-regulation observed in myotonic dystrophy.* Human molecular genetics, 2005. **14**(11): p. 1539-47.
184. Ward, A.J., et al., *CUGBP1 overexpression in mouse skeletal muscle reproduces features of myotonic dystrophy type 1.* Human molecular genetics, 2010. **19**(18): p. 3614-22.
185. Rudich, P. and T. Lamitina, *Models and mechanisms of repeat expansion disorders: a worm's eye view.* Journal of genetics, 2018. **97**(3): p. 665-677.
186. Hutten, S. and D. Dormann, *RAN translation down.* Nature Neuroscience, 2019. **22**(9): p. 1379-1380.
187. Zu, T., et al., *Non-ATG-initiated translation directed by microsatellite expansions.* Proceedings of the National Academy of Sciences, 2011. **108**(1): p. 260-5.
188. Cleary, J.D., A. Pattamatta, and L.P.W. Ranum, *Repeat-associated non-ATG (RAN) translation.* Journal of Biological Chemistry, 2018. **293**(42): p. 16127-16141.

189. Willson, J., *A matter of life and death for caspase 8.* Nature Reviews Molecular Cell Biology, 2020. **21**(2): p. 63-63.
190. André, L.M., et al., *Abnormalities in Skeletal Muscle Myogenesis, Growth, and Regeneration in Myotonic Dystrophy.* Frontiers in neurology, 2018. **9**: p. 368-368.
191. Charlet, B.N., et al., *Loss of the muscle-specific chloride channel in type 1 myotonic dystrophy due to misregulated alternative splicing.* Molecular cell, 2002. **10**(1): p. 45-53.
192. Kanadia, R.N., et al., *Reversal of RNA missplicing and myotonia after muscleblind overexpression in a mouse poly(CUG) model for myotonic dystrophy.* Proceedings of the National Academy of Sciences 2006. **103**(31): p. 11748-53.
193. Jacobs, A.E.M., et al., *The calcium homeostasis and the membrane potential of cultured muscle cells from patients with myotonic dystrophy.* Biochimica et Biophysica Acta (BBA) - Molecular Basis of Disease, 1990. **1096**(1): p. 14-19.
194. Tang, Z.Z., et al., *Muscle weakness in myotonic dystrophy associated with misregulated splicing and altered gating of Ca(V)1.1 calcium channel.* Human Molecular Genetics, 2012. **21**(6): p. 1312-24.
195. Hino, S., et al., *Molecular mechanisms responsible for aberrant splicing of SERCA1 in myotonic dystrophy type 1.* Hum Mol Genet, 2007. **16**(23): p. 2834-43.
196. Kimura, T., et al., *Alternative splicing of RyR1 alters the efficacy of skeletal EC coupling.* Cell Calcium, 2009. **45**(3): p. 264-74.
197. Zhao, Y., et al., *Functional analysis of SERCA1b, a highly expressed SERCA1 variant in myotonic dystrophy type 1 muscle.* Biochimica et Biophysica Acta (BBA) - Molecular Basis of Disease, 2015. **1852**(10, Part A): p. 2042-2047.
198. Sobczak, K., et al., *RNA interference targeting CUG repeats in a mouse model of myotonic dystrophy.* Molecular Therapy, 2013. **21**(2): p. 380-7.
199. Suenaga, K., et al., *Muscleblind-like 1 knockout mice reveal novel splicing defects in the myotonic dystrophy brain.* PLoS One, 2012. **7**(3): p. e33218.
200. Salmaninejad, A., et al., *Duchenne muscular dystrophy: an updated review of common available therapies.* The International journal of neuroscience, 2018. **128**(9): p. 854-864.
201. Nakamori, M., et al., *Altered mRNA splicing of dystrophin in type 1 myotonic dystrophy.* Muscle Nerve, 2007. **36**(2): p. 251-7.
202. Rau, F., et al., *Abnormal splicing switch of DMD's penultimate exon compromises muscle fibre maintenance in myotonic dystrophy.* Nature Communication, 2015. **6**: p. 7205.
203. Nakamori, M., et al., *Aberrantly spliced alpha-dystrobrevin alters alpha-syntrophin binding in myotonic dystrophy type 1.* Neurology, 2008. **70**(9): p. 677-85.
204. Fugier, C., et al., *Misregulated alternative splicing of BIN1 is associated with T tubule alterations and muscle weakness in myotonic dystrophy.* Nature Medicine, 2011. **17**(6): p. 720-5.
205. Jungbluth, H., C. Wallgren-Pettersson, and J. Laporte, *Centronuclear (myotubular) myopathy.* Orphanet Journal of Rare Diseases, 2008. **3**(1): p. 26.
206. Wu, T., Z. Shi, and T. Baumgart, *Mutations in BIN1 associated with centronuclear myopathy disrupt membrane remodeling by affecting protein density and oligomerization.* PloS one, 2014. **9**(4): p. e93060-e93060.
207. Razzaq, A., et al., *Amphiphysin is necessary for organization of the excitation–contraction coupling machinery of muscles, but not for synaptic vesicle endocytosis in Drosophila.* Genes and Development, 2001. **15**(22): p. 2967-2979.
208. Ueda, H., et al., *Decreased expression of myotonic dystrophy protein kinase and disorganization of sarcoplasmic reticulum in skeletal muscle of myotonic dystrophy.* Journal of the neurological sciences, 1999. **162**(1): p. 38-50.
209. Furling, D., A. Marette, and J. Puymirat, *Insulin-Like Growth Factor I Circumvents Defective Insulin Action in Human Myotonic Dystrophy Skeletal Muscle Cells1.* Endocrinology, 1999. **140**(9): p. 4244-4250.
210. Gomes-Pereira, M., T.A. Cooper, and G. Gourdon, *Myotonic dystrophy mouse models: towards rational therapy development.* Trends in molecular medicine, 2011. **17**(9): p. 10.1016/j.molmed.2011.05.004.
211. Llagostera, E., et al., *Role of myotonic dystrophy protein kinase (DMPK) in glucose homeostasis and muscle insulin action.* PLoS One, 2007. **2**(11): p. e1134.

212. Jones, K., et al., *GSK3beta mediates muscle pathology in myotonic dystrophy.* Journal of Clinical Investigation, 2012. **122**(12): p. 4461-72.
213. Beffy, P., et al., *Altered signal transduction pathways and induction of autophagy in human myotonic dystrophy type 1 myoblasts.* The international journal of biochemistry & cell biology, 2010. **42**(12): p. 1973-83.
214. Bargiela, A., et al., *Increased autophagy and apoptosis contribute to muscle atrophy in a myotonic dystrophy type 1 Drosophila model.* Disease models & mechanisms, 2015. **8**(7): p. 679-90.
215. Morriss, G.R., et al., *Mechanisms of skeletal muscle wasting in a mouse model for myotonic dystrophy type 1.* Human Molecular Genetics, 2018. **27**(16): p. 2789-2804.
216. Brockhoff, M., et al., *Targeting deregulated AMPK/mTORC1 pathways improves muscle function in myotonic dystrophy type I.* The Journal of clinical investigation, 2017. **127**(2): p. 549-563.
217. Sato, S., Y. Ogura, and A. Kumar, *TWEAK/Fn14 Signaling Axis Mediates Skeletal Muscle Atrophy and Metabolic Dysfunction.* Frontiers in Immunology, 2014. **5**(18).
218. Yadava, R.S., et al., *TWEAK/Fn14, a pathway and novel therapeutic target in myotonic dystrophy.* Human molecular genetics, 2015. **24**(7): p. 2035-48.
219. Cappella, M., et al., *High-throughput analysis of the RNA-induced silencing complex in myotonic dystrophy type 1 patients identifies the dysregulation of miR-29c and its target ASB2.* Cell Death & Disease, 2018. **9**(7): p. 729.
220. Sabater-Arcis, M., et al., *miR-7 Restores Phenotypes in Myotonic Dystrophy Muscle Cells by Repressing Hyperactivated Autophagy.* Molecular Therapy - Nucleic Acids, 2020. **19**: p. 278-292.
221. Nakamori, M., et al., *Splicing biomarkers of disease severity in myotonic dystrophy.* Annals of neurology, 2013. **74**(6): p. 862-72.
222. Wang, A.H. and X.J. Yang, *Histone deacetylase 4 possesses intrinsic nuclear import and export signals.* Molecular and cellular biology, 2001. **21**(17): p. 5992-6005.
223. Tang, H., et al., *A histone deacetylase 4/myogenin positive feedback loop coordinates denervation-dependent gene induction and suppression.* Molecular Biology of the Cell, 2009. **20**(4): p. 1120-31.
224. Macdermot, V., *The histology of the neuromuscular junction in dystrophia myotonica.* Brain : a journal of neurology, 1961. **84**: p. 75-84.
225. Allen, D.E., A.G. Johnson, and A.L. Woolf, *The intramuscular nerve endings in dystrophia myotonica--a biopsy study by vital staining and electron microscopy.* Journal of Anatomy, 1969. **105**(Pt 1): p. 1-26.
226. Coers, C., N. Telerman-Toppet, and J.M. Gerard, *Terminal innervation ratio in neuromuscular disease. II. Disorders of lower motor neuron, peripheral nerve, and muscle.* Archives of neurology, 1973. **29**(4): p. 215-22.
227. Engel, A., et al., *The neuromuscular junction in myopathies: a quantitative ultrastructural study*, in *Recent Advances in Myology: Proceedings of the Third International Congress on Muscle Diseases, International Congress Series no. 360*, W. Bradley, D. Gardner-Medwin, and J. Walton, Editors. 1975, Elsevier: New York. p. 132-143.
228. Drachman, D.B. and D.M. Fambrough, *Are muscle fibers denervated in myotonic dystrophy?* Archive in Neurology, 1976. **33**(7): p. 485-8.
229. Spilker, K.A., et al., *Caenorhabditis elegans Muscleblind homolog mbl-1 functions in neurons to regulate synapse formation.* Neural development, 2012. **7**: p. 7.
230. Wheeler, T.M., M.C. Krym, and C.A. Thornton, *Ribonuclear foci at the neuromuscular junction in myotonic dystrophy type 1.* Neuromuscular disorders : NMD, 2007. **17**(3): p. 242-7.
231. Strack, S., et al., *Turnover of acetylcholine receptors at the endplate revisited: novel insights into nerve-dependent behavior.* Journal of muscle research and cell motility, 2015. **36**(6): p. 517-24.
232. Castets, P., et al., *mTORC1 and PKB/Akt control the muscle response to denervation by regulating autophagy and HDAC4.* Nature Communication, 2019. **10**(1): p. 3187.
233. Cohen, T.J., et al., *The histone deacetylase HDAC4 connects neural activity to muscle transcriptional reprogramming.* Journal of Biological Chemistry, 2007. **282**(46): p. 33752-9.

234. Strack, S., et al., *A Novel Labeling Approach Identifies Three Stability Levels of Acetylcholine Receptors in the Mouse Neuromuscular Junction In Vivo.* PLoS One, 2011. **6**(6): p. e20524.
235. Lee, K.Y., et al., *Compound loss of muscleblind-like function in myotonic dystrophy.* EMBO Molecular Medicine, 2013. **5**(12): p. 1887-900.
236. Willadt, S., M. Nash, and C.R. Slater, *Age-related fragmentation of the motor endplate is not associated with impaired neuromuscular transmission in the mouse diaphragm.* Scientific Reports, 2016. **6**: p. 24849.
237. Martinez-Pena y Valenzuela, I., et al., *Nicotinic acetylcholine receptor stability at the NMJ deficient in alpha-syntrophin in vivo.* Journal of Neurosciences, 2011. **31**(43): p. 15586-96.
238. Cohen, T.J., et al., *The deacetylase HDAC4 controls myocyte enhancing factor-2-dependent structural gene expression in response to neural activity.* FASEB Journal, 2009. **23**(1): p. 99-106.
239. Castets, P., et al., *Sustained activation of mTORC1 in skeletal muscle inhibits constitutive and starvation-induced autophagy and causes a severe, late-onset myopathy.* Cell Metabolism, 2013. **17**(5): p. 731-44.
240. Moyer, M., et al., *Differential susceptibility of muscles to myotonia and force impairment in a mouse model of myotonic dystrophy.* Muscle Nerve, 2011. **43**(6): p. 818-27.
241. Dimauro, I., et al., *A simple protocol for the subcellular fractionation of skeletal muscle cells and tissue.* BMC research notes, 2012. **5**: p. 513.
242. Hilton-Jones, D., *Myotonic dystrophy, 3rd edition: major problems in neurology series, No 37.* Journal of Neurology, Neurosurgery & Psychiatry, 2002. **72**(3): p. 422.
243. Tang, C.-Y. and T.-Y. Chen, *Physiology and pathophysiology of CLC-1: mechanisms of a chloride channel disease, myotonia.* Journal of biomedicine & biotechnology, 2011. **2011**: p. 685328-685328.
244. Wheeler, T.M., et al., *Correction of ClC-1 splicing eliminates chloride channelopathy and myotonia in mouse models of myotonic dystrophy.* Journal of Clinical Investigation, 2007. **117**(12): p. 3952-7.
245. Klein, A.F., et al., *Peptide-conjugated oligonucleotides evoke long-lasting myotonic dystrophy correction in patient-derived cells and mice.* The Journal of Clinical Investigation, 2019. **129**(11): p. 4739-4744.
246. Bryant, S.H. and A. Morales-Aguilera, *Chloride conductance in normal and myotonic muscle fibres and the action of monocarboxylic aromatic acids.* The Journal of Physiology, 1971. **219**(2): p. 367-383.
247. Renaud, J.F., et al., *Expression of apamin receptor in muscles of patients with myotonic muscular dystrophy.* Nature, 1986. **319**(6055): p. 678-80.
248. Corrochano, S., et al., *Novel mutations in human and mouse SCN4A implicate AMPK in myotonia and periodic paralysis.* Brain, 2014. **137**(Pt 12): p. 3171-85.
249. Wheeler, T.M., et al., *Targeting nuclear RNA for in vivo correction of myotonic dystrophy.* Nature, 2012. **488**(7409): p. 111-5.
250. Sharma, A., et al., *CLCA2 is a positive regulator of store-operated calcium entry and TMEM16A.* PLoS One, 2018. **13**(5): p. e0196512.
251. Patel, A.C., T.J. Brett, and M.J. Holtzman, *The role of CLCA proteins in inflammatory airway disease.* Annual review of physiology, 2009. **71**: p. 425-449.
252. Loewen, M.E. and G.W. Forsyth, *Structure and Function of CLCA Proteins.* Physiological Reviews, 2005. **85**(3): p. 1061-1092.
253. Sala-Rabanal, M., et al., *Modulation of TMEM16A channel activity by the von Willebrand factor type A (VWA) domain of the calcium-activated chloride channel regulator 1 (CLCA1).* Journal of Biological Chemistry, 2017. **292**(22): p. 9164-9174.
254. Dayal, A., S.F.J. Ng, and M. Grabner, *Ca2+-activated Cl- channel TMEM16A/ANO1 identified in zebrafish skeletal muscle is crucial for action potential acceleration.* Nature Communication, 2019. **10**.
255. Pedemonte, N. and L.J. Galietta, *Structure and function of TMEM16 proteins (anoctamins).* Physiological Reviews, 2014. **94**(2): p. 419-59.
256. Sung, T.S., et al., *Influence of intracellular Ca2+ and alternative splicing on the pharmacological profile of ANO1 channels.* American Journal of Physiology-Cell Physiology, 2016. **311**(3): p. C437-51.

257. Freyermuth, F., et al., *Splicing misregulation of SCN5A contributes to cardiac-conduction delay and heart arrhythmia in myotonic dystrophy.* Nature Communication, 2016. **7**: p. 11067.
258. Lee, R.M. and S.M. Jeong, *Identification of a novel calcium (Ca2+)-activated chloride channel accessory gene in Xenopus laevis.* Molecular Biology, 2016. **50**(1): p. 91-97.
259. Mundhenk, L., et al., *Interspecies diversity of chloride channel regulators, calcium-activated 3 genes.* PloS one, 2018. **13**(1): p. e0191512-e0191512.
260. Yurtsever, Z., et al., *Self-cleavage of Human CLCA1 Protein by a Novel Internal Metalloprotease Domain Controls Calcium-activated Chloride Channel Activation.* Journal of Biological Chemistry, 2012. **287**(50): p. 42138-42149.
261. Bombelli, F., et al., *Neuromuscular transmission abnormalities in myotonic dystrophy type 1: A neurophysiological study.* Clinical Neurology and Neurosurgery, 2016. **150**: p. 84-88.
262. Panaite, P.-A., et al., *Peripheral Neuropathy Is Linked to a Severe Form of Myotonic Dystrophy in Transgenic Mice.* Journal of Neuropathology & Experimental Neurology, 2011. **70**(8): p. 678-685.
263. Shiao, T., et al., *Defects in neuromuscular junction structure in dystrophic muscle are corrected by expression of a NOS transgene in dystrophin-deficient muscles, but not in muscles lacking α- and β1-syntrophins.* Human Molecular Genetics, 2004. **13**(17): p. 1873-1884.
264. Grady, R.M., et al., *Skeletal and Cardiac Myopathies in Mice Lacking Utrophin and Dystrophin: A Model for Duchenne Muscular Dystrophy.* Cell, 1997. **90**(4): p. 729-738.
265. Lyons, P.R. and C.R. Slater, *Structure and function of the neuromuscular junction in young adult mdx mice.* Journal of neurocytology, 1991. **20**(12): p. 969-81.
266. Rudolf, R., et al., *Degeneration of neuromuscular junction in age and dystrophy.* Frontiers in aging neuroscience, 2014. **6**: p. 99.
267. Belotti, E. and L. Schaeffer, *Regulation of Gene expression at the neuromuscular Junction.* Neuroscience Letters, 2020. **735**: p. 135163.
268. Adams, M.E., et al., *Absence of α-Syntrophin Leads to Structurally Aberrant Neuromuscular Synapses Deficient in Utrophin.* Journal of Cell Biology, 2000. **150**(6): p. 1385-1398.
269. Jones, R.A., et al., *NMJ-morph reveals principal components of synaptic morphology influencing structure-function relationships at the neuromuscular junction.* Open biology, 2016. **6**(12): p. 160240.
270. García-Puga, M., et al., *Myotonic Dystrophy type 1 cells display impaired metabolism and mitochondrial dysfunction that are reversed by metformin.* Aging, 2020. **12**(7): p. 6260-6275.
271. Campione, E., et al., *Cutaneous features of myotonic dystrophy types 1 and 2: Implication of premature aging and vitamin D homeostasis.* Neuromuscular disorders : NMD, 2017. **27**(2): p. 163-169.
272. Mateos-Aierdi, A.J., et al., *Muscle wasting in myotonic dystrophies: a model of premature aging.* Frontiers in Aging Neuroscience, 2015. **7**: p. 125.
273. Vandervoort, A.A., *Aging of the human neuromuscular system.* MUSCLE & NERVE, 2002. **25**(1): p. 17-25.
274. Elkerdany, M.K. and M.A. Fahim, *Age changes in neuromuscular junctions of masseter muscle.* Neurobiology, 1993. **237**(2): p. 291-295.
275. Fahim, M., J. Holley, and N.J.J.o.n. Robbins, *Scanning and light microscopic study of age changes at a neuromuscular junction in the mouse.* Journal of Neurocytology, 1983. **12**(1): p. 13-25.
276. Smith, D.O., K.D. Williams, and M. Emmerling, *Changes in acetylcholine receptor distribution and binding properties at the neuromuscular junction during aging.* International Journal of Developmental Neuroscience, 1990. **8**(6): p. 629-631.
277. Lin, I.H., et al., *Skeletal muscle in aged mice reveals extensive transformation of muscle gene expression.* BMC Genetics, 2018. **19**(1): p. 55.
278. Xie, F., et al., *Advanced age enhances the sepsis-induced up-regulation of the γ- and α7-nicotinic acetylcholine receptors in different parts of the skeletal muscles.* Archives of gerontology and geriatrics, 2016. **65**: p. 1-8.
279. Fan, J., et al., *Autophagy as a Potential Target for Sarcopenia.* Journal of cellular physiology, 2016. **231**(7): p. 1450-9.
280. Jiao, J. and F. Demontis, *Skeletal muscle autophagy and its role in sarcopenia and organismal aging.* Current opinion in pharmacology, 2017. **34**: p. 1-6.

281. Liu, W., et al., *Loss of adult skeletal muscle stem cells drives age-related neuromuscular junction degeneration.* eLife, 2017. **6**: p. e26464.
282. Thornell, L.E., et al., *Satellite cell dysfunction contributes to the progressive muscle atrophy in myotonic dystrophy type 1.* Neuropathol Appl Neurobiol, 2009. **35**(6): p. 603-13.
283. Perfetti, A., et al., *Genome wide identification of aberrant alternative splicing events in myotonic dystrophy type 2.* PloS one, 2014. **9**(4): p. e93983-e93983.
284. van Woerden, G.M., et al., *βCaMKII controls the direction of plasticity at parallel fiber–Purkinje cell synapses.* Nature Neuroscience, 2009. **12**(7): p. 823-825.
285. Okamoto, K., M. Bosch, and Y. Hayashi, *The Roles of CaMKII and F-Actin in the Structural Plasticity of Dendritic Spines: A Potential Molecular Identity of a Synaptic Tag?* Physiology (Bethesda), 2009. **24**(6): p. 357-366.
286. Yamasaki, N., et al., *Alpha-CaMKII deficiency causes immature dentate gyrus, a novel candidate endophenotype of psychiatric disorders.* Molecular Brain, 2008. **1**(1): p. 6.
287. Silva, A., et al., *Impaired spatial learning in alpha-calcium-calmodulin kinase II mutant mice.* Science, 1992. **257**(5067): p. 206-211.
288. Cohen, S.M., et al., *Calmodulin shuttling mediates cytonuclear signaling to trigger experience-dependent transcription and memory.* Nature Communications, 2018. **9**(1): p. 2451.
289. Singh, P., M. Salih, and B.S. Tuana, *Alpha-kinase anchoring protein alphaKAP interacts with SERCA2A to spatially position Ca2+/calmodulin-dependent protein kinase II and modulate phospholamban phosphorylation.* The Journal of biological chemistry, 2009. **284**(41): p. 28212-21.
290. Zhang, T. and J.H. Brown, *Role of Ca2+/calmodulin-dependent protein kinase II in cardiac hypertrophy and heart failure.* Cardiovascular Research, 2004. **63**(3): p. 476-486.
291. Bachstetter, A.D., et al., *Generation and behavior characterization of CaMKIIβ knockout mice.* PloS one, 2014. **9**(8): p. e105191-e105191.
292. O'Leary, H., E. Lasda, and K.U. Bayer, *CaMKIIβ Association with the Actin Cytoskeleton Is Regulated by Alternative Splicing.* Molecular Biology of the Cell (MBoC), 2006. **17**(11): p. 4656-4665.
293. GuptaRoy, B., et al., *Alternative splicing of Drosophila calcium/calmodulin-dependent protein kinase II regulates substrate specificity and activation.* Molecular Brain Research, 2000. **80**(1): p. 26-34.
294. Bayer, K.U., et al., *Developmental expression of the CaM kinase II isoforms: ubiquitous gamma- and delta-CaM kinase II are the early isoforms and most abundant in the developing nervous system.* Brain research. Molecular brain research, 1999. **70**(1): p. 147-54.
295. Mouslim, C., et al., *A Role for the Calmodulin Kinase II-Related Anchoring Protein (αkap) in Maintaining the Stability of Nicotinic Acetylcholine Receptors.* Journal of Neurosciences, 2012. **32**(15): p. 5177-5185.
296. Zhang, M., et al., *Abstract 457: Ca2+/calmodulin Dependent Kinase II Exacerbates Heart Failure Progression Through Activation of Class I Histone Deacetylases.* Circulation Research, 2018. **123**(Suppl_1): p. A457-A457.
297. Hudmon, A., et al., *CaMKII tethers to L-type Ca2+ channels, establishing a local and dedicated integrator of Ca2+ signals for facilitation.* The Journal of cell biology, 2005. **171**(3): p. 537-47.
298. Martinez-Pena, Y.V.I., et al., *The knockdown of alphakap alters the postsynaptic apparatus of neuromuscular junctions in living mice.* The Journal of neuroscience : the official journal of the Society for Neuroscience, 2015. **35**(13): p. 5118-27.
299. O'Leary, H., et al., *Nuclear targeting of the CaMKII anchoring protein αKAP is regulated by alternative splicing and protein kinases.* Brain Research, 2006. **1086**(1): p. 17-26.
300. Yuasa, K., et al., *Targeted ablation of p38α MAPK suppresses denervation-induced muscle atrophy.* Scientific reports, 2018. **8**(1): p. 9037-9037.
301. Laplante, M. and D.M. Sabatini, *mTOR signaling at a glance.* Journal of cell science, 2009. **122**(Pt 20): p. 3589-94.
302. Sanchez, A.M., et al., *AMPK promotes skeletal muscle autophagy through activation of forkhead FoxO3a and interaction with Ulk1.* Journal of cellular biochemistry, 2012. **113**(2): p. 695-710.

303. Pond, A., et al., *History, Mechanisms and Clinical Value of Fibrillation Analyses in Muscle Denervation and Reinnervation by Single Fiber Electromyography and Dynamic Echomyography.* European journal of translational myology, 2014. **24**(1): p. 3297-3297.
304. Ware, J., A.L. Bennett, and A.R. McIntyre, *Membrane Resting Potential of Denervated Mammalian Skeletal Muscle Measured in Vivo.* American Journal of Physiology, 1954. **177**(1): p. 115-118.
305. Cisterna, B.A., et al., *Connexin hemichannels explain the ionic imbalance and lead to atrophy in denervated skeletal muscles.* Biochimica et Biophysica Acta (BBA) - Molecular Basis of Disease, 2016. **1862**(11): p. 2168-2176.
306. Konieczny, P., E. Stepniak-Konieczna, and K. Sobczak, *MBNL proteins and their target RNAs, interaction and splicing regulation.* Nucleic acids research, 2014. **42**(17): p. 10873-10887.
307. Philips, A.V., L.T. Timchenko, and T.A. Cooper, *Disruption of splicing regulated by a CUG-binding protein in myotonic dystrophy.* Science, 1998. **280**(5364): p. 737-41.
308. Klocke, R., et al., *Role of innervation, excitability, and myogenic factors in the expression of the muscular chloride channel ClC-1. A study on normal and myotonic muscle.* The Journal of biological chemistry, 1994. **269**(44): p. 27635-9.
309. McManaman, J.L., J.C. Blosser, and S.H. Appel, *Inhibitors of membrane depolarization regulate acetylcholine receptor synthesis by a calcium-dependent, cyclic nucleotide-independent mechanism.* Biochimica et Biophysica Acta (BBA) - Molecular Basis of Disease, 1982. **720**(1): p. 28-35.
310. Birnbaum, M., M.A. Reis, and A. Shainberg, *Role of calcium in the regulation of acetylcholine receptor synthese in cultured muscle cells*.* Pflugers Archiv : European journal of physiology, 1980. **385**(1): p. 37-43.